Cruise report JC057 on RRS James Cook

GEOTRACES West Atlantic leg 3

Punta Arenas (Chile) 02-03-2011 to Las Palmas (Spain) 06-04-2011

Micha J.A. Rijkenberg

With contributions of participants

Royal Netherlands Institute for Sea Research

Acknowledgements

On behalf of all participants I want to thank Captain Bill Richardson for his help, advice and hospitality on his ship RRS James Cook. Jason Scott from the NERC Marine Facilities (NMF) has been of great help in getting our Dutch equipment to work on a British ship, his enthusiastic and expert help during the scientific deck operations was greatly appreciated. We received the same expert help from Gareth Knight (NMF) who took care of the digital data collection of underway data. The crew of the James Cook were very helpful whenever and wherever needed. They made our stay on the James Cook a convenient and happy time. The post-cruise data management by Hendrik van Aken and the data management group was excellent as usual. Other people I want to thank for their help to make this cruise possible are Jez Evans (NMF), Jane Thompson (NMF), Mark Westcott (NMF), Hilde Kooijman (NIOZ), Erica Koning (NIOZ), Jack Schilling (NIOZ) and everybody from the NIOZ MTEC department involved in getting all our heavy equipment organised and transported to Punta Arenas! We acknowledge ZKO (project number 839.08.410) for funding of this work.

Front page: the titanium ultraclean CTD frame with 24 x 27L PVDF samplers during recovery on the RRS James Cook

CONTENTS

Cruise summary

Research cruise

The Geotraces West Atlantic cruise leg 3; JC057 on RRS James Cook started 2 March 2011 departing from Punta Arenas (Chile) and ended in Las Palmas (Canary Islands, Spain) on 06 April 2011 with Micha Rijkenberg (Royal NIOZ) as chief scientist.

Stations

Initially 25 stations were planned for leg 3 of the Dutch Geotraces cruises, however, the speed of the ship was strongly reduced due to a damaged propeller. We nevertheless managed to do a total of 18 full depth stations. St. 1 was a test station to check system performance and to rinse the UC CTD. However, because st 1 was fully sampled over the full depth of the water column and no signs of contamination or malfunction were detected, it was counted as a normal station. Overall we did 12 normal stations (st 1, 3, 4, 5, 7, 8, 10, 11, 13, 15, 16, 18), 2 superstations (st 9, 14) and 4 hyperstations (st 2, 6, 12, 17) (Figure 1). Normal stations typically consisted of 1 CTD 25L and 1 UC CTD to the bottom. Superstations were defined by the additional use of *in situ* pumps. Hyperstations consisted typically of 1 x CTD 25 L to the bottom, 2 x UC CTD to the bottom and the use of the *in situ* pumps. In addition 4 x CTD 25 L casts to 3500 m depth were performed (st 2, 7, 11, 16) for deep sea microbiology.

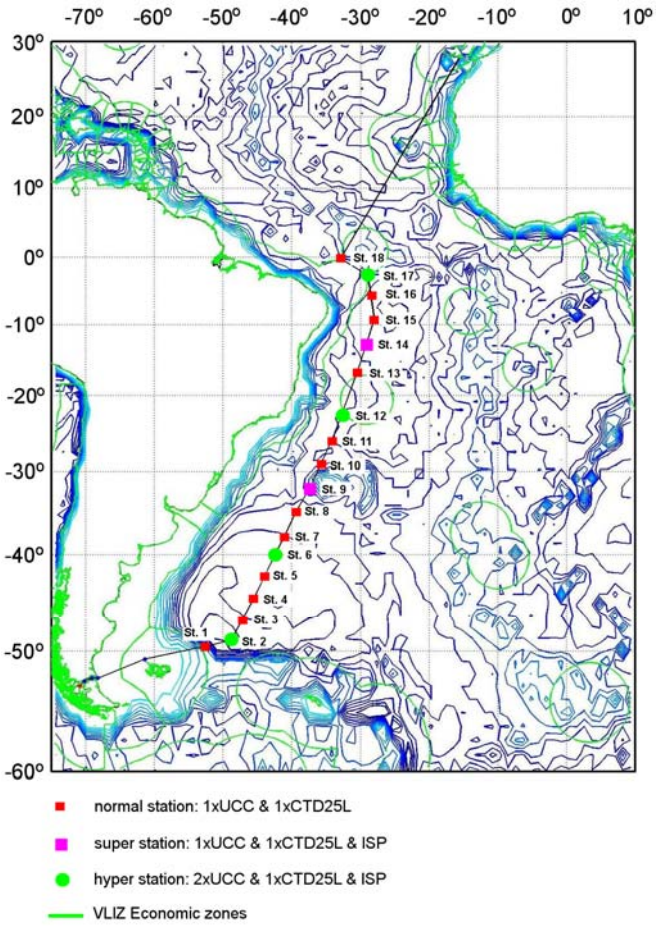

Figure 1. The cruise track of JC067, red squares indicate normal stations, pink squares indicate superstations and green circles indicate hyperstations.

Cruise narrative

The participants joined the RRS James Cook from 26 to 28 March 2011. The RRS James Cook departed from the harbour in Punta Arenas (Chile) on the 1st of March to bunker fuel at Cabo Negro. On the 2nd of March around 13:00 the RRS James Cook departed for its transit to our first station. Our first station would normally be a test station to check system performance and to rinse the UC CTD, however, due to reduced ship time for scientific work we decided to call the test station a normal station. Dissolved aluminium and manganese concentrations showed that the ultraclean sample bottles were clean and that we could use the data. Our 2nd station was a hyperstation. According to the software PERPLEX the water depth at this station was 6000 m. The CTD sensors were certified for a depth of 6000 m. One of the altimeters broke down on the first down cast so it was decided that the CTD's would not go to the bottom but instead to a depth of 5930 m. Although the bottom was not reached the first bottle was closed within the nepheloid layer.

Station 6, at about 40°S, was also a hyperstation. This station is of particular importance as a cross over station with the UK Geotraces cruise along 40°S. Although this UK Geotraces cruise was not able to reach our position, a future planned UK Geotraces cruise along 40°S will use the same position as a cross over hyperstation with our cruise.

The location choice of hyperstations 12 and 17 was based on the equal distance between these stations relative to the hyperstations 2 and 6. The location choice of the superstations, i.e. the use of *in situ* pumps, was based on the creation of a regular sampling pattern.

Where the cruise track crossed the Brazilian economic zones, i.e. between stations 12–13 and stations 17-18, the distance between stations were above average.

Ship's clock

The ship left the harbour on 2 March 2011 with ship time on UTC-3hr. The ship time was advanced on 5 March 2011 to UTC-2hr, on 20 March 2011 to UTC-1hr, on 1 April 2011 to UTC and on 4 April 2011 to UTC+1 hr.

Weather

The weather conditions were excellent during the whole expedition. Wind speed did not exceed 20-25 knots.

Hydrography

The depth of the water column on the stations during our cruise varied from 6000 m at station 2 to 3892 m at station 10. Station 1 was situated on the shelf north of the Falkland Islands and was "only" 2414 m deep. Some of the water masses that we encountered are clearly visible in the ocean section plots of salinity (Figure 2), potential temperature (Figure 3), oxygen (Figure 4) and the nutrients (Figure 5, 6 & 7). Low salinities of around 34 indicate the Antarctic Intermediate Water (AAIW) that appears around 50ºS and flows at a depth between about 500-1000 m northwards. The North Atlantic Deep Water (NADW) with salinities around 35 flows at a depth between 1200-3900 m southwards until about 45ºS after which it flows eastwards (Stramma et al. 1999). The nutrients silicate, phosphate and NO_3^- + NO_2^- clearly distinguish NADW (Figure 5, 6 & 7). Until 25ºS, low silicate concentrations and a salinity maximum within the NADW indicate the Upper NADW. In the south the NADW penetrates the Circumpolar Water (CPW) entering from the Drake Passage dividing the CPW in an Upper and Lower Circumpolar Deep Water. The Upper Circumpolar Deep Water (UCDW) flows below the AAIW around 1000 m depth. In the south till about 25ºS, the

UCDW is indicated by an oxygen minimum. Towards the north, the UCDW is indicated by high silicate and a phosphate maximum (Stramma et al. 1999). The UCDW most northern reaches are found near the equator (Stramma et al. 1999). Good visible in the ocean section plot of the potential temperature is the cold Antarctic Bottom Water (AABW) that flows below 4000 m northwards. The identity of the AABW is further confirmed by the high concentrations in silicate (Figure 5). The surface South Atlantic Central Water (SACW) is unrecognizable in the ocean section plots, however, SACW can be recognized in a property-property plot of the potential temperature against salinity (Figure 8) as a straight line between 5 ºC, 34.3 and 20 ºC, 36.0 (Stramma et al, 1999).

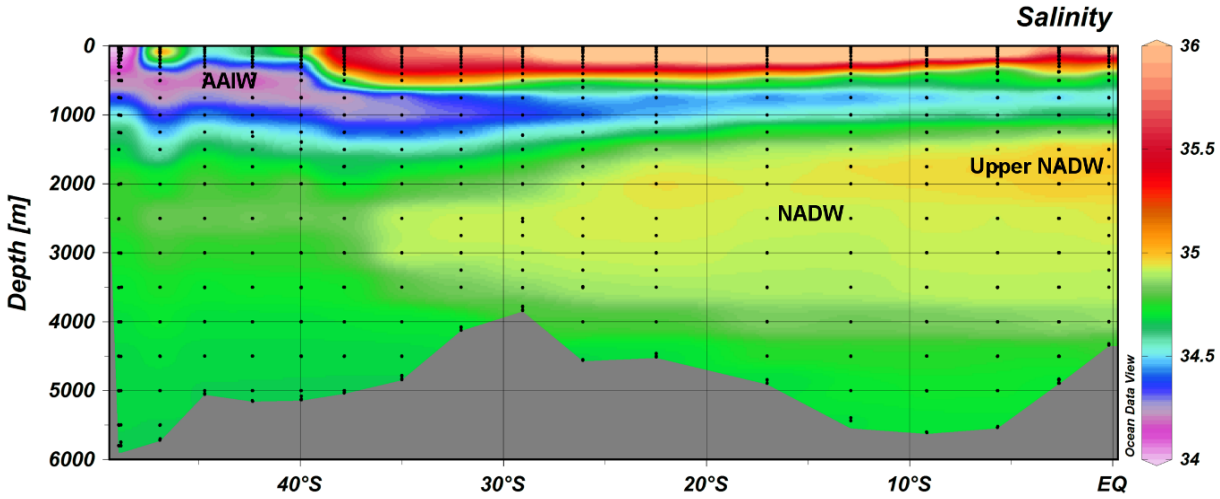

Figure 2. Ocean section of preliminary salinity data from the CTD bottle files of the UC CTD and CTD 25L during JC057 (data Sven Ober).

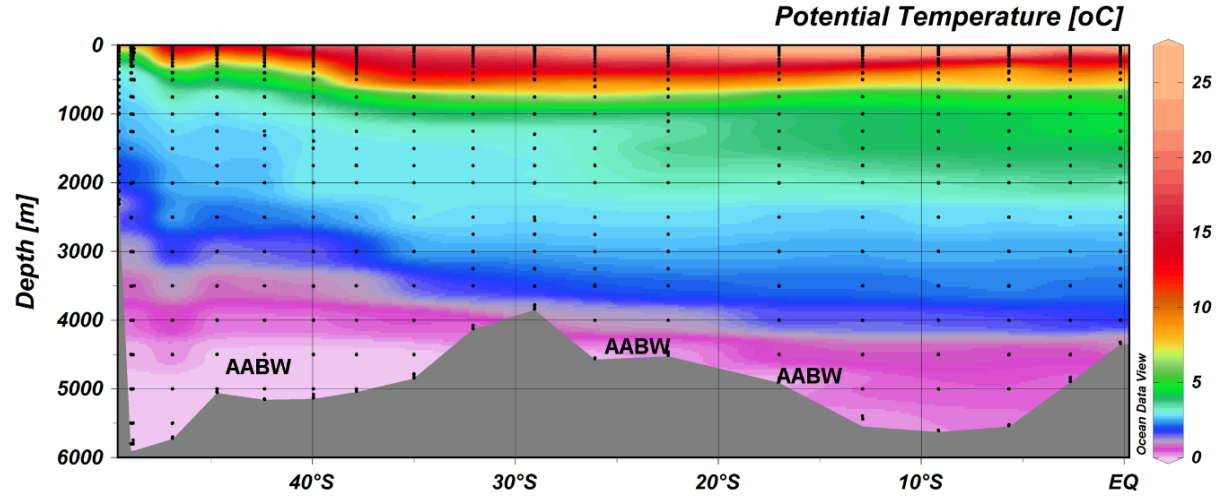

Figure 3. Ocean section of the preliminary potential temperature data from the CTD bottle files of the UC CTD and CTD 25L during JC057 (data Sven Ober).

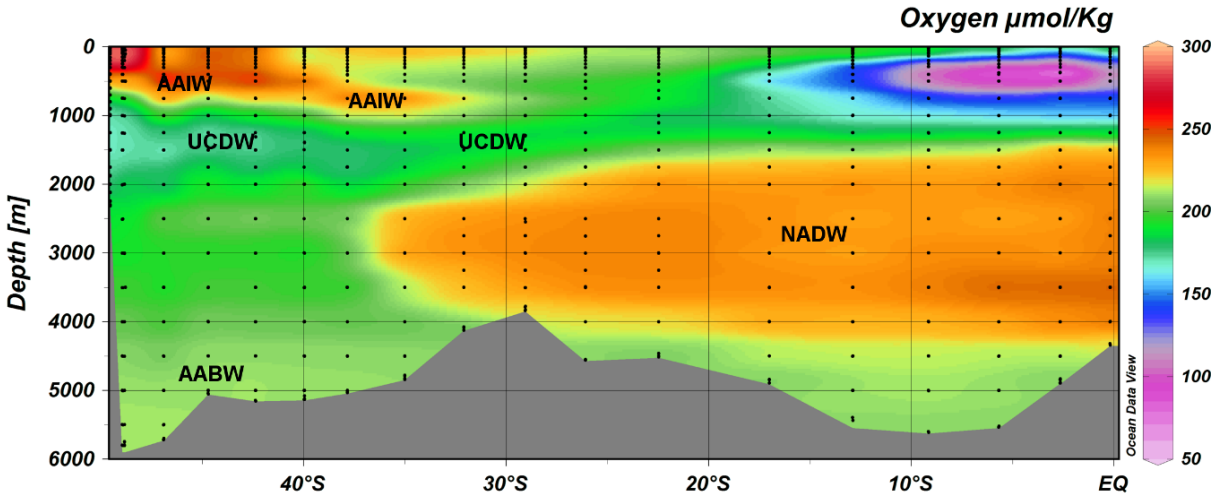

Figure 4. Ocean section of the preliminary potential oxygen data (µmol/kg) from the CTD bottle files of the UC CTD and CTD 25L during JC057 (data Sven Ober).

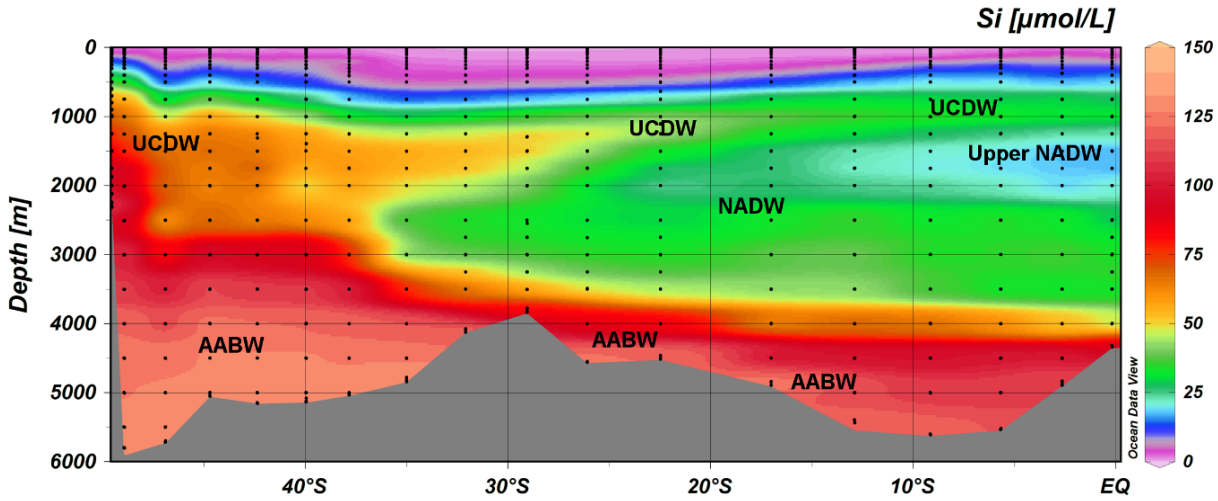

Figure 5. Ocean section of the preliminary silicate data as measured from the UC CTD and CTD 25L during JC057 (data Evaline van Weerlee).

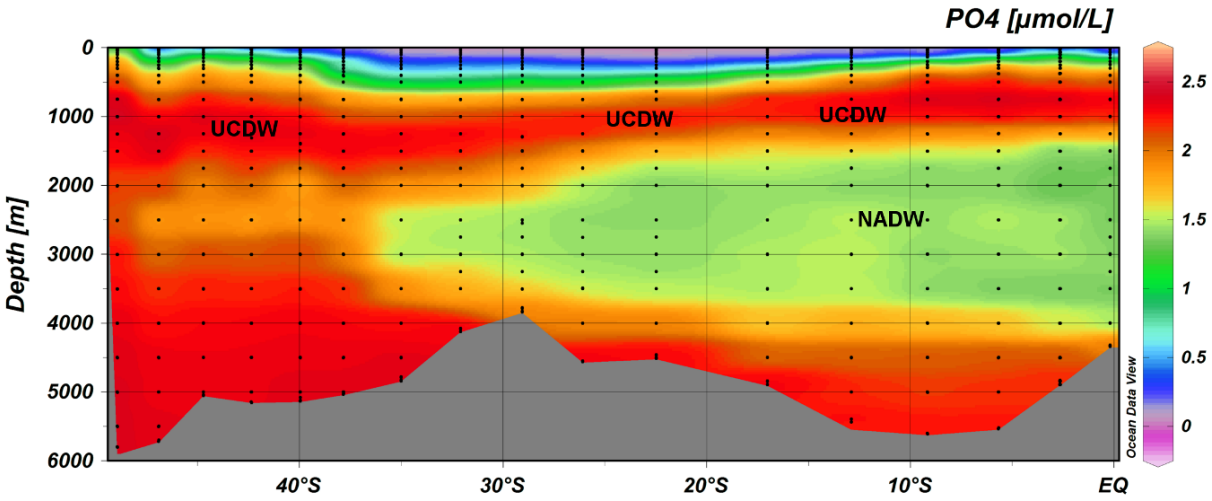

Figure 6. Ocean section of the preliminary phosphate data as measured from the UC CTD and CTD 25L during JC057 (data Evaline van Weerlee).

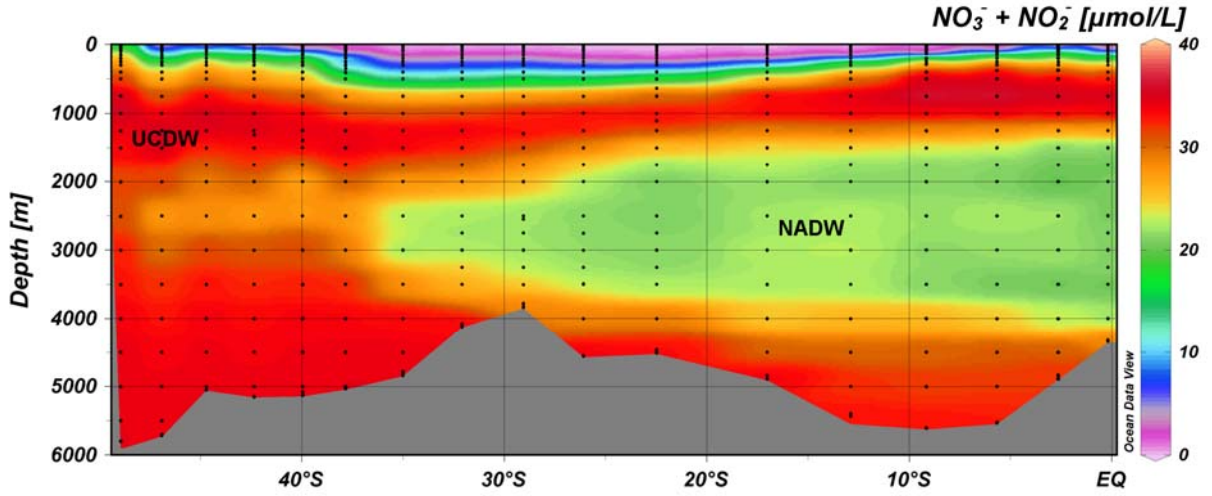

Figure 7. Ocean section of the preliminary NO_3^- + NO_2^- data as measured from the UC CTD and CTD 25L during JC057 (data Evaline van Weerlee).

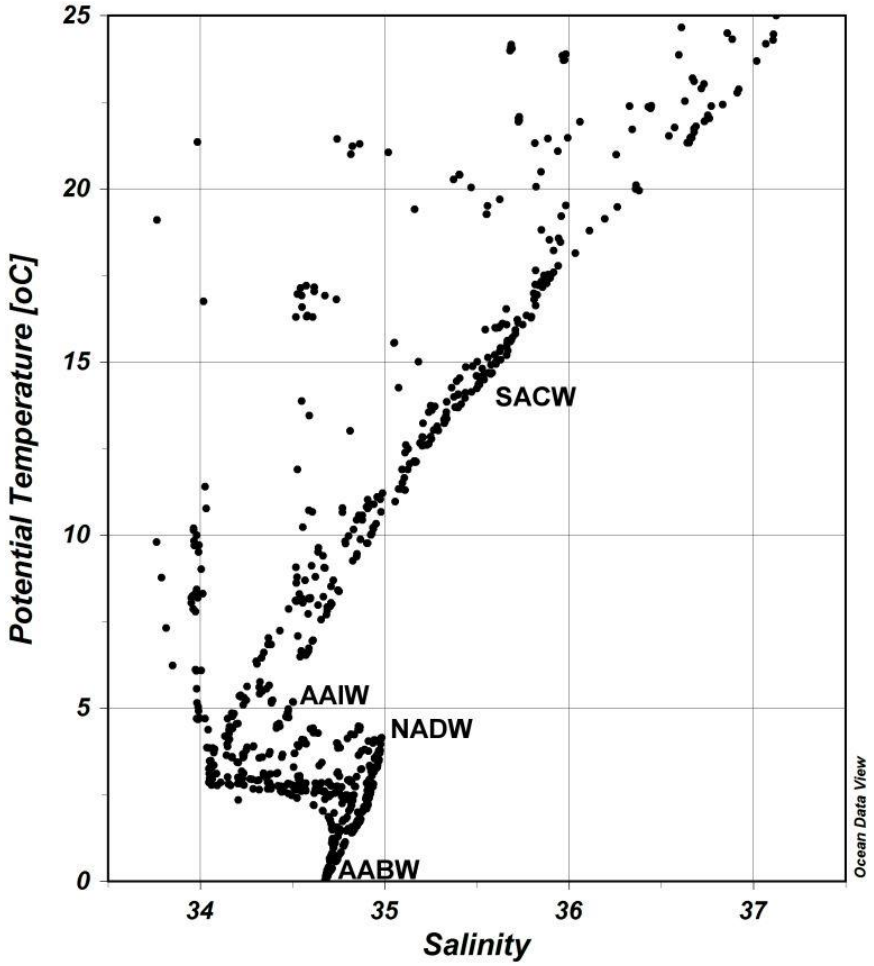

Figure 8. Potential temperature versus salinity plot from the preliminary CTD data shows the AABW, NADW, AAIW and SACW (data Sven Ober).

Underway surface data

Surface seawater has been sampled using a towed fish. The list of parameters sampled from the towed fish and the non-toxic surface seawater supply of the ship can be found in section 2.3.

Figure 9 shows the underway surface seawater data as measured by the ship's systems (see section 3.1.3.). As expected the seawater temperature rose steadily from about 10°C at 50°S to about 28-29°C at the equator (Figure 9 a). The salinity of the surface seawater ranged between 33.8 and 37.5 with the highest salinities found near 20°S (Figure 9 b). The fluorescence data (Figure 9 c) show that the biological productivity was highest south of 40°S and north of 20°N. Between 40°S and 20°N we sailed through parts of the oligotrophic gyres of the Atlantic Ocean.

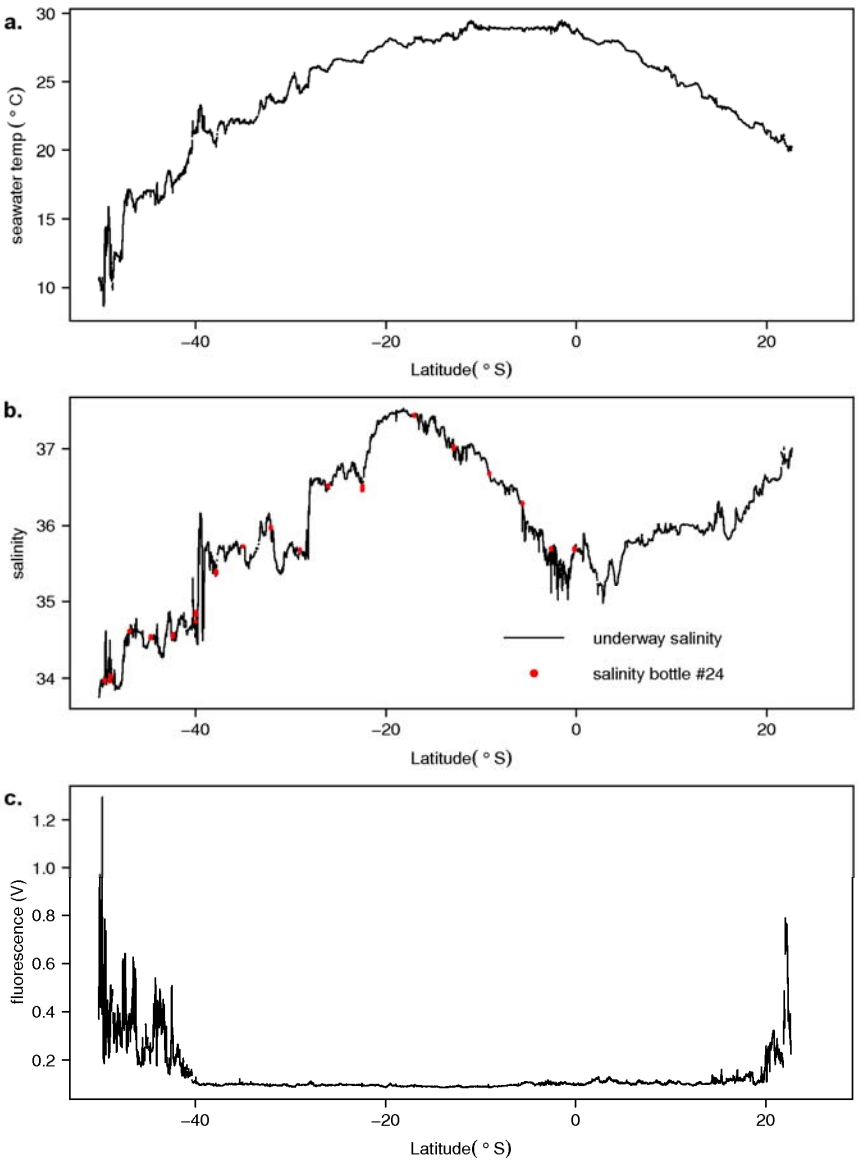

Figure 9. The preliminary surface data as measured with the ship's underway systems, with: a) the surface seawater temperature in degrees Celcius, b) the surface seawater salinity (underway measurements as black line) as confirmed by the preliminary CTD salinity data of bottle #24 (10 m depth, red dots), and c) the fluorescence (Volts).

Description of sample equipment and deployment

We used two rosette systems. Both systems were deployed to deep ocean waters by a 17.7 mm diameter Kevlar hydrowire with seven independent internal signal/conductor cables (Cousin Trestec S.A.) deployed from the Kley France winch (Figure 10 a). One rosette system was used for ultra clean trace metal sampling and consisted of an all-titanium frame with 24 sample bottles of 27 L each made of PVDF plastic (Figure 10 c, UC CTD; UCC in the cruise summary file). Sampling of the UC CTD occurred in a class 100 clean-room container (de Baar et al., 2008). Filtered samples were directly filtered from the UC sample bottles under nitrogen pressure using 0.2 µ. Sartobran 300 cartridges (Sartorius). The second rosette system consisted of 24 new Niskin-type samplers of 25L each mounted on a stainless steel rosette sampler (Figure 10 d, CTD 25L). At each station a mono corer, to collect sediment samples, replaced the bottom weight of the CTD25L (Figure 10 e). Three *in situ* pumps (Woods Hole oceanographic institute) were used for the collection of particulate matter (Figure 10 f). Underway surface seawater was pumped into a trace metal clean laboratory container using a peristaltic pump connected by a braided PVC tubing to a towed fish positioned at approximately 3m depth alongside the ship (Figure 10 b). The seawater samples from the fish was filtered in-line using a Sartobran 300 filter capsule (Sartorius) with a 0.2 µm cut-off. Except for the Brazilian economic zones between station 12–13 and from station 17 until 29 March 10:00 am UTC, the fish has continuously been in the water between station 1 and the Cape Verde economic zone. Other parameters measured underway were the navigation parameters, weather parameters and sea-surface water temperature. For more details see section 2.3 for the list of parameters, and appendix 2 Station list and Devices list.

Challenges during the deployment of the equipment included: i) difficult deployment and recovery of both CTD frames due to the close positioning of the winch in relation to the ships structure, ii) some Niskin bottles failed to close properly as concluded from nutrient data, see Table 1.

Table 1. Niskin bottles that according to nutrient data failed to close properly.

Station	Cast	CTD	Bottle	Status
4	1	UCC	18	failure
6	4	UCC	18	failure
6	4	UCC	10	failure
7	2	UCC	18	failure
1	2	CTD25L	16	doubt
3	1	UCC	8	doubt

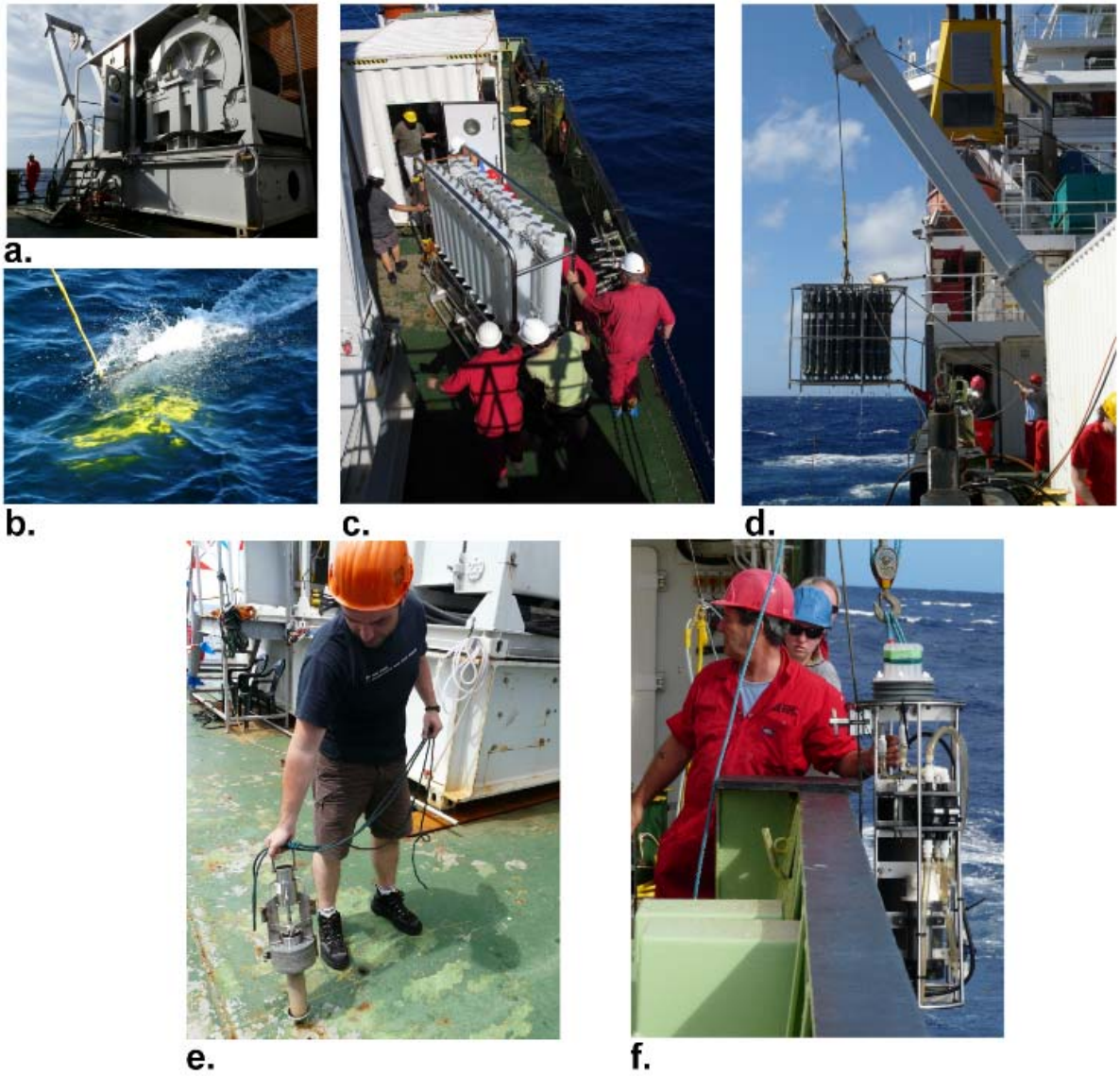

Figure 10. Equipment used during JC057: a) Kley France winch with mounted A frame, b) the towed fish used for underway surface sampling of seawater, c) the ultraclean all titanium CTD transported to its custom made cleanroom container for sampling, d) the high volume CTD25L during recovery, e) Leo Pena holding the mono corer used underneath the CTD25L to sample bottom sediments for Nd isotopes, f) the Chief Petty Officer Scientific Mick Minnock and Stephanie Owens deploying an in situ pump. Pictures a, b, d, e and f by Micha Rijkenberg, Picture c by Elizabeth Jones.

Concluding

We have completed the third and last leg of the Dutch Geotraces project. The Dutch Geotraces project aimed to map the distribution of important trace elements and isotopes in the West Atlantic Ocean. With 18 full depth stations sampled during this leg 3 we completed a transect of 59 stations from 65ºN to 50ºS, (Figure 11). On board were scientists from Brazil, Germany, France, UK, USA, Austria and the Netherlands. We sampled a extensive set of parameters with direct on board measurement of the trace metals Fe, Al, Mn, Co, Zn and Cd, the CO_2 system, nutrients, organic speciation and size fractionation of Fe, ^{234}Th and bacterial and Archaeal production. We also sampled a large set of parameters for the international community including Ag, Pt, Cu, Zn, Hg, Ba, U, Mo, the rare earth elements, the isotopes of Cd, Cr, Ni, Nd (water column and bottom sediments), Pb, Fe, Zn, Si, ^{15}N, $^{13/14}$C, ^{230Th}, ^{231}Pa, ^{232}Th, ^{18}O, D and other parameters as CFC's and a whole range of parameters to increase our understanding of the deep sea microbiology.

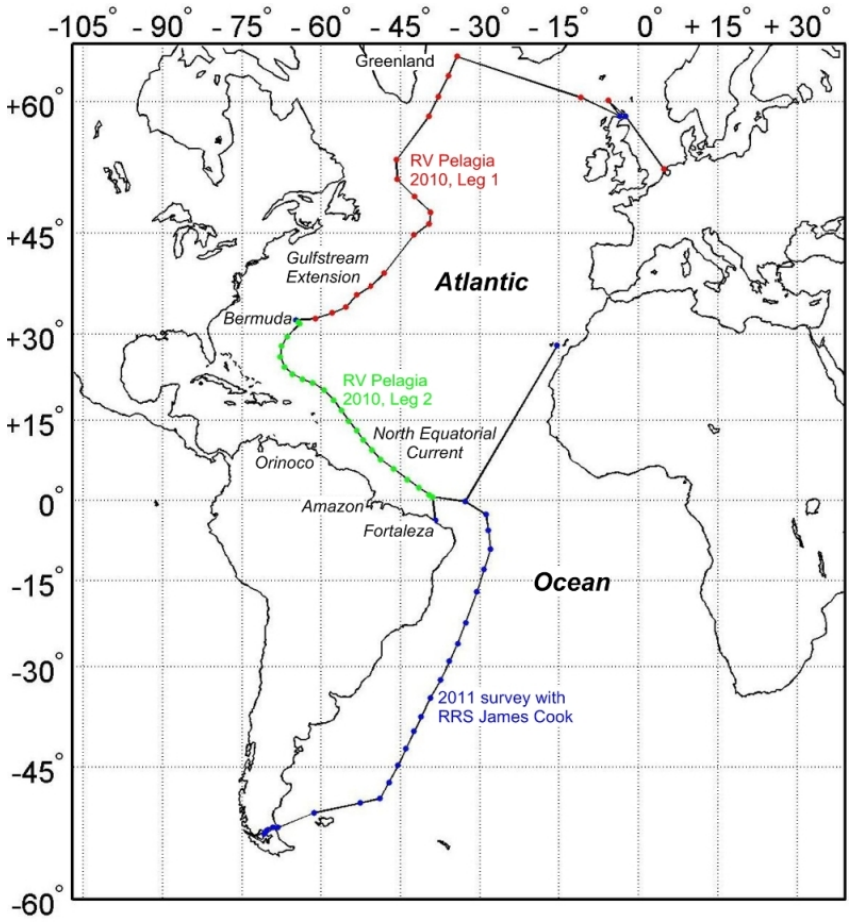

Figure 11. The completed West Atlantic transect of the Dutch Geotraces project.

References

Stramma, L. and England, M., 1999. On the water masses and mean circulation of the South Atlantic Ocean. Journal of Geophysical Research-Oceans, 104(C9): 20863-20883

1. General introduction of the GEOTRACES project

The goal of the GEOTRACES project is to re-visit in 2010-2011 the West Atlantic GEOSECS-1972 cruise to produce complete ocean sections of (A) novel trace elements and several isotopes, (B) transient tracers of global change, (C) microbial biodiversity and metabolism, and (D) interpretation by ocean modelling where the ocean observations A-C serve for verification of the models.

Many of these 'tracers in the sea' are the first-ever ocean sections (sub-projects A, (B), C), while others (sub-project B) will allow unravelling of transient global changes over the past ~35 years by comparison with data of 1972-1973 GEOSECS and later cruises (notably 1981-1983 TTO, WOCE 1990's; CLIVAR).

A) Trace elements and isotopes of the international GEOTRACES program

The first-ever high resolution Atlantic deep section of trace metals Fe, Al, Zn, Mn, Cd, Cu, Co, Ni, Ag were sampled, in conjunction with lower resolution sampling for Rare Earths, natural isotopes ^{234}Th, ^{230}Th, ^{231}Pa, ^{223}Ra, ^{224}Ra, ^{226}Ra, ^{228}Ra, ^{227}Ac and anthropogenic isotopes ^{129}I, ^{99}Tc, ^{137}Cs, ^{239,240}Pu, ^{238}Pu.

More than thirty years after GEOSECS the techniques for ultraclean sampling in a time efficient manner (De Baar et al., 2008) and final analyses have improved enormously. Nowadays it is feasible to determine for the first time ever the oceanic distributions of key trace metals, other trace elements, and various isotopes, along ocean sections throughout the full 4-6 km depth of the oceans. In the GEOTRACES Science Plan (www.geotraces.org) we have defined 6 key trace metals Fe, Al, Zn, Mn, Cd, Cu, which, together with additional metals Co, Ni, Ag is investigated with high priority in the GEOTRACES West Atlantic Ocean sections. The distribution and biological availability of Fe is strongly controlled by its physical-chemical speciation within seawater, where colloids and Fe-organic complexes are dominant actors. For phytoplankton growth, Cu at the cell wall acts in reductive dissociation of Fe-organic complexes, hence facilitates Fe uptake. This may partly explain the nutrient-type distribution of Cu in the oceans. The external sources of Fe into the oceans are either from above (dust) and below (sediments) and will be constrained by Al and Mn for aeolian dust input and sedimentary redox cycling sources, respectively. Iron enhances phytoplankton growth, which in turn controls the biological pump for uptake of CO_2 from the atmosphere. Due to fossil fuel burning the CO_2 also increases in ocean waters and this may affect phytoplankton ecophysiology, with key links of metals Fe and Zn in overall photosynthesis and in carbonic anhydrase, respectively, where Cd and Co may substitute for Zn in the latter carbonic anhydrase.

B) Global change of anthropogenic CO_2 invasion and other transient anthropogenic tracers

Water masses, circulation and mixing are defined by classical S, T, p combined with datasets of dissolved nutrients and O_2, as well as transient tracers DIC, CFCs, novel SF6, ^{3}H/^{3}He and $^{13}CO_2$, $^{14}CO_2$ also to derive 'ages' of a water mass. The invasion of transients is mostly in the North Atlantic Ocean and partly overlaps with warming of upper ocean waters, and with the increase of CO_2 inventory, hence ocean acidification.

Aim is the determination of anthropogenic CO_2 inventory by measurements of DIC, Alkalinity and transient radiocarbon, and interpretation relying also on other transients

(CFC's; SF6; $^{3}H/^{3}He$; other noble gases) measured by international partners. The overarching hypothesis is the very obvious statement: **The best possible estimate of the inventory of anthropogenic CO_2 in the Atlantic Ocean can be achieved by optimizing between a suite of transient tracers and approaches, for optimal concordance between them.**

The first major objective is to quantify the inventory of anthropogenic CO_2 along the transect in the West Atlantic Ocean by a suite of different approaches, as follows:
(i) simple (or simplistic) comparison of DIC inventories over the period between 1981-1983 and 2009-2010, as to derive an inventory increase over this circa three decades time interval;
(ii) instantaneous back calculations using DIC, nutrients, O_2, by several methods like delta C*, TROCA, eMLR;
(iii) combinations of DIC data and one or more transient tracers.

Each one of these approaches requires insight and skill, but is in itself quite feasible to pursue. Afterwards these various findings will be evaluated, and the most promising approaches will be applied for an expansion both in time and in space, by developing a time history of increasing anthropogenic CO_2 inventory in the complete North Atlantic Ocean basin, also relying on preceding data in the CARINA database. This expansion towards a basin wide estimate will be in conjunction with the sub-project D. global ocean modelling.

C) Microbial oceanography: biodiversity and turnover rates of prokaryotes, eukaryotes and viruses

Biodiversity, abundance and metabolic rates of microbes (eukaryotes, prokaryotes and viruses) were determined in the meso- and bathypelagic ocean. Particularly, the role of chemoautotrophy in the deep ocean is investigated as it might represent an unrecognized source of dark ocean 'primary productivity'.

The main objective of the proposed study is to mechanistically understand the dynamics in diversity and function of the meso- and bathypelagic food web in relation to hydrodynamic conditions in distinct deep-water masses of the North Atlantic and at water-mass boundaries where diversity hotspots are expected to occur as predicted by the ecotone concept. The main objective translates into the following **specific objectives**:
i) To link phylogenetic prokaryotic diversity to selected prokaryotic functions relevant for the dark ocean's biogeochemical fluxes (remineralisation of organic matter, organic matter production, ectoenzymatic activity, etc.) using a combination of approaches.
ii) To differentiate between the distribution of abundant and rare prokaryotic taxa and to determine the significance of rare taxa for the functioning of the community.
iii) To determine the extent of the recently discovered archaeal chemoautotrophy in the meso- and bathypelagic realm.
iv) To relate dynamics in abundance and activity of the dark ocean biota to changes in the quantity and quality of the organic matter, water mass age and remineralisation activity.
v) To determine the expression of selected functional genes for Archaea and Bacteria indicative of major metabolic pathways using targeted Q-PCR analyses in specific deep-water masses.
vi) To assess the role of viruses as compared to protists as consumers of prokaryotes.

The overarching hypothesis is that the seemingly homogenous water column of the dark ocean is highly structured due to the hydrodynamics of the different water masses. Each water mass carries its specific biogeochemical characteristics and allows the expression of distinct diversity and function patterns of the dark ocean biota. At the interface and mixing zones of deepwater masses, persistent deep-sea ecotones exist, representing 'hotspots' in

diversity and activity of microbes with significant influence on the overall biogeochemical cycles of the dark ocean.

D) Ocean Biogeochemical Climate Modelling

The above datasets A,B,C are in mutual support and moreover combine to serve for Ocean Biogeochemical Climate Modelling towards more rigorous, integrated understanding of processes including the role of the Atlantic Ocean in global change.

References

de Baar, H.J.W., Timmermans, K.R., Laan, P., De Porto, H.H., Ober, S., Blom, J.J., Bakker, M.C., Schilling, J., Sarthou, G., Smit, M.G. and Klunder, M., 2008. Titan: A new facility for ultraclean sampling of trace elements and isotopes in the deep oceans in the international Geotraces program. Marine Chemistry, 111(1-2): 4-21.

2. Participants and parameters

2.1. List of participants

1	**Micha Rijkenberg PI**	NIOZ; BIO-Chemical Oceanography
2	**Kristin Bergauer**	University of Vienna
3	**Marie Boyé**	LEMAR IUEM
4	**Maaike Claus**	NIOZ/RuG
5	**Feifei Deng**	Oxford University
6	**Jonathan Dérot**	LEMAR IUEM
7	**Loes Gerringa**	NIOZ; BIO-Chemical Oceanography
8	**Jose Marcus Godoy**	PUC-RIO
9	**Santiago Gonzalez**	NIOZ; BIO-Chemical Oceanography
10	**Lennart Groot**	NIOZ/Hogeschool Utrecht
11	**Alison Hartman**	Lamont-Doherty Earth Observatory, Columbia University
12	**Elizabeth Jones**	NIOZ; BIO-Chemical Oceanography
13	**Jeroen de Jong**	NIOZ; Université Libre, Bruxelles (ULB)
14	**Adam Klimiuk**	University of Vienna/NIOZ
15	**Patrick Laan**	NIOZ; BIO-Chemical Oceanography
16	**Itziar Lekunberri**	University of Vienna
17	**Rob Middag**	NIOZ; University of California Santa Cruz
18	**Sven Ober**	NIOZ; MTE
19	**Stephanie Owens**	Woods Hole Oceanografic Institute
20	**Leo Pena**	Lamont-Doherty Earth Observatory, Columbia University
21	**Lesley Salt**	NIOZ; BIO-Chemical Oceanography
22	**Patrick Schmidt**	University Bremen (UB)
23	**Jan-Dirk de Visser**	NIOZ;MTE
24	**Evaline van Weerlee**	NIOZ; GEO
25	**Dominik Weiss**	Imperial College London
26	**Leon Wuis**	NIOZ; MTEC

For complete addresses and email see Appendix 1

Figure 12. Scientists and part of the crew of GEOTRACES leg 3 (JC057) on the RRS James Cook in the South West Atlantic Ocean.

2.2. UCC Sample Team

The following people have been part of the general UCC sampling team in the ultraclean container:

1) Lennart Groot
2) Dominik Weiss
3) Patrick Laan
4) Jeroen de Jong
5) Micha Rijkenberg
6) Rob Middag
7) Leo Pena
8) Alison Hartman
9) José Marcus Godoy
10) Loes Gerringa
11) Marie Boyé
12) Jonathan Dérot

Figure 13. Rob, José Marcus, Leo, Lennart, Alison and Patrick sampling in the ultraclean container.

2 .3. List of parameters

sample equipment & parameters	collected by	responsible for analysis and data
UC CTD (UCC)		
Library metals totals	P. Laan	P. Laan, H. de Baar
Library metals dissolved	P. Laan	P. Laan, H. de Baar
Nutrients	E. van Weerlee	E. van Weerlee
Unfiltered Fe	P. Laan	P. Laan, L Gerringa
Dissolved Fe	P. Laan, L. Groot	P. Laan, M. Rijkenberg
Dissolved Mn	R. Middag	R. Middag
Dissolved Al	R. Middag	R. Middag
Fe ultra filtration	M. Rijkenberg, L. Gerringa	M. Rijkenberg
Fe Speciation	L. Gerringa	L. Gerringa
Dissolved Ag	P. Laan	E. Achterberg
Dissolved Pt	P. Laan	A. Cobelo/D. Lopez Sanchez
Dissolved Co, Zn, Cd	M. Boyé/J. Dérot	M. Boyé
Co-speciation	M. Boyé	M. Boyé
Cd, Cr, Ni Isotopes	J. de Jong	W. Abouchami
Nd isotopes	L. Pena/A. Hartman	L. Pena, S. Goldstein
Rare Earth Elements	L. Pena/A. Hartman	L. Pena, S. Goldstein
^{234}Th	S. Owens	S. Owens, K. Buesseler
Si-isotopes	P. Laan	L. Pichevin
T Fe and Zn isotopes	J. de Jong	J. de Jong, V. Schoemann
Dissolved Fe and Zn isotopes	J. de Jong	J. de Jong, V. Schoemann
Dissolved Fe, Cu, Zn	J. de Jong	J. de Jong, V. Schoemann
^{14}C/^{13}C	L. Jones, L. Salt, M. Claus, P. Schmidt	S. van Heuven, H. Meijer
Dissolved Pb Isotopes	D. Weiss, J. de Jong	D. Weiss, S. Galer
Rubisco	UCC sample team	M. Orellano
O_2	M. Claus, L. Salt, L. Jones	L. Salt
Dissolved ^{15}N isotopes	UCC sample team	P. Rafter
Dissolved ^{230}Th and ^{231}Pa	F. Deng	F. Deng, G. Henderson
Salinity	S. Ober	S. Ober
^{18}O, D, Ba, U, Mo	J. M. Godoy	J. M. Godoy
Dissolved Hg	UCC sample team	C. Lamborg
Dissolved ^{232}Th	UCC sample team	P. Anderson

CTD25L

CFC	P. Schmidt	R. Steinfeldt
O_2	M. Claus, L. Salt, L. Jones	L.Salt
DIC-ALK	E. Jones, L. Salt	L. Jones, L. Salt
DOC	S. Gonzalez	S. Gonzalez
FDOM	S. Gonzalez	G. Herndl
Nutrients	E. van Weerlee	E. van Weerlee
BA / Vir/ Abundance	A. Klimiuk	A. Klimiuk, G. Herndl
3H-Leu / Bacterial prod.	I. Lekunberri	I. Lekunberri, G. Herndl
14C-DIC / Archaeal Prod.	S. Gonzalez	G. Herndl
3H-FISH	I. Lekunberri	I. Lekunberri, G. Herndl
14C-FISH	I. Lekunberri	I. Lekunberri, G. Herndl
FISH	I. Lekunberri	I. Lekunberri, , G. Herndl
DNA	K. Bergauer	K. Bergauer, G. Herndl
Proteomics	K. Bergauer	K. Bergauer, G. Herndl
qPCR Nitrifiers	deep sea microbiologists	P. Berube
Enzymatic activity	A. Klimiuk	A. Klimiuk, G. Herndl
Dissolved ^{230}Th and ^{231}Pa	F. Deng	F. Deng, G. Henderson
Dissolved ^{232}Th	L. Pena/A. Hartman	P. Anderson

In Situ Pumps

Particulate ^{234}Th	S. Owens	S. Owens, K. Buesseler

Sediment mono corer

Nd	L. Pena, A. Hartman	L. Pena, S. Goldstein

FISH

Dissolved Pt	J. de Jong, D. Weiss	A. Cobelo/D, Lopez Sanchez
Dissolved Cd, Cr, Ni-isotopes	J. de Jong, D. Weiss	W. Abouchami
Pb-isotopes (filt. & unfilt.)	J. de Jong, D. Weiss	D. Weiss
Dissolved Fe	J. de Jong, D. Weiss	P. Laan, M. Rijkenberg
Dissolved Mn	J. de Jong, D. Weiss	R. Middag
Dissolved Al	J. de Jong, D. Weiss	R. Middag
Fe speciation	J. de Jong, D. Weiss	L. Gerringa
Nutrients	J. de Jong, D. Weiss	E. van Weerlee
Library metals dissolved	J. de Jong, D. Weiss	P. Laan, H. de Baar
Library metals totals	J. de Jong, D. Weiss	P. Laan, H. de Baar
^{18}O & Ba	J. de Jong, D. Weiss	J. M. Godoy
Co (filt. & unfilt.)	J. de Jong, D. Weiss	M. Boye
Fe/Cu/Zn (filt. & unfilt.)	J. de Jong, D. Weiss	J. de Jong. V. Schoemann

Non-toxic underway seawater supply

Enzymatic activity	A. Klimiuk	A. Klimiuk, G. Herndl
DIC-Alk	E. Jones, L. Salt	E. Jones, L. Salt

3. Analyses and measurements

3.1. General parameters and Data management

3.1.1. Data Management

Lesley Salt & Loes Gerringa

NIOZ

A MATLAB script was written that allowed straightforward concatenation of CTD bottle files (SeaBird's standard .btl format) and user-provided datasets (listing either measurement results or notifications of which samples were collected). Output consisted of a single large datafile which were used in Ocean Data View to create section plots of all submitted parameters. Many of the figures provided in this cruise report are output of this script used in Ocean Data View.

3.1.2. CTD systems

Sven Ober

NIOZ

Introduction

During the cruise 2 CTD-systems were used. One system, the Ultra Clean CTD-system (UCC) was used for ultra clean trace metal sampling and the second one, the Large Volume CTD, for the rest of the sampling. Both systems are more or less off-standard and therefore briefly described below. During the stations the CTD's were deployed 2, 3 or 4 times. In between most of the casts it was necessary to disconnect (mechanical and electrical) the CTD-cable from one CTD and connect it to the other. This was in all cases done by the CTD-operator. This job was checked each time by the winch-operator and both operators had to sign for this on the CTD-form of that cast. This procedure was introduced this cruise as a safety measure to prevent the loss of a frame due to small mistakes like forgetting a safety pin.

Both systems were deployed 22 times, worked reliable and showed only minor technical problems. In 3 cases a bottle of the UCC-system did not function properly (due to human errors) and the samples were rejected. The user-protocol of the UCC-system has been adapted in order to prevent these errors in the future. Two interconnecting cables (T- and DO-sensor) in the UCC-system had to be exchanged by spares after showing broken conductors probably due to fatigue. This happened as well with the cable that interconnects the CTD with the towlink-cable in the LV-CTD. Detailed inspection of this cable learned that this was due to a production problem.. The altimeter of the LV-CTD died at approx. 5500 m due to pressure. This instrument was rated for 6000 m so after the cruise the manufacturer will be asked for a warranty-repair.

During most of the casts of the LV-CTD a small NIOZ-made mono-corer was used as bottom-weight. The corer worked very well (only one failure due to a stone) resulting in 15 sediment-samples.

Both systems were equipped with a Seabird reference-thermometer for in situ calibration of the SBE-3 profiling thermometers. A first analysis of the temperature calibration data showed that the both profiling thermometers have a small pressure-effect. The manufacturer is contacted about this feature and is asked to provide software to correct the data as part of the post processing.

From most casts of both the UCC as the LV-CTD salinity-samples were tapped and analyzed on board with a Guildline 8400B Autosal using OSIL standard water batch P149. A first analysis of the salinity data showed a pressure-effect in the conductivity-sensor of the UCC-system and the conductivity-sensor of the LV-CTD showed a small offset. As part of the post processing the data will be corrected.

From most casts of both the UCC as the LV-CTD samples were tapped for Winkler titrations in order to calibrate the dissolved oxygen (DO)-sensors. Analysis of the Winkler results has not been finished. The DO-sensors of both systems appeared to function very well.

The Ultra Clean CTD-system (UCC)

The system consists of 3 major modules:

- A box-shaped titanium CTD frame with 24 sampling bottles made of PVDF and titanium
- A clean air container for contamination-free (sub)sampling
- A special deep sea winch with an iron-free Dyneema CTD-cable

To avoid contamination the frame of the UCC- system is made of titanium and all the electronic pressure housings and other parts are made of titanium or clean plastics like Teflon, PVDF or POM. The frame can be parked and ‘seasave’ secured inside the clean air container. Prior to a cast the frame is prepared inside that container and transported to the CTD-launching spot using a custom made aluminium pallet and a long bedded forklift. After the cast the frame can be returned to the clean air container within minutes avoiding contamination of the equipment with grease, rust or smoke particles from the ship. After closing of the container the air treatment system starts to clean the air using HEPA-filters (meeting class 100 clean-room specifications after 15 minutes) and the frame, sampling-bottles and electronics can be rinsed with fresh water.

The electronic system consists of a SBE9plus underwater unit, a SBE11plusV2 deckunit, a NIOZ developed multivalve bottle-controller, a SBE3plus thermometer, a SBE4 conductivity sensor, a SBE5T underwater pump, a SBE43 dissolved oxygen sensor, a Chelsea Aquatracka MKIII fluorometer, a Wetlabs C-Star transmissiometer (25 cm, deep, red). For Ultra Clean water sampling 24 samplers (27 liter each) are applied. The UC samplers are produced by NIOZ and are made of PVDF and titanium. Due to the butterfly-type closure on both ends of the sampler the flow-through is excellent. The samplers are controlled with a hydraulic system. The heart of the sampling system is the NIOZ developed Multivalve. For bottom-detection 2 devices are installed: A Benthos PSA-916 altimeter and a bottom switch with a weight. The SBE11+ has a NMEA interface for navigational data. On the logging computer Seasoft for Windows is installed (Seasave V7.20 and SBE Data Processing V7.20). For calibration of the profiling thermometer (SBE3) a high-accuracy reference-thermometer (SBE35) was mounted.

The Large Volume CTD-system (LV-CTD)

The CTD-system consists of a SBE9plus underwater unit, a SBE11plusV2 deck unit, a SBE32 carousel, a SBE3plus thermometer, a SBE4 conductivity sensor, a SBE5T underwater pump, a SBE43 dissolved oxygen sensor, a Chelsea Aquatracka MKIII fluorometer, a Wetlabs C-Star transmissiometer (25 cm, deep, red), a Satlantic logarithmic PAR-sensor for underwater PAR and a Satlantic linear PAR-sensor for deck reference. For large volume water sampling 24 water samplers each with a volume of 25 liter manufactured by Ocean Test Equipment is applied. These 25-liter samplers are equipped with an internal stainless steel spring and a horizontally mounted Teflon drain assembly. Via this drain assembly flexible jerry cans can be filled easily and the horizontal orientation of the drain enables easy and efficient CFC-sampling. For bottom detection 2 devices are installed: A Benthos PSA-916 altimeter and a bottom switch with a weight. The SBE11+ has a NMEA interface for navigational data. On the logging computer Seasoft for Windows is installed (Seasave V7.20 and SBE Data Processing V7.20). For in situ calibration of the profiling thermometer (SBE3) a high-accuracy reference-thermometer (SBE35) was installed.

3.1.3. RRS James Cook systems

Gareth Knight

NMF-SS

For any further information on this report please contact:

Gareth Knight
National Marine Facilities
National Oceanography Centre
Waterfront Campus
Southampton
SO14 3ZH
+44(2380) 596281
E-mail: gck@noc.soton.ac.uk

Description of the Cruise

CTD clean sampling cruise from Punta Arenas to Las Palmas for NIOZ

End of Cruise Data Deliverables

Final data deliverables were loaded onto portable hard disks with copies of the entire data set going to the BODC and the principal scientist.

As per the new template on the Cook file server used for the last two cruises by Leighton Rolley

Descriptions of Science Systems Used during JC057, COOKFS, Drobo and daily data backup

Backups were made daily from all active systems to the COOKFS server. In addition copies of the data were also loaded onto the drobo NAS as required by the scientific party.

COOKFS

A Dell Data server was delivered to the ship on JC54 to act as a new file storage system for cruise data.

Kongsberg Network	192.168.1.149
Ships Network	192.168.62.57

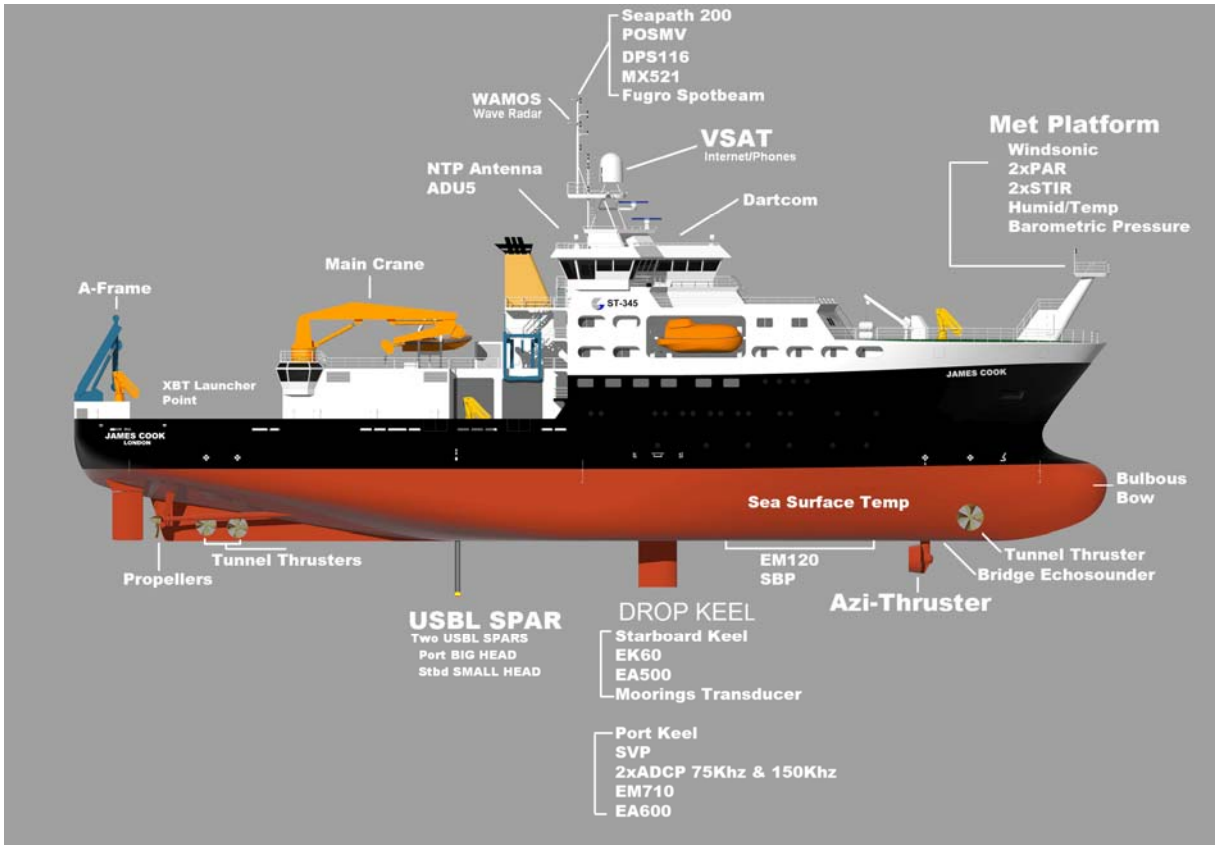

Figure 14. Guide to Ship Fitted Systems

DROBO

The Drobo NAS was utilized by the scientific part as the main science data store and copied to the cruise data disk at the end of the cruise.

Printing facilities

We continue to be short on printers and should have replacements for the terminal room multi function and another 2605 printer at the end of the next passage leg.
Currently we have the following.

2605dn terminal Room

2605dn Main Lab
A0 Plotter Main Lab
A0 Plotter Terminal Room

Having to use the ships office printer for the PS was not a problem during this cruise and it was setup on the NOC provided PC which for a change was used by the PS.

Internet Facilities, Phones, Exinda and Firewall

New internet guidance document written for users and supplied to the purser for inclusion in cabin welcome pack. On the whole the internet worked well throughout the cruise with minimal downtime.

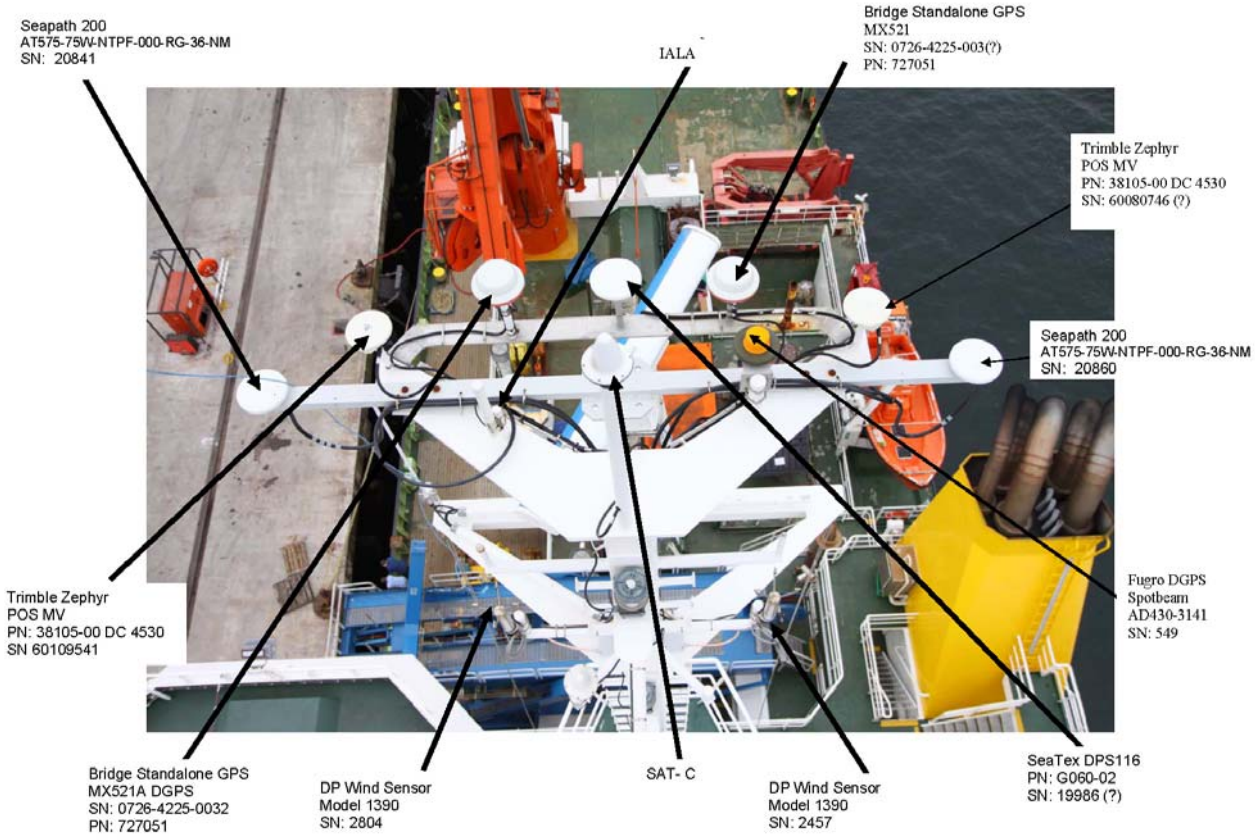

Figure 15. Guide to RRS James Cook GPS Antenna

Inspection of VSAT System – Planned Maintenance

The VSAT system was inspected prior to the cruise and during calm conditions when access ups the mast was possible at roughly the midpoint of the cruise this was near the equator. This was during a period when we had tracking problems for about half an hour around midday. It was put down to sun activity and was common to a number of vessels in the area according to Invsat. The period of disruption lasted for about four days.

No issues were identified with the hardware during these inspections. The securing bolts were also inspected and found to be tight.

Coverage

The Vsat coverage was good other than the problem with the sun activity mentioned. The system was turned to a new frequency in Punta Arenas prior to sailing. This was at the request of Nescco Invsat.

Chernikief

The Chernikief log continues to be reading quite high values – usually about 10-20% higher than the GPS or Skipper Log. The system was fully calibrated on leaving the vessel refit (October 2010). The system should have retained its calibration for this period. Readings whilst on station are still reasonable and this proved to be satisfactory for the cruise.

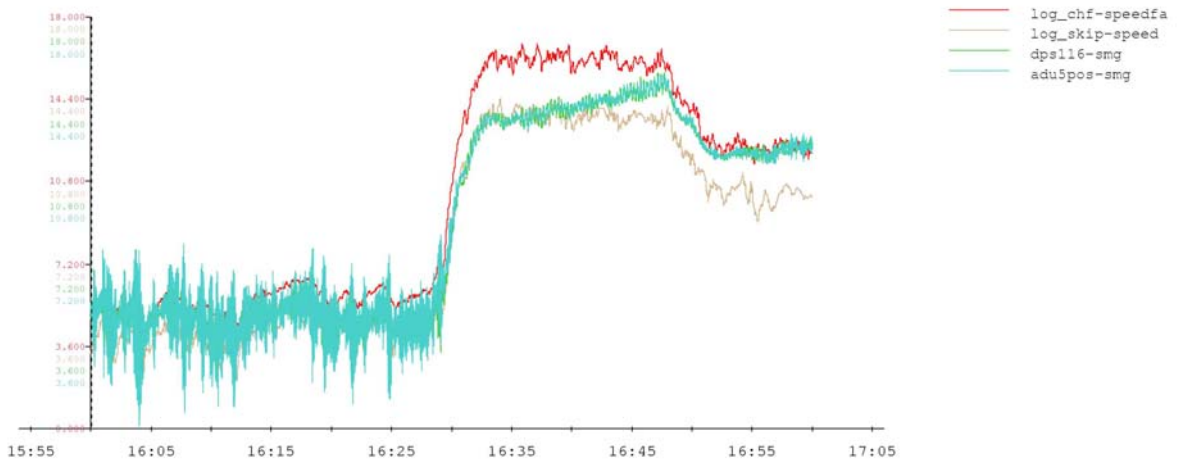

Figure 16. Graph showing the differences in speed logged by each system

Sound Velocity Profiles

Profiles were produced from the CTD casts as it was not possible to attach our sv profilers to the clean system without compromising its cleanness. No time could be allocated for a separate cast.

Olex

The Olex system used for displaying charts and acquired swath failed during the previous cruise. A new computer was brought to the ship for the start of the cruise and the hard drive which is licensed was swopped over. The new system failed to boot. It was not clear if the new computer had issues with hardware even though it was specifically purchased to be the same. Or if the hard drive was faulty. The system will need to be reinstalled by our Olex support and then we can try to clone it to the spare we now have.

Replacement Sea path 200

This continues to be used. It does not accept the differential input. Our old unit did accept differential and should return in Govan at the end of the next passage leg. For the remainder of the cruise with no pitch, roll or heave compensation

EM120

The EM120 was used throughout the cruise to collect raw data and provide monitoring at the stations. Raw data is copied to the cruise archive disk.

3.1.4. Nutrient measurements

Evaline van Weerlee

NIOZ

Summary

On this cruise, more than 1000 samples were analyzed on phosphate, silicate, nitrate and nitrite. 912 samples from CTD bottles, 112 samples from 'fish device' and 96 samples from experiments

During the cruise there were about 4000 analysis processed on a Bran en Luebbe trAAcs 800 Auto-analyzer. The different nutrients were determined colorimetrical as described by Grashoff et all. (1983).

Methods

Samples were obtained from a large volume CTD rosette sampler with 24 bottles of 25 Liter each and an ultra clean CTD with 24 bottles of 27 Liter. All samples were collected directly after the DIC and DOC -sampling in 125ml polypropylene bottles and stored in a fridge at 4˚C. 'Fish' samples were filtrated over a 0.2 µm filter collected in 125ml polypropylene bottles and stored at 4˚C prior to analysis. Experiment samples were filtrated using an Acrodisc Syringe filter with 0.2 µm Supor membranes and stored in 4 ml vials at 4˚C.

Calibration Standards were prepared fresh every day diluted from stock solutions of the different nutrients in 0.2µm filtered low nutrient seawater (LNSW). The LNSW is surface seawater depleted for most nutrients, and is also used as baseline water for the analysis in-between the samples.

The samples were measured from the lowest to the highest concentration in order to keep carry-over effects as small as possible, so from surface to deep waters. Prior to analysis all samples and standards were brought to room temperature of 23˚C, concentrations were recorded in µM per Liter at this temperature.

In every run a daily freshly diluted mixed nutrient standard, containing silicate, phosphate and nitrate a so called nutrient-cocktail, was measured in triplicate. Secondly a natural sterilized Reference Nutrient Sample (RMNS Kanso, Japan) containing a known concentration of silicate, phosphate, nitrate and nitrite in Pacific Ocean water, was analyzed in triplicate every run. The cocktail and the RMNS were both used to monitor the performance of the analysis. Finally the RMNS was used to adjust all data by means of computing with a factor, to obtain the final data set, so all referred to the same RMNS values for each analysis. This made data international comparable and comparable to the first legs of GEOTRACES.

From every station the deepest sample is sub sampled for nutrients in duplicate, the duplicate sample-vials were all stored dark at 4 °C, and measured again with the next station, for statistics.

Chemistry

Silicate reacts with ammonium molybdate to a yellow complex, after reduction with ascorbic acid, the obtained blue silica-molybdenum complex is measured at 800nm. Oxalic acid is used to prevent formation of the blue phosphate-molybdenum.

Phosphate reacts with ammonium molybdate at pH 1.0, and potassium antimonyl-tartrate is used as an inhibitor. The yellow phosphate-molybdenum complex is reduced by ascorbic acid and measured at 880nm.

Nitrate plus nitrite (NO_3^- + NO_2^-) is mixed with an imidazol buffer at pH 7.5 and reduced by a copperized cadmium column to nitrite. The nitrite is diazotated with sulphanylamide and naphtylethylene diamine to a pink colored complex and measured at 550nm.

Nitrate is calculated by subtracting the nitrite value of the nitrite channel from the NO_3^- + NO_2^- value.

Nitrite is diazotated with sulphanylamide and naphtylethylenediamine to a pink colored complex and measured at 550nm.

Described by K. Grasshoff et al, 1983.

Table 2) Statistics of the analysis of this cruise.

	PO4 µmol/L	Si µmol/L	NO_3^- + NO_2^- µmol/L	NO2 µmol/L
JRM target value	1,64	60,5	22,6	0,39
cruise average	1,65	59,9	22,7	0,38
stdev	0,01	0,2	0,2	0,01
stdev%	0,65	0,40	0,79	3,22

Problems during the cruise

The nitrite channel has a sinus baseline signal during the cruise due to sensitive adjustment of the system. The detection limit is therefore increased to 0.04 µmol/L.

References

K. Grasshoff et al, 1983. Methods of seawater analysis. Verlag Chemie GmbH, Weinheim.

3.1.5. Dissolved oxygen

Lesley Salt, Maaike Claus

NIOZ

Water samples were taken from the CTD 25L and UCC at every station for the determination of the concentration of dissolved oxygen, in order to calibrate the CTD sensors. Samples were taken from a minimum of five depths, in duplicate, from the 25L and a minimum of three depths were taken from the UC CTD, also in duplicate, to verify the calibration of the UC CTD to the CTD 25L. Samples were drawn into volume-calibrated ~120ml Pyrex glass bottles using Tygon tubing, flushing the bottle with at least 3 times its volume. Addition of chemicals was performed immediately afterwards, after which glass stoppers were secured in place with an elastic band. The samples were stored underwater and in the dark at 20ºC. Analysis of series of circa 20 samples at a time took place at the same temperature at least 15 hours after sampling.

The determination of the volumetric dissolved oxygen concentration of water samples was performed colourimetrically by measuring the absorbance of iodine at 456nm on a Hitachi U-1100 Spectrophotometer (see Su-Chen Pai et al., 1993). The spectrophotometer was calibrated using standards of seawater spiked with known amounts of KIO_3 (a stock solution of KIO_3 of concentration 73.344M was used). The R^2 value of the calibration line was never less than 0.9997, the average residuals between theoretical values and measured standards having a standard deviation of 0.66 μmol l^{-1} .

The absorbance and the voltage of the photo-cell were recorded manually and oxygen values calculated later, expressed in μmol l^{-1}, for later conversion to μmol kg^{-1} when calibrated salinity values become available. At each station at least one sample was taken in triplicate to measure during the following run for continuity. The standard deviation (1 S.D.) of circa 123 replicates was 0.64 μmol l^{-1}, after discarding 12 samples with unacceptable replicate differences of > 2 μmol l^{-1}. The average difference between circa 123 replicates was 0.98 μmol l^{-1}.

Subsequent utilization of the bottle oxygen measurements for the calibration of the CTD frames' oxygen sensors will be performed back at NIOZ by Hendrik van Aken.

References

Su-Chen Pai et al., 1993) Marine Chemistry **41** (1993), 343-351

3.2. Analyses and Measurements of key parameters

A. Metals and isotopes

3.2.A.1. Dissolved Fe

Patrick Laan and Lennart Groot

NIOZ

Introduction

The trace metal iron (Fe) is one of the 6 key elements in the GEOTRACES Science plan. It is an important factor in biogeochemical cycles of the world oceans [*Martin and Gordon*, 1988*; De Baar et al.,*1995*;*28 *Bruland et al.,*1995*; Boyd et al.* 2000] and is therefore of major importance for marine ecosystems. In recent decades a major step forward is made in understanding the role of Fe in global marine biogeochemical cycles [*De Baar and De Jong*, 2001]. However, there is still very little data available on trace metal concentrations in the especially deeper parts of the world oceans [*Middag et al.*, 2009].

Work at sea

Dissolved iron (DFe) concentrations of all 18 stations with 24 depths each, were measured directly on board by automated Flow Injection Analysis (FIA) system using a modified method (*De Jong et al.* 1998, *De Baar et al.* 2008) of *Obata et al.,* 1993. In addition, unfiltered samples were acidified and stored to determine the total dissolvable Fe (TDFe) concentrations in the NIOZ laboratory after 6-12 months of dissolution. At some selected stations water filtered into different size fractions were measured for DFe directly on board (See Rijkenberg3.2.A.2). Also samples from the towed fish were taken and analyzed on board.

Filtered (0.2µm) and acidified (pH 1.8, 2ml/L 12M Baseline grade Seastar HCl) seawater was concentrated on a column containing aminodiacetid acid (IDA).This material binds only transition metals and not the interfering salts. After washing the column with ultrapure water, the column is eluted with diluted hydrochloric acid. After mixing with luminol, peroxide and ammonium, the oxidation of luminol with peroxide is catalyzed by iron and a blue light is produced and detected with a photon counter. The concentration of iron is calculated using a standard calibration line, where a known amount of iron is added to low iron containing seawater. Using this calibration line a number of counts per nM iron is obtained. Samples were analyzed in triplicate and average DFe concentrations and standard deviation are given. Concentrations of DFe measured during the JC057 cruise ranged from 17 pM in the oligotrophic surface waters up to 6 nM in the deep water and some surface areas. The standard deviation varied between 0% and 40% (the latter being exceptional), but was on average 2.9%. Since samples containing less than 0.06nM DFe values are near the detection limit of the system; the standard deviation of these measurements were higher than the average value. The average blank was determined at 0.019±0.017nM and was defined as a sample loaded for 5 seconds and measured daily. The average limit of detection was determined at 0.018±0.017nM and was defined as 3*standard deviation of the mean blank and measured daily. To better understand the day to day variation duplicate samples were reanalyzed the day after. The differences between these measurements were, in the order of

15%. To correct for this day to day variation a so-called lab standard sample was measured daily. All data will be corrected for the mean average of this value after the cruise and all data presented so far is uncorrected for this day to day variation. The consistency of the FIA system over the course of the day was verified using a drift standard. Drift has been observed and seemed to be variable from day to day. All data will be corrected for this daily drift after the cruise and all results so far are not corrected. A certified SAFe standard (*Johnson et al*. 2007) for the long term consistency and absolute accuracy was measured on a regular basis.

Preliminary results

Figure 17 shows a depth profile obtained during the cruise. Station 18 is a profile sampled at the end of the cruise near the equator. Low surface values and a minor subsurface maximum corresponding with the oxygen minimum zone. Elevated iron concentration around 2500 meters is most likely caused by hydrothermal activity.

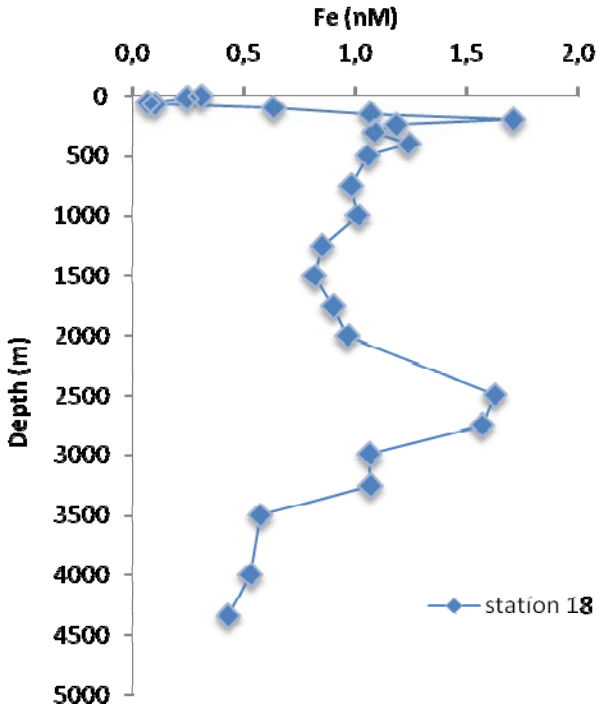

Figure 17. Depth profile of dissolved iron from station 18

References

Boyd, P. W., et al. (2000), A mesoscale phytoplankton bloom in the polar Southern Ocean stimulated by iron fertilization, *Nature*, *407*, 695–702, 2000

Bruland, K.W., N.M. Price, M.L. Wells (1995), Iron chemistry in seawater and its relationship to phytoplankton: a workshop report, *Marine Chemistry,48(1), 157-182*

De Baar, H.J.W., J.T.M. De Jong, D.C.E. Bakker, B.M. Löscher, C. Veth, U. Bathmann and V. Smetacek (1995), Importance of Iron for Phytoplankton Spring Blooms and CO2Drawdown in the Southern Ocean. *Nature*, 373: 412-415.

De Baar, H.J.W., J.T.M. De Jong (2001), Distributions, sources and sinks of iron in seawater. In: Turner, D., Hunter, K.A. (Eds.), Biogeochemistry of iron n seawater, IUPAC Book

De Baar, H.J.W., K.R. Timmermans, P. Laan , H.H. De Porto, S. Ober, J.J. Blom, M.C. Bakker, J. Schilling,G. Sarthou, M.G. Smit and M. Klunder (2008) Titan: A new facility for ultraclean sampling of trace elements and isotopes in the deep oceans in the international Geotraces program, Marine Chemistry, 2008.

De Jong, J.T.M, den Das, J. , Bathman, U., Stoll, M. H.C., Kattner, G., Nolting, R.F., and de Baar, H.J.W.(1998). Dissolved iron at subnanomolar levels in the Southern Ocean as determined by shipboard analysis. Analytica Chimica Acta, 377, 113-124.

Johnson et al., 2007. Developing standards for dissolved iron in Seawater. Eos, Vol 88, n. 11.

Martin, J. H., and R. Michael Gordon (1988), Northeast Pacific iron distributions in relation to phytoplankton productivity, *Deep Sea Research Part A. Oceanographic Research Papers*, 680 *35*(2), 177-196.

Middag, R., H. J. W. de Baar, P. Laan, and K. Bakker (2009), Dissolved aluminium and the silicon cycle in the Arctic Ocean, *Marine Chemistry*, *115*(3-4), 176-195.

Obata, H., Karatani, H., Nakayama, E., (1993). Automated determination of iron in seawater by chelating resin concentration and chemiluminescence. Analytical Chemistry 65, 1524–1528.

3.2.A.2. Size fractionation of iron

Micha J.A. Rijkenberg, Loes J.A. Gerringa, Patrick Laan

NIOZ

Introduction

Iron (Fe) is a critical nutrient for oceanic primary productivity. It's an important element in many proteins, enzymes and pigments. Due to its low solubility, Fe limits phytoplankton growth in large parts of the ocean (Martin and Fitzwater, 1988; de Baar et al. 1990). Notwithstanding its low solubility concentrations of dissolved Fe (DFe, < 0.2 μm) are higher than predicted by its solubility product alone and vary widely over the water column and across the surface ocean. This variation in DFe concentrations can be explained by i) the chemistry of Fe in the dissolved phase, ii) the proximity of Fe sources, and iii) biological processes (e.g. high DFe at the oxygen minimum).

DFe consists of several distinguishable and measurable fractions such as a truly soluble Fe fraction (Fe(III) and Fe(II)), a truly soluble organically complexed Fe fraction and a colloidal Fe fraction. These different size fractions are often defined by the pore size of the filters and may vary with study.

We used size fractionation (filters with 1000 kDa pore size) to investigate the distribution of the different size fractions of Fe over the water column, the interplay between these fractions, and the relation between relative differences in Fe concentration of the size fractions and environmental parameters such as the excess organic Fe-binding ligand concentration, oxygen etc.

Materials and methods

Filtered seawater (0.2 μm, Sartobran 300 cartridges) samples of different depths, representing the entire water column, were sampled from the ultraclean titanium CTD (de Baar et al. 2008). 1000 kDa hollow fiber filters (Mitsubishi) was used for further size fractionation. The 1000 kDa hollow fibre filters were pre-cleaned in the home laboratory with 10 ml quartz-distilled HCl (5 ml/min), 10 ml MQ water (5 ml/min), 60 ml HCl (Merck, suprapur) (20 ml/day), 210 ml MQ water (7 ml/min) followed by storage in 0.025% HCl (Merck, suprapur) until use. Before use the 1000 kDa hollow fibre filters were cleaned with 210 ml 0.05% HCl (Merck, suprapur) (7 ml/min), 210 ml MQ water (7 ml/min) and 210 ml sample (7 ml/min) before sample collection. Samples filtered with 1000 kDa hollow fibre filters were measured for DFe and organic Fe-binding ligand concentration (FeL).

Samples for ultra filtration

Samples for ultra filtration were taken at hyperstations (Table 3).

Table 3. Water column samples taken from the ultraclean titanium UC CTD at hyperstations

station	cast	bottles	filter	sampled for
2	1	1,2, 4, 6, 8, 10, 12, 14, 16, 18, 20, 23	1000 kDa	DFe & FeL
6	1	1,2, 4, 6, 8, 10, 12, 14, 16, 18, 20, 23	1000 kDa	DFe & FeL
12	1	1,2, 4, 6, 8, 10, 12, 14, 16, 18, 20, 23	1000 kDa	DFe & FeL
17	1	1,2, 4, 6, 8, 10, 12, 14, 16, 18, 20, 23	1000 kDa	DFe & FeL

Results

Preliminary data of station 17 shows that the < 1000 kDa Fe fraction is smaller or equal to the dissolved Fe (< 0.2 μm) fraction (Figure 18).

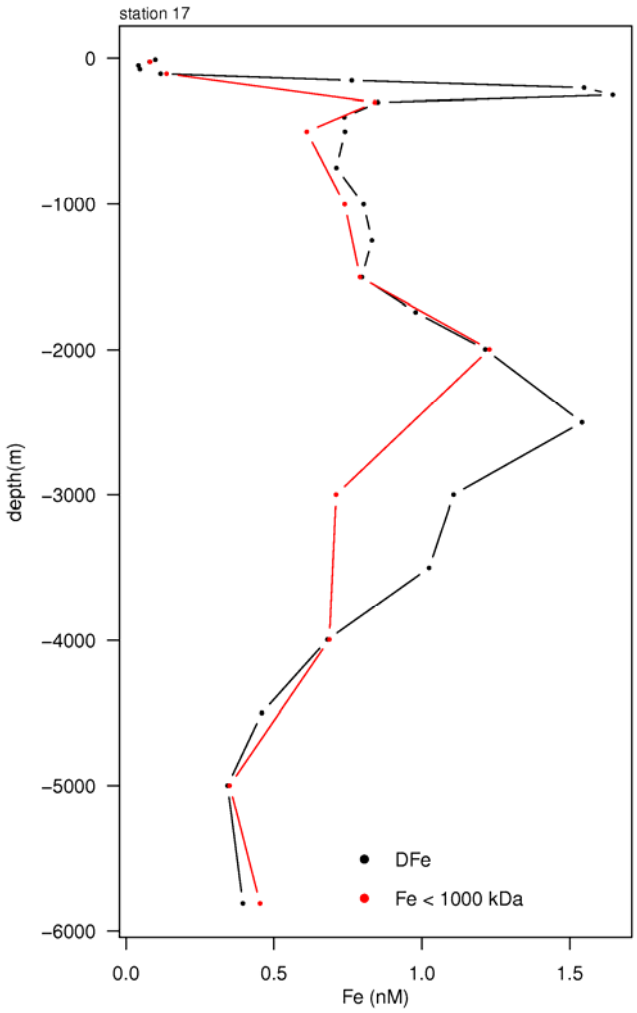

Figure 18. Dissolved Fe and < 1000 kDa Fe in the water column of station 17.

Acknowledgements

We want to thank Marc Sterken, Charles-Edouard Thuróczy, Maarten Klunder and Rob Middag for their help in the preparations for the cruise.

References

de Baar, H.J.W., K.R. Timmermans, P. Laan, H.H. De Porto, S. Ober, J.J. Blom, M.C. Bakker, J. Schilling, G. Sarthou, M.G. Smit and M. Klunder (2008) Titan: A new facility for ultraclean sampling of trace elements and isotopes in the deep oceans in the international Geotraces program, Marine Chemistry, 2008

de Baar, H.J.W., Buma, A.G.J., Nolting, R.F., Cadee, G.C., Jacques, G. and Treguer, P.J., 1990. On iron limitation of the Southern Ocean - experimental- observations in the Weddell and Scotia seas. Mar. Ecol. Progr. Ser., 65(2): 105-122.

Martin, J.H. and Fitzwater, S.E., 1988. Iron-deficiency limits phytoplankton growth in the northeast Pacific subarctic. Nature, 331(6154): 341-343.

3.2.A.3. Organic speciation of Fe

Loes Gerringa, Micha Rijkenberg and Patrick Laan

NIOZ

Introduction

Fe is an interesting element in the ocean and has been studied intensively because it is essential micronutrient for phytoplankton growth and the concentrations in seawater are extremely low. High Nutrient Low Chlorophyll (HNLC) regions in the oceans can partly be explained by a lack of Fe (de Baar et al, 1990, 1995; Johnson et al, 1997). Outside the HNLC regions Fe apparently is not limiting but still present in relatively low concentrations. The concentrations of Fe are so very low in seawater because the solubility product of the oxy-hydroxides of Fe is very low at the pH and oxygen concentrations of normal seawater (Liu and Millero, 2002). However, the dissolved Fe concentrations below the photic zone are higher than predicted by this solubility product. Since 1994 it is known that around 99% of dissolved Fe in seawater is bound to organic molecules that bind Fe very strongly (Geldhill and van den Berg, 1994). This so called organic complexation is important because it increases the solubility of Fe in seawater and enables concentrations above the solubility product. The binding by dissolved organic molecules, called ligands, prevents or at least retards precipitation of Fe as insoluble oxides. Organic complexation also influences the bioavailability of Fe. Part of the complexed Fe must be taken up by phytoplankton, although it is not quite clear how (Shaked et al., 2005, Salmon et al., 2006).

In order to study the distribution chemical species of Fe over the whole water depth the chemical speciation is determined in two different size fractions, the filtered <0.2 μm and the <1000 kDa fractions (Thuróczy et al., 2010, 2011). Special attention was given that distinct water masses present were sampled as well.

Methods

Samples were filtered (<0.2 μm or <1000 kDa).

Samples were collected by the UC CTD at stations 1, 2, 6, 8, 12, 15 and 17 and during transit samples were taken with a towed fish once or twice a day, preferably in the dark. The reason for the preference of dark sampling is to prevent variable conditions of photo-reduction of Fe and/or photo-oxidation of ligands. Different weather conditions and times of day could cause variations in the results that would not be connected to the geographical position of sampling.

These samples are complementary to samples that have been processed during the previous GEOTRACES Western Atlantic cruise leg 1 and leg 2 (64PE319 and 64PE321, respectively).

The analysis is so time consuming that not all analyses could be executed within the time limits of the cruise.. The remaining samples are frozen and will be analyzed in the NIOZ home laboratory. Since more samples than foreseen had to be frozen, there was a storage problem. This problem was solved by the Cook's cook Wilmot Isby. We are very grateful to him for allowing to store (untreated) filtered seawater in the galley freezers.

Analysis

The natural ligand characteristics were determined by doing a complexing ligand titration with addition of iron (between 0 and 8 nM of Fe added) in buffered seawater (mixed

NH_3/NH_4OH borate buffer, 5 mM). The competing ligand 'TAC' (2-(2-Thiazolylazo)-p-cresol) with a final concentration of 10 µM was used and the complex $(TAC)_2$-Fe was measured after equilibration (> 6 h) by cathodic stripping voltammetry (CSV) (Croot and Johansson, 2000). The electrical signal recorded with this method (nA) was converted as a concentration (nM), then the ligand concentration and the binding strength were estimated using the non-linear regression of the Langmuir isotherm (Gerringa and al., 1995).

The samples were stored at 4 ºC when analysis could be performed within three days after sampling, otherwise they were stored frozen (-20 ºC). When a sample was prepared for analysis of Fe speciation, always a separate sample for DFe was taken (30 ml). Patrick Laan and Lennart Groot analysed these (see section3.2.A.1, DFe).

Figure 19. The voltammetric equipment with in front the sample changer. The electrode stand is mounted in a NIOZ home-made aluminium frame on a wooden board that is hanging in elastic bands, preventing scans to be disturbed by motions of the ship. At the left is a sample that was taken to test the influence of bacterial activity on the characteristics of the ligands. The sample is kept in the laboratory at room temperature to stimulate bacterial activity.

The voltammetric equipment consisted of a µAutolab potentiostat (Type II, Ecochemie, The Netherlands), a mercury drop electrode (model VA 663 from Metrohm) and a sample changer. All equipment was protected against electrical noise by a current filter (Fortress 750, Best Power).

Tests

To investigate bacterial production of organic Fe-binding ligands a large volume of filtered seawater was sampled at station 17 bottle 21. It was filtered and kept at room temperature and sampled regularly during 1.5 week. DFe samples were taken and samples for bacterial counts. For bacterial counts 1 ml samples were taken, 30 µl of glutar-aldehyde was added. Next the sample was shaken and kept in the refrigerator for 30 minutes, after which they were put in liquid nitrogen for 5 minutes and stored at -80 ºC. Analysis will be done back at the NIOZ Laboratory in co-operation with Corina Brussaard and Claire Evans.

To investigate the effect of sampling and storing of filtered seawater in 1 L LDPE on the

organic complexation of Fe a sample was directly taken from the UCC bottles and compared to a sample as taken from the UUC bottles and subsequently stored in a 1 L LDPE bottle before analysis.

Results

Station 17 was analysed and some fish samples <0.2µm, but not yet calculated into the proper parameters: the ligand concentration and the conditional binding constant.

Bottle 21 from station 17 was kept in the laboratory at 20 ºC in the light. Two processes are expected to take place:

1. adsorption of Fe at the wall of the bottle. This is expected to be a relatively quick process in which the bottle wall and the Fe binding ligands get equilibrated with respect to Fe. Preliminary results of experiments from Rijkenberg, Gerringa and Laan during GEOTRACES leg 1, showed that after about 8 hours equilibrium is reached.

2. bacterial activity changes the character and possibly the concentration of the organic ligands.

Preliminary results indicate an increase in empty ligand sites. This increase was about 0.3 nM during 5 days and it was a steady increase. This can be explained in two ways, either Fe is lost to the bottle wall and thus creating more empty ligand sites or ligands are created out of organic material present. Since the increase in empty ligand sites was observed during days instead of hours, the last explanation seems the more plausible.

The test, whether transfer from the UC CTD bottles into 1 liter LDPE bottle influenced the speciation measurement, was executed three times. Adsorption of Fe to the bottle wall of the 1 L LDPE sampling bottle could be a disturbing factor of all measurements (see also section ultrafiltration of Fe). Thus far no influence could be detected of the 1L LDPE sample bottles.

References

Croot P.L., Johanson M., 2000. Determination of iron speciation by cathodic stripping voltammetry in seawater using the competing ligand 2-(2-Thiazolylazo)-p-cresol (TAC). Electroanalysis. 12, No.8, 565-576.

de Baar, H.J.W., Buma, A.G.J., Nolting, R.F., Cadee, G.C., Jacques, G., Tréguer, P.J., 1990. On iron limitation of the Southern Ocean: experimental observations in the Weddell and Scotia Seas. Mar. Ecol. Progress Ser. 65, 105–122.

de Baar, H.J.W., de Jong, J.T.M., Bakker, D.C.E., Löscher, B.M., Veth, C., Bathmann, U., Smetacek, V., 1995. Importance of iron for phytoplankton spring blooms and CO2 drawdown in the Southern Ocean. Nature 373, 412–415.

Gerringa, L.J.A., Herman, P.M.J., Poortvliet, T.C.W., 1995. Comparison of the linear Van den Berg/Ruzic transformation and a non-linear fit of the Langmuir isotherm applied to Cu speciation data in the estuarine environment. Mar. Chem., 48, 131-142.

Gledhill, M. and van den Berg, C.M.G., 1994. Determination of complexation of iron (III) with natural organic complexing ligands in seawater using cathodic stripping voltammetry. Mar. Chem., 47: 41-54.

Johnson, K.S., R. M Gordon, K. H. Coale, 1997. What controls dissolved iron concentrations in the world ocean? Marine Chemistry 57, 137-161

Liu, X., Millero, F.J., 2002. The solubility of iron in seawater. Mar. Chem. 77, 43-54.

Shaked, Y., Kustka, A.B., Morel, F.M.M., 2005. A general kinetic model for iron acquisition by eukaryotic phytoplankton. Limnol. Oceanogr. 50: 872–882.

Salmon, T.P., Andrew L. Rose, A.L., Neilan, B.A., Waite, T.D., 2006. The FeL model of iron acquisition: Non-dissociative reduction of ferric complexes in the marine environment. Limnol. Oceanogr., 51, 1744–1754

Thuróczy, C.-E., L.J.A. Gerringa, M. Klunder, P. Laan, H.J.W. de Baar, 2011. Organic complexation of dissolved iron in the Atlantic sector of the Southern Ocean. Accepted by Deep Sea Res. II

Thuróczy, C.-E., Gerringa, L.J.A., Klunder, M,. Middag, R., Laan, P., Timmermans, K.R. and H.J.W. de Baar, 2010. Speciation of Fe in the North East Atlantic Ocean. Deep Sea Res I, 57, 1444-1453.

3.2.A.4. Dissolved Al and Mn

Rob Middag

NIOZ, University of California Santa Cruz

Introduction

Dissolved Al is a trace metal with a scavenged-type distribution and an extreme difference between the extremely low concentrations in the North Pacific and the elevated concentrations in the North Atlantic; varying by greater than two orders-of-magnitude (Orians and Bruland, 1985). The distribution of dissolved Al in surface waters of the open ocean is influenced by atmospheric dust inputs (Measures et al., 2008) and variations in the intensity of removal by scavenging. The surface distribution of dissolved Al can potentially be a tracer of atmospheric Fe inputs. For Al there is no known biological function within the cell, but it has been shown Al is build into the siliceous frustules of diatoms (Gehlen et al., 2002). The incorporation of Al in the frustules decreases the solubility of the frustule (e.g. Van Bennekom et al., 1991, Gehlen et al., 2002), making the frustule more durable. Al is known to co-vary with Si, but this co-variance disappears with aging of the water masses and depends on the sources and sinks of both Al and Si (Middag et al., 2011).

Dissolved Mn is a trace metal with a scavenged-type distribution due the formation of insoluble oxides in oxygenated sea water and the distribution of Mn is strongly influenced by external inputs. Dissolved Mn can be a tracer of hydrothermal sources and of reducing sediment input. Like dissolved Al, the distribution of dissolved Mn can potentially provide insight into Fe inputs as Mn and Fe can come from the same sources. Dissolved Mn is a trace nutrient that has been suggested to become quite important for phytoplankton (especially diatoms) under low Fe conditions (Peers and Price, 2004; Middag et al., 2010).

Work at sea

Dissolved Al and dissolved Mn were measured directly using shipboard FIA measurements. In a continuous FIA system, the acidified pH 1.8, filtered (0.2 μm) seawater is buffered to pH 5.5 and 8.5 for Al and Mn, respectively. The metals are concentrated on a column which contains the chelating material aminodiacetid acid (IDA). This material binds only transition metals and not the interfering salts. After washing of the column with ultra pure water (MQ) the column is eluted with diluted acid.

The Al is determined using lumogallion after Brown and Bruland (2008). Lumogallion is a fluorometric agent and reacts with aluminum. The change in the fluorescence detected by a fluorometer is used as a measure for the dissolved Al concentration.

In order to verify the consistency of the analysis, every day a sample was measured from a check sample that was taken in the beginning of the cruise. Also a duplicate sample was taken every cast and this sample was analysed with the samples of the next cast to further check for inter daily variation. Furthermore, SAFe and GEOTRACES seawater samples were analysed daily and the values are consistent with those found previously.

The Mn is detected using the chemoluminescence method of Doi et al. 2004. The oxidation of luminol by hydrogen peroxide produces a blue light. This oxidation reaction is catalyzed by manganese and the increase in the production of blue light is detected by a photon counter and used as a measure for the dissolved Mn concentration.

Also for Mn similar consistency checks as for Al have been performed with samples from the check sample and duplicate samples. Also SAFe and GEOTRACES seawater was analysed which was consistent with the values found previously. The daily consistency of the system was verified using a so-called drift standard.

Preliminary results

Concentrations of Al were low in the surface waters near the Falkland Islands (~ 1.5 nM) and increased in the northward direction towards the equator with values up to ~20 nM. There was an mid depth minimum of Al around 1000 m depth (AAIW), followed by and increase with depth to a maximum around 3000 m (NADW). In the deepest bottom waters (AABW) concentrations of Al decreased again (see Figure 20).

Concentrations of Mn were elevated in the surface waters with concentrations up to 2 nM, except in the southernmost part of the transect. There, the surface concentrations of Mn were depleted (<0.1 nM), and followed by a subsurface maximum. With depth the concentrations of Mn decreased to low concentrations in the deep basin (see Figure 21). Lowest concentrations of Mn (~0.1 nM) were found in the deepest bottom waters. Elevated concentrations of Mn were found around 3000 m depth in the northernmost part of the transect, possibly of hydrothermal origin.

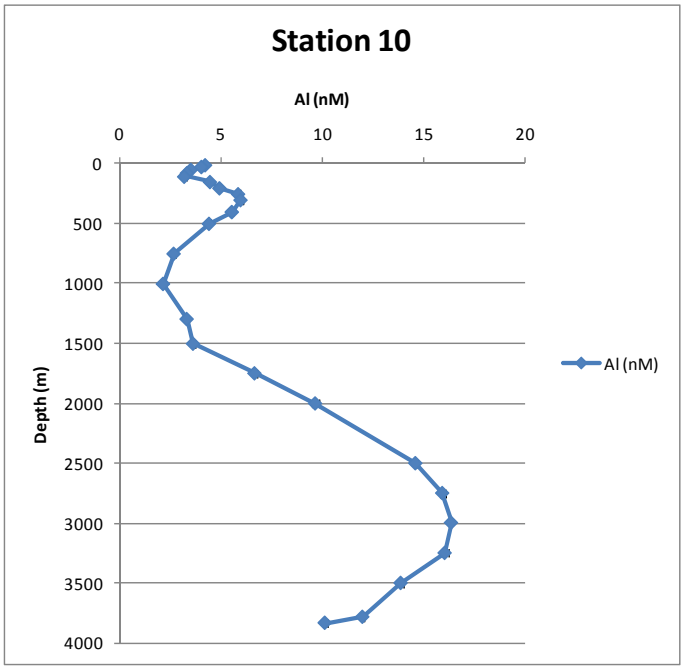

Figure 20. Dissolved Al (nM) versus depth (m) at station 10. Error bars representing standard deviation of triplicate measurement are not visible on this scale.

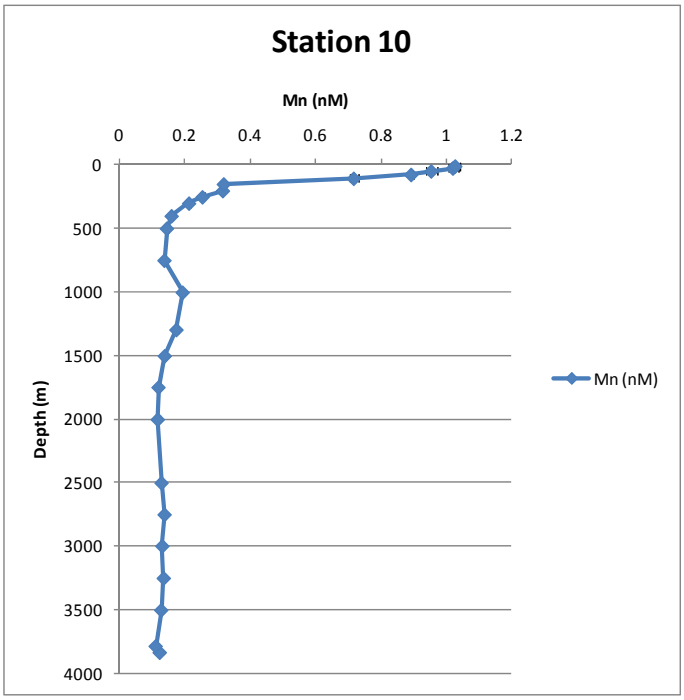

Figure 21. Dissolved Mn (nM) versus depth (m) at station 10. Error bars representing standard deviation of triplicate measurement are not visible on this scale.

References

Brown, M.T., Bruland, K.W., 2008. An improved flow-injection analysis method for the determination of dissolved aluminum in seawater. Limnology and Oceanography Methods 6, 87-95

Doi, T., Obata, H., Maruo, M., 2004. Shipboard analysis of picomolar levels of manganese in seawater by chelating resin concentration and chemiluminescence detection. Analytical and Bioanalytical Chemistry 378 (5), 1288-1293.

Gehlen, M., Beck, L., Calas, G. Flank, A.M., Van Bennekom, A.J., Van Beusekom, J.E.E., 2002. Unraveling the atomic structure of biogenic silica: Evidence of the structural association of Al and Si in diatom frustules. Geochimica et Cosmochimica Acta 66 (9), 1604-1609.

Measures, C.I., Landing, W.M., Brown, M.T., Buck, C.S. 2008. High-resolution Al and Fe data from the Atlantic Ocean CLIVAR-CO2 Repeat Hydrography A16N transect: Extensive linkages between atmospheric dust and upper ocean geochemistry. Global Biogeochemical Cycles 22, GB1005.

Middag, R., De Baar, H.J.W., Laan, P., Cai, P.H., Van Ooijen, J.C., 2010. Dissolved Manganese in the Atlantic section of the Southern Ocean, in press with *Deep-Sea Res. II,* doi:10.1016/j.dsr2.2010.10.043.

Middag, R., Van Slooten, C., De Baar, H.J.W., Laan, P., 2011. Dissolved Aluminium in the Southern Ocean, in press with *Deep-Sea Res. II,* doi:10.1016/ j.dsr2.2011.03.001

Orians, K.J., Bruland, K.W., 1985. Dissolved aluminum in the Central North Pacific. Nature 316 (6027), 427– 429.

Peers, G., Price, N.M., 2004. A role for manganese in superoxide dismutases and growth of iron-deficient diatoms. Limnology and Oceanography 49 (5), 1774–1783.

Van Bennekom, A.J., Buma, A.G.J., Nolting, R.F., 1991. Dissolved aluminium in the Weddell-Scotia Confluence and effect of Al on the dissolution kinetics of biogenic silica. Marine Chemistry 35 (1-4), 423-434.

3.2.A.5. Iron (Fe), zinc (Zn) and their stable isotopes in seawater of the southwest Atlantic Ocean.

Jeroen de Jong[1,2], Nadine Mattielli[2], Véronique Schoemann[1]

NIOZ[1], Université Libre de Bruxelles[2] (ULB)

Introduction

The availability of bio-essential trace metals such as Fe, Zn, Co, Cu and Mn may limit primary productivity and the associated uptake of carbon over large areas of the ocean. They play hence an important role in the carbon cycle, and changes in its supply to the surface ocean may have had a significant effect on atmospheric carbon dioxide concentrations over glacial–interglacial cycles (Martin, 1990).

Since recent years a continuing scientific effort was initiated by the development of sensitive multi-collector isotope dilution multi-collector inductively coupled mass spectrometry (ICP-MS) and Thermal Ionization MS (TIMS) techniques to expand isotope geochemistry research into the oceanic realm. Apart from the traditional isotopic systems (e.g. Pb, Nd, Sr and Hf) also the so-called non-traditional isotopes receive increased attention, in particular Li, B, Mg, Si, Ca, Fe, Cu, Zn, Mo, Ni, Cr and Cd. The idea is that biogeochemical

processes in the ocean interior leave distinct isotopic signatures, which may provide a means of tracking these processes. The first ocean profiles for Fe (Lacan et al., 2008), Cu and Zn (Bermin et al., 2006) were recently published.

During the GEOTRACES West Atlantic cruise leg 3 (JC-057) with RRS *James Cook*, samples were taken to study the evolution in the distribution and behavior of iron, zinc and their isotopes in seawater along a transect in the southwestern Atlantic. Results will be complementary to GEOTRACES West Atlantic cruises leg 1 and 2 (RV *Pelagia* cruises 64PE319 and 64PE321). On a south to north transect from Punta Arenas (Chile) to the northeast coast of Brazil, where leg 2 from Bermuda to Fortaleza (Brazil) ended, four full water column profiles (19 depths) were sampled for total dissolvable and dissolved iron, copper and zinc concentration measurement by Isotope Dilution MS (ID-MS), to provide new data for this ocean region for which only very few data exist. At each of these four stations, iron and zinc isotopic compositions at six selected depths (near-surface, chlorophyll-*a* maximum, oxygen minimum, deep water, bottom water – 50 m, bottom water), will be measured. This will hopefully shed some light on isotopic signatures of biological processes such autotrophic/heterotrophic uptake and remineralization; or a-biologic processes such as physical-chemically driven dissolution/precipitation processes associated with atmospheric input, organic complexation, oxygen minimum redox, sediment diffusion/resuspension. This sampling was coordinated with Cd, Ni and Cr isotopes, sampled for Wafa Abouchami and Steve Galer (Max Planck Institute Mainz, Germany).

Sampling for trace metal concentration measurement.

After finishing station work on the South Atlantic transect, fish samples were taken for total dissolvable (unfiltered) and dissolved (filtered) Fe, Cu and Zn concentrations while crossing the equatorial Atlantic from Brazil to the Cape Verde Islands. We expect to find an atmospheric input signal from the Sahara dust plume.

Water column samples were collected at four hyperstations from the extra UCC cast (Nos. 2, 6, 12 and 17) with the NIOZ 'Titan' ultraclean CTD ('UCC') (De Baar et al., 2008), Inside a class 100 clean air van, 250 mL sub-samples for total dissolvable (unfiltered) and dissolved (filtered) iron, copper and zinc concentrations were collected from each UCC sampler.

All samples were acidified to pH = 1.9 (1mL acid per liter of sample) with quartz-still subboiling triple-distilled ultrapure 14M nitric acid (HNO_3).

Sampling for iron isotopic ratio measurement

Seawater samples were directly filtered from the UCC samplers through 0.2 µm pore size 142mm diameter polycarbonate membrane filter in polycarbonate filtration units (GeoTech) in 20L Nalgene low density polyethylene carboys using about 0.5-1 bar N_2 overpressure. The filtrate was acidified to pH 1.9 and the filters stored at -20 °C.

Analytical methods

Trace metal concentrations. Fe, Cu and Zn concentrations will be measured in the home laboratory at ULB by multi-spike isotope dilution (MC-ICP-MS) using a Nu Plasma mass spectrometer. To this end, samples are amended with pure Fe-54, Cu-65 and Zn-68 spikes and ultraclean ammonium acetate buffer prior to simultaneous pre-concentration/separation on a resin with the NTA functional group (Lohan et al., 2005, de Jong et al., 2008).

Fe and Zn isotopic ratio measurement. Using the same Nu Plasma mass spectrometer, iron and zinc isotopic compositions of the dissolved phase will be measured after a newly developed lanthanum hydroxide co-precipitation technique (de Jong et al., in prep.), followed by purification of the sample by ion exchange chromatography with the BioRad AG-MP1 anion exchange resin For the determination of the Fe and Zn isotopic compositions of particulate matter, the polycarbonate filters will be acid-digested in a nitric acid/hydrofluoric acid/hydrogen peroxide digestion, and purified with the aforementioned resin as well (de Jong et al., 2007). Fe and Zn isotopic compositions will be determined by double-spike technique (Lacan et al., 2008, Bermin et al., 2006).

References

Bermin J., Vance D., Archer C., Statham P.J. (2006) The determination of the isotopic composition of Cu and Zn in seawater. *Chemical Geology* 226, 280– 297

de Baar H.J.W. et al. (2008) Titan: A new facility for ultraclean sampling of trace elements and isotopes in the deep oceans in the international Geotraces program. *Marine Chemistry* 111, 4–21.

de Jong J., Schoemann V., Tison J.-L., Becquevort S., Masson F., Lannuzel D., Petit J., Chou L., Weis D., Mattielli N. (2007) Precise measurement of Fe isotopes in marine samples by multi-collector inductively coupled plasma mass spectrometry (MC-ICP-MS). *Analytica Chimica Acta* 589, 105–119.

de Jong J., Schoemann V., Lannuzel D., Tison J.-L., Mattielli N. (2008) High-accuracy determination of iron in seawater by isotope dilution multiple collector inductively coupled plasma mass spectrometry (ID-MC-ICP-MS) using nitrilotriacetic acid chelating resin for pre-concentration and matrix separation. *Analytica Chimica Acta* 623 126–139.

de Jong J., V. Schoemann, H.J.W. de Baar and N. Mattielli (in preparation) Fe and Zn isotopes in seawater by double-spike MC-ICP-MS after lanthanum hydroxide coprecipitation and purification using AG-MP-1 anion exchange resin.

Lacan F., Radic A., Jeandel C., Poitrasson F., Sarthou G., Pradoux C., Freydier R. (2008) Measurement of the isotopic composition of dissolved iron in the open océan. Geophysical Research Letters 35, L24610, doi:10.1029/2008GL035841

Lohan M.C., Aguilar-Islas A.M., Franks R.P., Bruland K.W. (2005) Determination of iron and copper in seawater at pH 1.7 with a new commercially available chelating resin, NTA Superflow. *Analytica Chimica Acta* 530, 121–129.

Martin, J. H. (1990) Glacial-interglacial CO2 change: The iron hypothesis. *Paleoceanography* 5, 1–13.

3.2.A.6. The biogeochemical cycles of cobalt, zinc and cadmium in the South West Atlantic

Marie Boyé
Jonathan Dérot

Universitaire Européen de la Mer, Brest

1. Introduction and objectives

Cobalt (Co), zinc (Zn) and cadmium (Cd) are among the key trace metals highlighted in the GEOTRACES Science Plan. They are essential micronutrients, and they can drive the productivity and spatial distribution of specific taxa (Sunda and Huntsman, 1995; Saito *et al.,* 2002; Jakuba *et al.,* 2008). Furthermore the geochemical cycles of these elements have shown to be connected in the water column, through biochemical cambialistic substitutions (Saito *et al*., 2008; Lane *et al*., 2005; Roberts *et al*., 1997), which appear to be an important adaptation to life in ocean surface waters where these micronutrients are often depleted (Saito *et al*., 2010).

The internal cycle of Co within the oceans has been described by combining a nutrient-like cycling like that of major nutrient phosphate, with additional (versus P) removal of Co from deep waters by a scavenging removal term (Saito and Moffett, 2002; Saito *et al.,* 2010; Bown *et al*., in press) yet thus far the scarcity of field data of dissolved Co distributions prevents firm statements. By contrast the internal cycles of Zn and Cd are exclusively nutrient-like, especially, for Zn, resembling that of the major nutrient silicic acid (Lohan *et al*., 2002; Bruland, 1980; Martin *et al*., 1990; Ellwood, 2008) and of phosphate for Cd (de Baar et al., 1994; Saager et al., 1997; Ellwood, 2008). In the oligotrophic central Atlantic Co correlates with phosphate (Saito and Moffett, 2002) where the cobalt uptake relative to phosphate uptake is more than an order of magnitude higher in the surface waters than in the northeast Pacific but similar to that of zinc uptake relative to phosphate uptake in the northeast Pacific (Martin and Gordon, 1988; Martin *et al.*, 1989). This implies an increased biological importance of Co relative to Zn in the oligotrophic West Atlantic (Saito and Moffett, 2002). We hypothesize that the correlation between Co and P can be controlled by the concentration of and biological requirement for Zn in the West Atlantic. Furthermore the Cd uptake by phytoplankton and the particulate Cd:P ratios can both increase under Zn depletion or Fe limitation (Sunda and Huntsman, 2000; Cullen *et al*., 2006; Lane *et al*., 2008), which issue will be assessed in the South West Atlantic. In addition, the low solubility of Co may prevent its accumulation in deep water of the Pacific along the thermohaline circulation through the deep basins unlike the case for Zn and Cd. The Co cycle in the deep ocean can be controlled by the competition between its scavenging removal on settling particles and its stabilization in solution by the complexation with organic Co-binding ligands. In surface waters the organic complexation of cobalt may also serve to stabilize dissolved Co, preventing its microbial co-oxidation with manganese, an important removal pathway for cobalt in coastal environments (Moffett and Ho, 1996), and slowing down its scavenging process on settling particles. The internal processes of Co, Zn and Cd cycles furthermore include their interactions with particles that can act to scavenge metals (Co) from the upper ocean and/or to export these metals from the surface into biogenic particles, and to release them in deeper waters by remineralisation and possibly by desorption. The internal cycle of

these metals may interact with their external sources into the ocean when the particles are not biogenic or when biogenic particles incorporate the external signal. The origins and the potential for the metals interactions between the dissolved and particulate pool and the ratios metal:macro-nutrients in both pools will thus be investigated in collaborations for the use of tracers of particles sources and export fluxes. Among the potential external sources of these metals along the section, the natural dust inputs from Patagonia may be a significant source in surface waters, especially for Zn which is much more soluble in seawater when incorporated in crustal particles rather that in anthropogenic particles (Thuróczy et al., 2010). The transportation from rivers, continental shelf and slope waters towards the open ocean can be an additional external source along the section. For instance inputs of dissolved Co from the margins of South Africa with lateral advection of enriched intermediate and deep waters to the southeastern Atlantic Ocean, as well as advection from the Drake Passage and the southwestern Atlantic to the 0° meridian have recently been evidenced (Bown et al., in press). The deep section will also reveal internal processes of the Co cycle such as remineralisation and scavenging, as well as external inputs by reductive dissolution within sediment and diffusion into overlying bottom waters. Bottom enrichment of DCo in the Antarctic Bottom Waters was also evidenced, together with increasing water-mass pathway and ageing, possibly due to sediment resuspension and/or mixing with North Atlantic Deep waters (Bown et al., in press). Finally the concentrations in the well characterized water masses crossed along the section, such as NADW, SACW, AAIW, AABW, will be determined and compared to their levels in the source region of these waters. This will reveal Co, Zn and Cd dynamics over water-masses transportation in deep oceans. For example, southward increase of Cd may occur in the deep East Atlantic (Yeats et al., 1995), and input of low Cd:P ratio waters from the Antarctic via the northward flowing Antarctic Intermediate Water has not been observed in the Atlantic (Yeats, 1998).

2. Field work

Sampling of trace metals Cobalt, zinc and cadmium were sampled in the waters using the ultraclean sampling facilities of NIOZ for trace metals and several other variables, with ultraclean 24 large volume (27 L) samplers on TITAN frame with CTD and other sensors for oxygen, light transmission (inverse for particles abundance), and clean container holding the TITAN frame.

Dissolved metals were sampled at the deep 18 hydrocasts achieved along the section from Punta Arenas to the Equator. Unfiltered samples later used to estimate particulate metals concentrations (as the difference between unfiltered and filtered fractions) and filtered samples to determine the organic speciation of cobalt were sampled at 12 hydrocasts. The vertical resolution for these paramaters was 16 depths throughout the whole water column.

Furthermore 18 filtered and 18 unfiltered samples were samples underway using the fish during the transit back between north of the Equator and near Cape Verde.

Analyses of dissolved and total cobalt and its dissolved organic speciation Dissolved cobalt was measured on board by Marie Boye at 8 deep casts in filtered (0.2 microm), acidified (pH~1.9-2) and UV-digested samples by FIA-Chemiluminescence method with toyopearl preconcentrating column and acidified ammonium acetate (pH 4) as a column conditioning step prior to the sample loading and the rinse steps, following the method adapted by Shelley et al., 2010 (Bown et al., in press). Concentrations were estimated by two daily calibrations made at the start and the end of a serie of samples. The accuracy of the

method was evaluated by determining dissolved cobalt in acidified North Pacific deep and surface seawater samples from the Sampling and Analysis of Iron (SAFe) program. The method yields mean values of 2 ± 0.2 pM in surface and 24.3 ± 3 pM in deep which is in excellent agreement with the SAFe consensus values of 2.7 ± 1.3 pM and 26.9 ± 4.7 pM, in surface and deep reference waters respectively. Total dissolvable cobalt will be analysed in the unfiltered, acidified and UV-digested samples within the 1-2 coming years in the home lab by FIA-Chemiluminescence method (Bown et al., in press). The organic speciation of Co will be measured in the home lab in filtered (0.2 microm) and frozen-stored samples (-20°C) by Cathodic Stripping Voltammetry after Ellwood *et al.* (2005 ; 2001).

Analyses of dissolved and total zinc and cadmium Total and dissolved zinc and cadmium are measured simultaneously respectively in unfiltered and in filtered (0.2 microm) samples, after acidification (pH<1.8) by voltammetry method (Zn: Ellwood and van den Berg, 2000, Jakuba *et al*., 2008; Cd: Bruland, 1992, Ellwood, 2004). Successful analyses using these adapted methods were achieved in samples collected in the Southern Ocean at the home-lab. Dissolved zinc and cadmium were analysed on board by Jonathan Derot at 2 deep casts in the acidified samples without any added reagents using HMDE Anodic Stripping Voltammetry. Square wave was used with a scan rate of 148.5 mV, using a deposition potential of -1.4 V during 800 sec, a frequency of 30 Hz, and a scan in potential between -1.4 V and -0.4 V. Zinc was detected at the potential of -1 V and Cd at -0.6 V. The concentrations of Zn and Cd were calibrated against standards added into the samples at Zn concentrations of 3nM and 10 nM; and Cd of 1 nM and 3 nM. The accuracy of the method was verified using certified D2 SAFe standard of recently dispatched values for Zn and Cd. The method yields mean values of 7.47 nM for Zn and 1020 pM for Cd in deep waters which compare well with the SAFe consensus values of 7.19 ± 0.70 nM for Zn and 992 ± 35 pM for Cd in deep D2 reference water. The analyses at the HYPER stations will be completed right after the cruise in the home-lab, whereas the analyses of dissolved Zn and Cd at the other stations will be completed in the coming year in the home-lab. The concentrations of total Zn and Cd will be analysed at least 1 year after the sample collection and will be achieved in the home-lab, using voltammetry method.

3. Preliminary results

Dissolved cobalt Dissolved cobalt (DCo) distribution were much lower in the euphotic layer of the oligotrophic area (e.g., stations 8 and 12; Figure 22) compared to the southern part of the section (st 2, Figure 22), probably due to higher biological uptake. For instance cyanobacteria which often dominate the picophytoplankton assemblage in oligotrophic regions have an absolute cobalt requirement for growth (Saito et al., 2002). Biological uptake by cyanobacteria can be the dominant removal mechanism for cobalt in these regions (Saito and Moffett, 2001; Bown et al., in press). There were no clear meridional trend of DCo in the core of the SACW (Figure 22), but it should be further addressed using a larger space-scale.

The distribution of DCo at depth showed a small increase within the core of the UCDW which are marked by relative low dissolved oxygen content, although the concentrations can be in the same range than those recorded at intermediate depths in the AAIW (Figure 22). Furthermore the concentration of DCo may increase northward in the cores of UCDW and AAIW (Figure 22), suggesting additional sources of DCo along the water-masses transit such as lateral advection of Co-enriched waters at those depths and/or remineralisation processes in the water-column.

In the core of NADW, DCo was relatively high at depth at st 8 and 12 (about 70 pM; Figure 22). Comparison with preliminary data recorded in this water-mass further north (50 pM between Bermuda and Fortaleza; Boye, 2010) suggests an enrichment in DCo along its southward transit in the West Atlantic. However the signal was lost in the southern part of the section (st 2; Figure 22), probably due to mixing with UCDW waters which dispatched low DCo there (Figure 22).

In bottom waters the concentrations of DCo can be generally higher in the nepheloid layer than that at the sediment interface (data not shown), suggesting that the bottom sediments can be a source of DCo probably after dissolution of the benthic particles in the deepest waters. The concentrations of DCo in the AABW were lower than in overlying deep waters, generally <10-15 pM. Comparing with the higher concentrations recorded in AABW further north between Bermuda and Fortaleza (20 pM; Boye, 2010), it is suggested that bottom sediments could indeed be a source of DCo in the bottom waters along their northward transit.

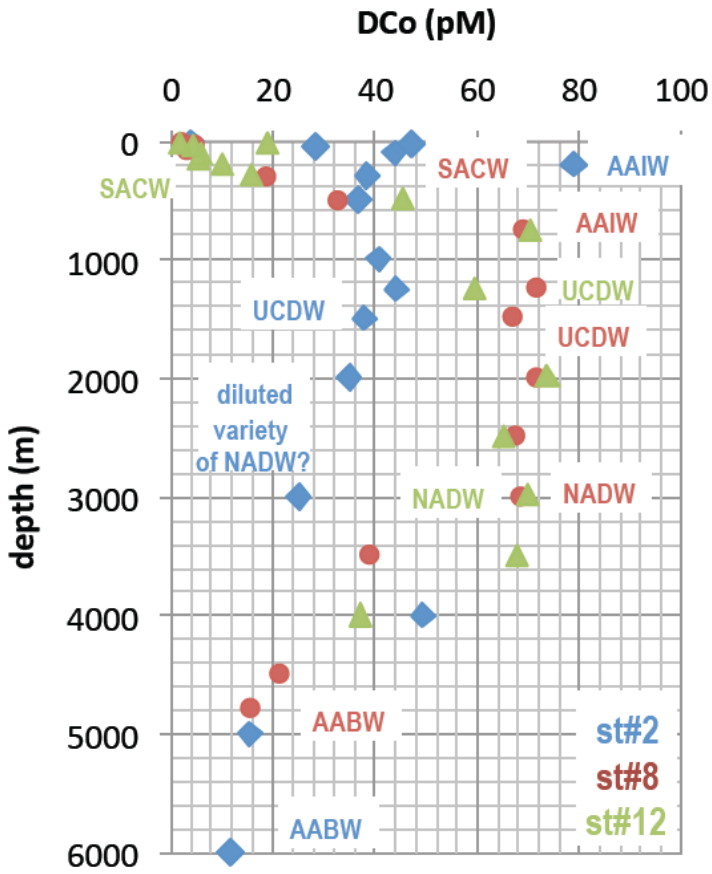

Figure 22- *Distribution at depth of dissolved cobalt (DCo) at stations 2-8 and 12. The water-masses are indicated for each station (SACW: South Atlantic Central Water, AAIW: Antarctic Intermediate Waters, UCDW: Upper Circumpolar Deep Waters, NADW: North Atlantic Deep Waters, AABW: Antarctic Bottom Waters).*

Dissolved zinc and cadmium

Preliminary results obtained at station 2 show low surface concentrations of Zn and Cd within the maximum of Chl-a (Figures 23, 24) due to the biological removal, possibly by enzymatic synthesis. The concentration in the shallowest water mass was higher than just below which can be interpreted as atmospheric deposition of these metals in surface waters at Station#2 (Figures 23, 24). Below the euphotic zone the concentrations of zinc and cadmium increase, which is possibly due to the reminalization process. In the depth of 1500 meters metals concentrations display relative maxima in the core of the Upper Circumpolar Deep Waters (Figures 23, 24). In the deepest waters below 4000 m cadmium concentration increases towards the bottom, whereas the zinc concentration is rather constant. Only a few data point makes it difficult to see a potential role of bottom sediment resuspension.

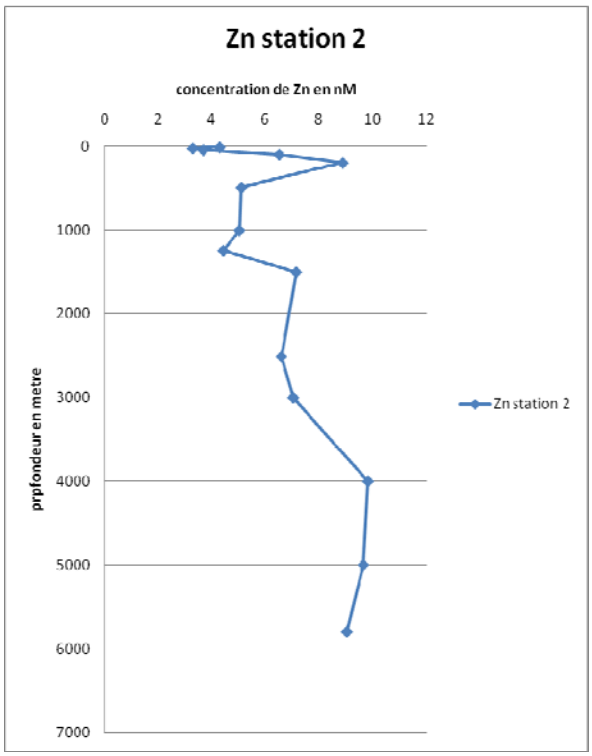

Figure 23- *Distribution at depth of dissolved zinc (DZn) at station 2.*

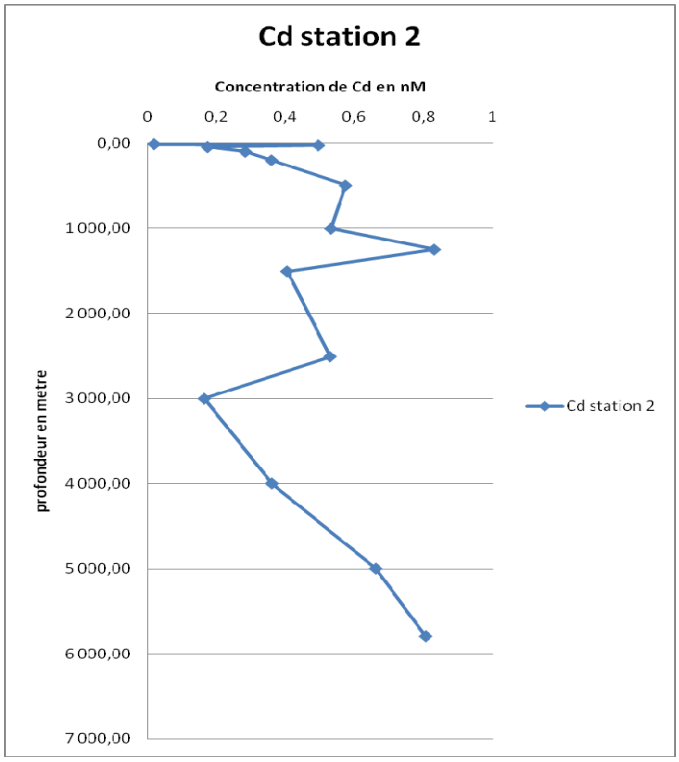

Figure 24*- Distribution at depth of dissolved cadmium (DCd) at station 2.*

References

Bown J., M. Boye, A. Baker, E. Duvieilbourg, F. Lacan, F. Le Moigne, F. Planchon, S. Speich, D.M. Nelson (in press). The biogeochemical cycle of dissolved cobalt in the Atlantic and the Southern Ocean south off the coast of South Africa. Marine Chemistry, in press.

Boye, 2010. The cobalt cycle in the North West Atlantic. Pelagia 64PE321 cruise report, Dutch GEOTRACES program in the West Atlantic, Edited by NIOZ.

Bruland, K.W., 1980. Oceanographic distributions of cadmium, zinc, nickel and copper in the North Pacific, Earth Planet. Sci. Lett., 47, 176–198.

Bruland, K.W., 1992. Complexation of cadmium by natural organic ligands in the central North Pacific. Limnol. Oceanogr. 37, 1008-1017.

Cullen, J. T., 2006. On the nonlinear relationship between dissolved cadmium and phosphate in the modern global ocean: could chronic iron limitation of phytoplankton growth cause the kink? Limnol. Oceanogr., 51, 1369–1380.

de Baar, H. J. W., Saager, P. M., Nolting, R. F., and van der Meer, J, 1994.: Cadmium versus phosphate in the world ocean, Mar. Chem., 46, 261–281.

Ellwood, M.J., 2004. Zinc and cadmium speciation in subantarctic waters east of New Zealand. Marine Chemistry 87, 37-58.

Ellwood, M.J., C.M.G. van den Berg, 2000. Zinc speciation in the northeastern Atlantic Ocean, Mar. Chem., 68, 295– 306.

Ellwood and van den Berg, 2001. Determination of organic complexation of cobalt in seawater by cathodic stripping voltammetry. *Marine Chemistry*, 75, 33-47.

Ellwood, van den Berg, Boye *et al.,* 2005. Organic complexation of cobalt across the Antarctic polar front in the Southern Ocean. *Marine and Freshwater Research*, 56, 1069-1075.

Ellwood, 2008. Wintertime trace metals (Zn, Cu, Ni, Cd, Pb and Co) and nutrient distributions in the Subantarctic Zone between 40-52°S; 155-160°E. Marine Chemistry, 112(1-2): 107-117.

Jakuba, R.W., Moffett, J.W. and 860 Dyhrman, S.T., 2008. Evidence for the linked biogeochemical cycling of zinc, cobalt, and phosphorus in the western North Atlantic Ocean. Global Biogeochemical Cycles, 22(4).

Lane, T. W., Saito, M. A., George, G. N., Pickering, I. J., Prince, R. C., and Morel, F. M. M., 2005. A cadmium enzyme from a marine diatom, Nature, 435, 42,.

Lane, E. S., Jang, K., Cullen, J. T., and Maldonado, M. T., 2008. The interaction between inorganic iron and cadmium uptake in the marine diatom *Thalassiosira oceanica*, Limnol. Oceanogr., 53, 1784–1789.

Lohan M.C., Statham P.J. and Crawford D.W., 2002. Total dissolved zinc in the upper water column of the subarctic North East Pacific. Deep Sea Res. II 49, 5793-5808.

Martin and Gordon, 1988. Northeast Pacific iron distribution in relation to phytoplankton productivity. *Deep-Sea Res.* 35, 177–196.

Martin *et al*., 1989. VERTEX: Phytoplankton/iron studies in the Gulf of Alaska. *Deep-Sea Res.* 36, 649 – 680.

Martin J.H., 1990. Glacial-interglacial CO_2 change: the iron hypothesis. *Paleoceanography*, 5: 1-13.

Moffett and Ho, 1996. Oxidation of cobalt and manganese in seawater via a common microbially catalyzed pathway. *Geochim. Cosmochim. Acta* 60, 3415–3424

Roberts, S., Lane, T., and Morel, F. M. M., 1997. Carbonic anhydrase in the marine diatom *Thalassiosira weissflogii* (*Bacillariophyceae*), J. Phycol., 33, 845–850.

Saager et al., 1997; Saager P.M., H.J.W. de Baar, J.T.M. de Jong, R.F. Nolting, J. Schijf, 1997. Hydrography and local sources of dissolved trace metals Mn, Ni, Cu, and Cd in the northeast Atlantic Ocean. *Marine Chemistry 57, 195-216.*

Saito and Moffett, 2001. Complexation of cobalt by natural organic ligands in the Sargasso Sea as determined by a new high-sensitivity electrochemical cobalt speciation method suitable for open ocean work. *Mar. Chem.* 75, 49 – 68.

Saito and Moffett, 2002. Temporal and spatial variability of cobalt in the Atlantic Ocean. *Geochimica et Cosmochimica Acta*, 66, 1943–1953.

Saito, M.A. and Goepfert, T.J., 2008. Zinc-cobalt colimitation of Phaeocystis antarctica. Limnology and Oceanography, 53(1): 266-275.

Saito, M.A., Goepfert, T.J., Noble, A.E., Bertrand, E.M., Sedwick, P. and DiTullio, G.R., 2010. Seasonal study of dissolved cobalt in the Ross Sea, Antarctica: micronutrient behavior, absence of scavenging, and relationships with Zn, Cd, and P. Biogeosciences Discussion 7, 6387–6439, 2010

Shelley, R.U., Zachhuber, B., Sedwick, P.N., Worsfold, P.J. and Lohan, M.C., 2010. Determination of total dissolved cobalt in UV-irradiated seawater using flow injection with chemiluminescence detection. Limnology and Oceanography: Methods., 8: 352-362.

Sunda, W.G. and Huntsman, S.A., 1995. Cobalt and zinc interreplacement in marine phytoplankton: Biological and geochemical implications. Limnology and Oceanography, 40(8): 1404-1417.

Sunda, W. G. and Huntsman, S. A., 2000. Effect of Zn, Mn, and Fe on Cd accumulation in

phytoplankton: implications for oceanic Cd cycling, Limnol. Oceanogr., 45, 1501–1516.
Thuróczy, C.E., Boye, M. and Losno, R., 2010. Dissolution of cobalt and zinc from natural and anthropogenic dusts in seawater. Biogeosciences, 7(6): 1927-1936.
Yeats P. A., S. Westerlund, A. R. Flegal, 1995. Cadmium, copper and nickel distributions at four stations in the eastern central and south Atlantic. *Marine Chemistry*, *49, 283-293*
Yeats P. A., 1998. An isopycnal analysis of cadmium distributions in the Atlantic Ocean. *Marine Chemistry 61, 15-23.*

3.2.A.7. Dissolved and particulate thorium-234 (^{234}Th)

Stephanie Owens, Ken Buesseler, Steve Pike

Woods Hole Oceanographic Institution, Woods Hole, MA USA

Overview

Thorium-234 is a tracer used for determining organic carbon export from the surface ocean and understanding particle dynamics on the time scale of days-weeks. The ^{238}U/^{234}Th disequilibrium method takes advantage of the contrasting chemical behavior of uranium and thorium in seawater (Buesseler, 1992). At pH values and CO_2 concentrations typical of oxic seawater, the predominant uranium species, U(IV), is highly soluble and occurs as a stable carbonate ion complex, $UO_2(CO_3)_3^{4-}$. In contrast, Th(IV), the stable ion of thorium under oxic conditions, is highly particle reactive (Santschi et al, 2006). At 4.47×10^9 years, the half-life of ^{238}U greatly exceeds the 24.1 day half-life of its daughter, ^{234}Th. Due to the large difference in the half-lives of this parent-daughter pair, when there are no external forces adding or removing either of the two isotopes from the system, ^{238}U and ^{234}Th can achieve a state of secular equilibrium. At secular equilibrium, the activity of ^{234}Th is equal to the activity of ^{238}U in the system. In the surface ocean, a deficit of ^{234}Th (relative to ^{238}U) occurs when ^{234}Th sorbs to particulate matter and is removed as that material sinks. An excess of ^{234}Th can occur when dissolution or remineralization of sinking particles occurs, releasing ^{234}Th into solution deeper in the water column. By integrating over the depth of the surface deficit, a ^{234}Th flux can be calculated which can be converted to a POC flux by multiplying by the POC/^{234}Th ratio on sinking particles. Due to its conservative behavior in seawater, the activity of uranium is typically derived from salinity.

Work at Sea

All sample processing and preliminary sample analysis by beta counting was completed on board, a requirement because of the short half-life of ^{234}Th (24.1 days). ^{234}Th was determined using the 4 L method of co-precipitating ^{234}Th with MnO_2 and beta counting the samples on low background, coincidence detectors (Risø National Laboratories; Benitez-Nelson, et al. 2001; Buesseler et al., 2001). On this cruise, 13-point profiles in the upper 1000 m were collected at each regular/super-station and 24-point profiles with additional samples for replicates were collected at each hyperstation (#2,6,12,17) for a total of 285 "total" or unfiltered ^{234}Th samples. All samples were collected from the UCC sampling system immediately after sampling for gases. Small volume (20 mL) archive samples for ^{238}U were also collected with each ^{234}Th sample. After collection, all ^{234}Th samples are acidified with concentrated nitric acid and spiked with a ^{230}Th tracer that will be used to determine the amount of ^{234}Th recovered by the method. Samples are allowed to equilibrate for 8 hours after which concentrated ammonium hydroxide is used to raise the pH to between and 8 and

9. A MnO_2 precipitate is formed with the addition of $KMnO_4$ and $MnCl_2$ and the samples are allowed to sit for a further 8 hours. The precipitate of each sample is then collected on a QMA filter and dried in an over for at least 12 hours. Samples are prepared for beta counting by covering them with a single layer of Mylar and a double layer of aluminum foil to prevent any low energy beta emissions. Detector efficiency and background were determined at the beginning and the conclusion of the cruise. Samples are counted twice for 12 hours each.

Samples for particulate ^{234}Th and organic carbon were collected using *in situ* McLane filtration pumps. Three pumps were deployed at depths of (50-200m) at stations 2, 6, 9, 12, 14, and 17. Depths were chosen so that the shallowest pump was at or below the deep chlorophyll maximum and so that pump depths matched depths sampled by the UCC and CTD. Pumps filtered on average 450 L during an hour period and particles were collected on a 53 µm mesh screen. These samples were subsequently rinsed onto Ag filters and counted for ^{234}Th as described above for total samples.

Preliminary Results

Figure 25 below shows data only from the upper 300 m across the 18 stations sampled. Before completion of final background counts and determination of sample recoveries, the average estimated uncertainty on these values is less than 1%. ^{234}Th and ^{238}U are in equilibrium at ~2.47 dpm/L, so in this contour plot areas of purple and blue in the surface are below equilibrium and green regions are at equilibrium. The surface deficit appears highest in the first 5 stations, meaning that particulate organic carbon export is highest at these stations. In the subtropical waters, there is little to no export, while export seems to increase slightly closer to the equator. Back in the lab, after ~5 months, samples will be counted for final background counts and sample recoveries will be determined using ICP-MS. Particulate samples will be analyzed for organic carbon content.

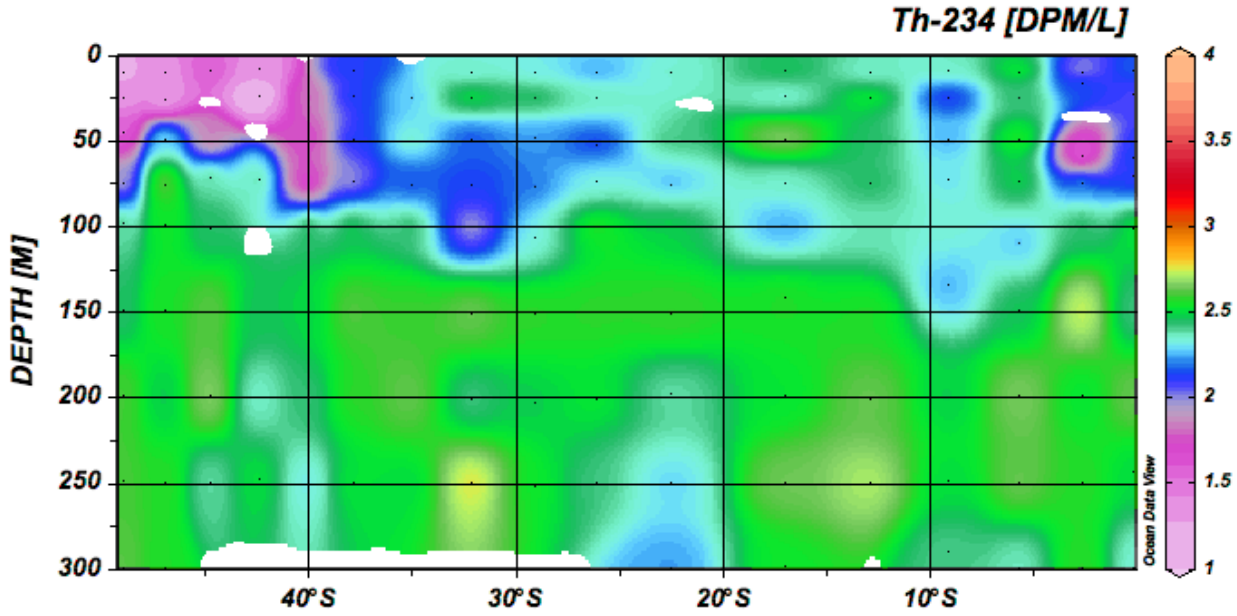

Figure 25: ^{234}Th distribution at 18 stations from 52°S to 0° in the Atlantic Ocean in the upper 300 meters. Blue/purple areas are below equilibrium while green/yellow areas are at or slightly above equilibrium.

References

Benitez-Nelson, C., Buesseler, K.O., Rutgers van der Loeff, M., Andrews, J., Ball, L., Crossin, G., Charette, M., 2001. Testing a new small-volume technique for determining thorium-234 in seawater. Journal of Radioanalytical and Nuclear Chemistry 248(3), 795-799.

Buesseler, K.O., Bacon, M.P., Cochran, J.K., Livingston, H.D., 1992. Carbon and nitrogen export during the JGOFS North Atlantic Bloom Experiment estimated from ^{234}Th:^{238}U disequilibria. Deep-Sea Research I 39(7-8), 1115-1137.

Buesseler, K. O., C. Benitez-Nelson, Rutgers van der Loeff, M., Andrews, J., Ball, L., Crossin, G., Charette, M., 2001. An intercomparison of small- and large-volume techniques for thorium-234 in seawater. Marine Chemistry, 74, 15-28.

Santschi, P. H., J. W. Murray, M. Baskaran, C. R. Benitez-Nelson, L. D. Guo, C.-C. Hung, C. Lamborg, S. B. Moran, U. Passow, Roy-Barman, M., 2006. Thorium speciation in seawater. Marine Chemistry 100: 250-268.

3.2.A.8. Lead concentrations and isotopes

Dominik Weiss

Imperial College London

Background

Emerging economies including Brazil and Mexico are likely to affect the global environment by their rapid industrial and population growth combined with poor air emission control in a similar way Northern America and Europe did in the last century (Reuer and Weiss, 2002). To date, however, studies assessing this possible impact are largely missing. This hinders the development of globally coordinated abetment policies.

Previous work pioneered by Clair Patterson and Ed Boyle in the Northern Hemisphere showed that lead concentration and isotope ratio measurements in the open ocean have the great potential (i) to act as sensitive gauges of impact that pollution has on the global environmental health and (ii) to identify major pollution sources (Schaule and Patterson, 1981; Wu and Boyle, 1997). Weiss and co workers used consequently Pb isotope and concentration measurements to suggest that during the 1980's, a shift occurred in the sources of anthropogenic pollution in the western Northern Atlantic (Weiss et al., 2003), with Mexico now likely a new major pollutant.

Aim and objectives

The Northern and Southern Atlantic basins are surrounded by major developing economies (i.e., Mexico, Brazil, and South Africa) and by two of the biggest urban conglomerates of the world, i.e. the Mexico City and the São Paulo Metropolitan Area, the latter being the largest and most industrialized area in South America with about 19.2 million inhabitants.

The aim of this study is to use Pb concentrations and isotope ratios measured in the open ocean to assess the extent of large range pollution caused by the growing economies in Northern (Leg 2) and Southern America (Leg 3). This is achieved by measuring the spatial development of Pb concentrations and isotope ratios along a surface water transect from Punta

Arenas to the Bermudas and gauging the temporal evolution by assessing depth profiles at selected stations.

Sampling during the cruise

During Leg 3, we collected 18 unfiltered surface water samples (2 l) using the fish at each station of the transect (i.e., 18 stations between Punta Arenas and the equator) and 10 depth samples/profile (2 l) at 4 stations using the UCC, namely stations 3, 7, 11, and 16. The samples collected along the depth profiles were chosen (i) to gauge the transition from polluted surface waters to unpolluted abyssal waters and (ii) to coincide with the major water masses. After collection, the samples were acidified using 2 ml/l 6 M HCl and double packed in plastic bags. At station 18, we collected in addition 3 x 10 l deep-sea water for method development and on the travel to Gran Canarias 1 x 10 l surface water samples.

Post cruise analysis

The collected samples will be analysed back at Imperial College London using electrochemical techniques (Weiss et al., 1999) for concentrations and mass spectrometry (Weiss et al., 2000) for isotope ratios.

References

Reuer, M.K., and Weiss, D.J., 2002, Anthropogenic lead dynamics in the terrestrial and marine environment: Phil. Trans. R. Soc. Lond. - Serie A, v. 360, p. 2889-2904.

Schaule, B.K., and Patterson, C.C., 1981, Lead concentrations in the north-east Pacific: evidence for global anthropogenic perturbations: Earth. Planet. Sci. Lett., v. 54, p. 97-116.

Weiss, D., Chavagnac, V., Boyle, E.A., Wu, J.F., and Herwegh, M., 2000, Determination of lead isotope ratios in seawater by quadrupole inductively coupled plasma mass spectrometry after $Mg(OH)_2$ co-precipitation: Spectrochim. Acta, B, v. 55, p. 363-374.

Weiss, D., Shotyk, W., Schäfer, J., Loyall, U., Grollimund, E., and Gloor, M., 1999, Microwave digestion of ancient peat and Pb determination by voltammetry: Fresenius J. Anal. Chem., v. 363, p. 300-305.

Weiss, D.J., Boyle, E.A., Chavagnac, V., Wu, J., Michel, A., and Reuer, M., 2003, Lead isotope evolution of the North Atlantic: pattern of deposition and source assessment: J. Geophys. Res., v. 108, p. 3306 doi:10.1029/2000JC000762.

Wu, J., and Boyle, E.A., 1997, Lead in the western North Atlantic Ocean: Completed response to leaded gasoline phaseout: Geochim. Cosmochim. Acta, v. 61, p. 3279-3283.

3.2.A.9. ^{231}Pa and ^{230}Th in the southwest Atlantic Ocean

Feifei Deng

Oxford University

Introduction

Naturally occurring ^{231}Pa (half-life 32.5 kyr) and ^{230}Th (half-life 75.2 kyr) are produced in seawater through the α-decay of dissolved ^{235}U and ^{234}U, respectively. Since uranium in seawater is uniformly distributed spatially and temporally, ^{231}Pa and ^{230}Th are produced in water column at a constant production ratio of 0.093.

Dissolved ^{231}Pa and ^{230}Th are removed from the water column through scavenging by falling particles and subsequent burial in sediments. ^{230}Th is more insoluble with an oceanic residence time of approximately 20~40 yrs with respect to the sediments [McManus et al., 2004]. Thus, ^{230}Th is removed from seawater effectively so that its rain to the seafloor is largely independent of particle flux, and approximately equal to its rate of production by decay of ^{234}U in the overlying water column. In contrast, less insoluble ^{231}Pa has a longer residence time of approximately 100~200 yrs (McManus et al., 2004), which permits more extensive lateral redistribution, than for ^{230}Th, from regions of low scavenging intensity to regions of high scavenging intensity prior to its removal from the water column.

Based on this fractionation of ^{231}Pa from ^{230}Th, ^{231}Pa/ ^{230}Th ratio can be used to reconstruct the rate of past deep-ocean circulation. When these nuclides form from Uranium decay, the short residence time of ^{230}Th does not allow it to be advected far before it is removed to the sediment. The longer residence time of ^{231}Pa, on the other hand, allows it to be advected so that, if the water mass is moving, ^{231}Pa may be transported downstream to be removed in regions of high particle flux (Henderson and Anderson, 2003). In regions where water mass residence times are similar to the scavenging residence times of ^{230}Th and ^{231}Pa, the distributions of ^{231}Pa/^{230}Th are particularly sensitive to deep water age. As the water mass ages, the preferential removal of ^{230}Th will result in an increase in the water's ^{231}Pa/^{230}Th. The increasing tendency will continue until the output of ^{213}Pa and ^{230}Th to the sediments occurs at the production ratio (i.e. 0.093). The closer to the production ratio that the sediment (^{231}Pa/ ^{230}Th) is, the longer it is since that water left the surface (or had disequilibrium imposed in some other way) (Thomas et al., 2007). The effective "age" of the water since ventilation is therefore reflected, which provides the potential of this proxy for assessment of changes in past ocean circulation.

Work at Sea

Samples for dissolved ^{231}Pa and ^{230}Th were collected at 18 stations throughout the water column in 25L Niskin bottles from the CTD rosette. At stations 1, 2, 3, 4, 5, 6, 7, 9, 12, 14, 16 18, samples were taken from 12 water depths, 5-10 L each. At other stations, samples were taken from the 25 meters water depth, 10L each. Filtration of samples was conducted directly from the Niskin, through Supor filters (0.8mm, 0.45μm) (Figure 26). The seawater was filtered into the acid cleaned sample bottles and was then acidified with 6-14 mL concentrated hydrochloric acid (32%) to lower the pH to <1.7 in a fume hood in the chemistry laboratory on board (Figure 27). Samples were sealed with a screw top and Parafilm, packed in zip-lock bags and stored in the container at room temperature until arrival at home laboratory. All further treatment and analysis will be carried out in clean laboratories in Oxford University. These include spiking the sample with standards, chemical separation and

purification of Pa and Th by column chromatography, and isotope analysis by ICP-Mass Spectrometer.

Figure 26: Sampling and filtration of seawater on board. The acid cleaned sample bottle was kept in two zip-lock bags and the sample was filtered directly from the Niskin bottle, which minimized the contamination from the ship.

Figure 27: Fume hood in the chemistry lab aboard, where acidification of samples was conducted.

References

Henderson, G. M., and R. F. Anderson (2003), The U-series toolbox for paleoceanography, in Reviews in Mineralogy and Geochemistry "Uranium Series Geochemistry", edited by Bourdon, B. et al., pp. 493-531, Mineral. Soc. Of Am., Washington, D. C.

McManus, J. F., Francois, R., Gherardl, J.-M., Kelgwin, L., Brown-Leger, S. (2004), Collapse and rapid resumption of Atlantic meridional circulation linked to deglacial climate changes, Nature, 428: 834-837.

Thomas, A. L., Henderson, G. M., McCave, I. N. (2007), Constant bottom water flow into the Indian Ocean for the past 140ka indicated by sediment 231Pa/230Th ratios, Paleoceanography, 22: PA 4210.

3.2.A.10. Neodymium isotopes ($^{143}Nd/^{144}Nd$) and rare earth elements (REE)

Leopoldo D. Pena and Alison Hartman

Lamont-Doherty Earth Observatory of Columbia University

Introduction

The value of Nd isotopes as an oceanographic and paleoceanographic tracer is increasingly recognized, in large part due to efforts by our lab at LDEO. For example, they have been targeted as part of the suite of key trace elements and isotopes (TEIs) that will be analyzed in every ocean section associated with the US GEOTRACES Program [GEOTRACES Science Plan, 2006]. The use of Nd isotope ratios as a water mass tracer is based on distinct isotopic compositions of different water masses and the quasi-conservative behavior of Nd isotopes in the ocean. ^{143}Nd is produced through radioactive decay of ^{147}Sm ($t_{1/2}$ = 106 Ga). Nd is enriched relative to Sm in the continents compared to the bulk Earth. As a result the continents have lower $^{143}Nd/^{144}Nd$ ratios than the bulk Earth and the mantle, and values vary with crustal age such that older continents have lower Nd isotope ratios. In the oceans, Nd isotope ratios show distinct and systematic geographic variability that is controlled by the isotopic composition of the local inputs, which is in turn controlled by the age of the continental crustal sources of Nd, and the advection of the Nd by ocean circulation. In the modern oceans Nd isotopes show variability by location and depth that enables distinct isotopic fingerprinting of different water masses [e.g. Fig. 28, Frank, 2002; Goldstein and Hemming, 2003].

Measured Nd isotopic values are usually normalized to a known standard and expressed as ε_{Nd} (Eq. 1). Modern intermediate and deep water from the Southern Ocean has Nd isotope ratios of ε_{Nd} between ca. -6 and -9, clearly distinguishable from the deep North Atlantic value of around -13.5 and North Pacific values of 0 to -4 [Piepgras and Jacobsen, 1988]. Due to the relatively short residence time of Nd in the oceans (500-1000 years) [Piepgras et al., 1979; Goldstein and O'Nions, 1981; Tachikawa et al., 1999] it stays in seawater long enough to be dispersed but short enough to prevent the isotopic composition from becoming homogenized [Piepgras and Jacobsen, 1988; Tachikawa et al., 1999]. As a result, Nd isotopes respond rapidly to changes in patterns of ocean circulation. Moreover, in comparison to other nutrient-based tracers of ocean circulation, Nd isotope ratios have the great advantage that they are not affected by productivity, air-sea gas exchange, or temperature, and in archival samples they do not change as a result of dissolution. As a consequence the Nd isotope ratios in deep water samples behave "quasi-conservatively" (for

example, in the Atlantic they reflect mixtures of NADW and Southern Ocean water [Goldstein and Hemming, 2003]), at least away from ocean margins where exchange processes with bottom sediments may be significant [e.g. Lacan and Jeandel, 2005]. The quasi-conservative behavior also applies to intermediate water. This potentially allows the Nd isotope ratio of any part of the water column to yield the mix between two (or more) end-member water masses with distinct Nd isotopic compositions.

$$\varepsilon_{Nd} = \left(\frac{\left({}^{143}Nd/{}^{144}Nd \right)_{SMP}}{\left({}^{143}Nd/{}^{144}Nd \right)_{CHUR}} - 1 \right) \times 10000 \qquad \text{Eq. 1}$$

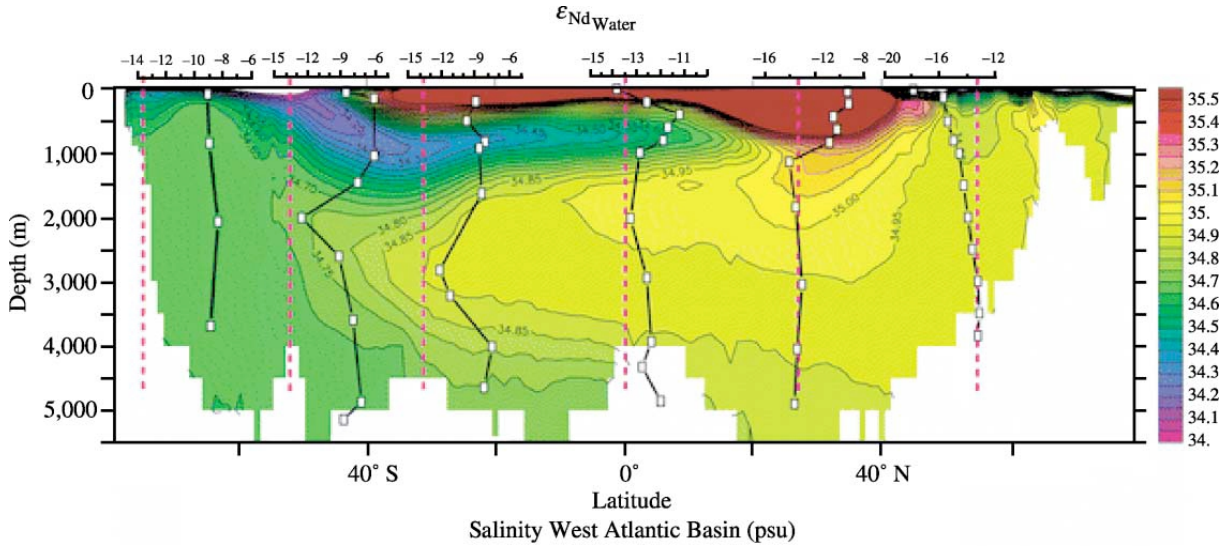

Figure 28: Nd isotope profiles in the Atlantic basin compared with salinity distributions [von Blanckenburg, 1999].

Materials and methods

During the GEOTRACES JC057 cruise we have sampled 17 stations on a latitudinal transect from the Falkland Islands to the equatorial region off Brazil. At each station, 16 samples were collected at different depths. The selection criteria for sample depth were based on the distribution of the different water masses present in the area of study. The concentration of Neodymium in seawater ranges from 10 pmol/Kg in surface waters to 40 pmol/Kg in deep waters. Based on these ranges our sampling volumes ranged from 5 to 10 L of seawater depending on the depth. For samples shallower than 1000 m we collected 10L of seawater, >7L for samples between 1000-2000 m and 5L for samples deeper than 2000 m. Assuming full recovery, the total Nd mass in the samples will range from 15 to 30 ng, enough to perform accurate isotopic measurements by TIMS. The majority of the samples were collected from the Ultra Clean Cast (UCC) and only in a few occasions a few samples were collected from the regular CTD when the water budget was very tight. In all cases the seawater was filtered through 0.2 μm Sartobran cartridges in order to remove particulate material. After collection the samples were acidified using ultrapure Seastar HCl at a rate of approximately 1mL/L in order to decrease the pH to ~2. The purpose of this acidification is twofold: first it kills all the bacteria and algae and prevents further biologically mediated

chemical reactions and second it helps to keep the Nd (and all the REEs) in solution and to prevent them from 'sticking' to the walls of the cubitainers.

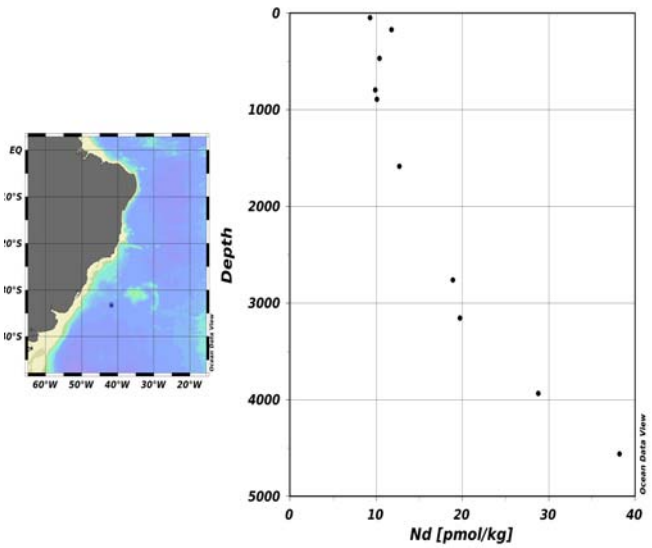

Figure 29: Typical Nd concentration (pmol/Kg) depth profile in the south West Atlantic [Jeandel, 1993]. Nd concentrations are typically low in surface waters and the concentration increasing with depth.

In addition to the water samples, at every station we have deployed a small gravity core attached to the bottom alert cable in the regular CTD cast. With the exceptions of the first 2 stations the gravity core has been able to recover an average of 20 cm of undisturbed sediments from the sea floor. Once on deck, the sediments were sliced every 1 cm and stored for further analyses back in the lab.

Results

No results to be reported during the cruise.

Future work

The complexity of the neodymium extraction and purification process forbids any sample processing aboard the RSS James Cook. Therefore our main workload will start back in the ultra clean lab at LDEO. Once there, the Nd and other REEs will be extracted by co-precipitation in the seawater and purified through a series of chromatographic columns. After these steps the Nd isotopes will be measured using Thermal Ionization Mass Spectrometry (TIMS) due to the relatively low concentration of Nd in seawater. The concentration of the different REEs in seawater will be determined by multi isotope dilution ICP-MS using an in house spike specifically targeted for this purpose.

The sediment samples will allow us to establish a basin wide calibration between the seawater signature and the different sedimentary substrates where Nd can be measured (disperse FeMn nodules, carbonate microfossils, fish teeth and fish debris, ...etc). This calibration will be important in order to understand the transference of the modern signal to the sedimentary record, where the Nd isotopes can be used to reconstruct paleoceanographic variations in the water masses circulation.

Acknowledgements

We want to thank all the crewmembers of the RSS James Cook for their invaluable help and hospitality during the JC057 cruise.

References

Frank, M. (2002), Radiogenic isotopes: tracers of past ocean circulation and erosional input, *Reviews of Geophysics*, *40*(1), 10.1029/2000RG000094.

GEOTRACES Science Plan (2006), Scientific Committee on Oceanic Research, Baltimore, Maryland (http://www.geotraces.org).

Goldstein, S. L., and R. K. O'Nions (1981), Nd and Sr isotopic relationships in pelagic clays and ferromanganese deposits, *Nature*, *292*, 324-327.

Goldstein, S., and S. Hemming (2003), Long-lived Isotopic Tracers in Oceanography, Paleoceanography, and Ice-sheet Dynamics, in *Treatise on Geochemistry*, pp. 453-498, Elsevier, New York.

Jeandel, C. (1993), Concentration and isotopic composition of Nd in the Southern Atlantic Ocean, *Earth and Planetary Science Letters*, *117*, 581-591.

Piepgras, D., and S. B. Jacobsen (1988), The isotopic composition of neodymium in the North Pacific, *Geochimica et Cosmochimica Acta*, *52*, 1373-1381.

Piepgras, D., G. Wasseburg, and E. J. Dasch (1979), The isotopic composition of Nd in different ocean masses, *Earth and Planetary Science Letters*, *45*(2), 223-236.

Tachikawa, K., C. Jeandel, and M. Roy (1999), A new approach to the Nd residence time in the ocean: the role of atmospheric inputs, *Earth and Planetary Science Letters*, *170*, 433-446.

Lacan, F., and C. Jeandel (2005), Neodymium isotopes as a new tool for quantifying exchange fluxes at the continent–ocean interface, *Earth and Planetary Science Letters*, *232*.

3.2.A.11. Uranium, barium, molybdenum, δ(^{18}O) and δ(D)

José Marcus Godoy

Chemistry Department, Pontifical Catholic University of Rio de Janeiro

Introduction

The decision to take part on the present GEOTRACES cruise came after our Department head has joined the project committee in 2010. After the invitation to send a Brazilian researcher to participate on the present cruise, we have decided to send one of our professors, instead of a Ph.D. student, in order to verify how we could contribute to some extension to an already on-going project and also verify *in-situ* the sampling procedures and the analytical methods for trace elements adopted, in particular, for iron.

After asking the principal scientist, Micha Rijkenberg, about the existing interested parties and the parameters already assigned to them, and based on our analytical capability related to the implemented methods able to accept an additional large number of samples, it was decided to use this opportunity to collect samples for the determination of the following parameters: uranium, barium, molybdenum, δ(^{18}O) and δ(D).

Uranium and barium are used currently in our water mixing studies related to submarine ground water discharge (SGD) and estuarine areas (Souza *et al.*, 2010). Although a

redox sensitive element, uranium shows, generally, a conservative behavior in seawater and is correlated with the salinity, similar behavior is expected for molybdenum (Turetta *et al.*, 2010). Dissolved barium is depleted at surface waters and enriched at the bottom; it is also highly correlated with silicate and can be applied as an additional tracer of the Antarctic Bottom Water.

Oxygen and hydrogen isotopic composition changes with the water cycle and depends on factors as geographical position and temperature changes. In seawater they are depleted on fresher, cooler and less saline water masses and enriched on warmer and saltier sub-tropical waters (Povinec *et al.*, 2011). Figure 30, below, shows their application on tracing of water masses in the southern Indian Ocean (Povinec *et al.*, 2011).

Samples collected and measurements

Filtered seawater samples (0.2 μm) from the UC CTD of each station and depth were collected in 2mL glass vials, with a total of 420 samples. Additionally, also 0.2 μm filtered surface samples from the FISH were collected regularly after station 11 and every six hours after station 18. The samples vials were kept in plastic boxes at 4^{o}C. Due to the isotopic measurements it is not possible to add acids to the sample.

Uranium, barium and molybdenum will be determined by ICP-MS after 1:20 dilution and indium and thallium as internal standards. For the determination of $\delta(^{18}O)$ and $\delta(D)$ we will use a Picarro laser based cavity down spectrometer, which measures directly the isotopic ratio based on the peak height of the water molecules IR spectrum at vapor state as shown on Fig. 31.

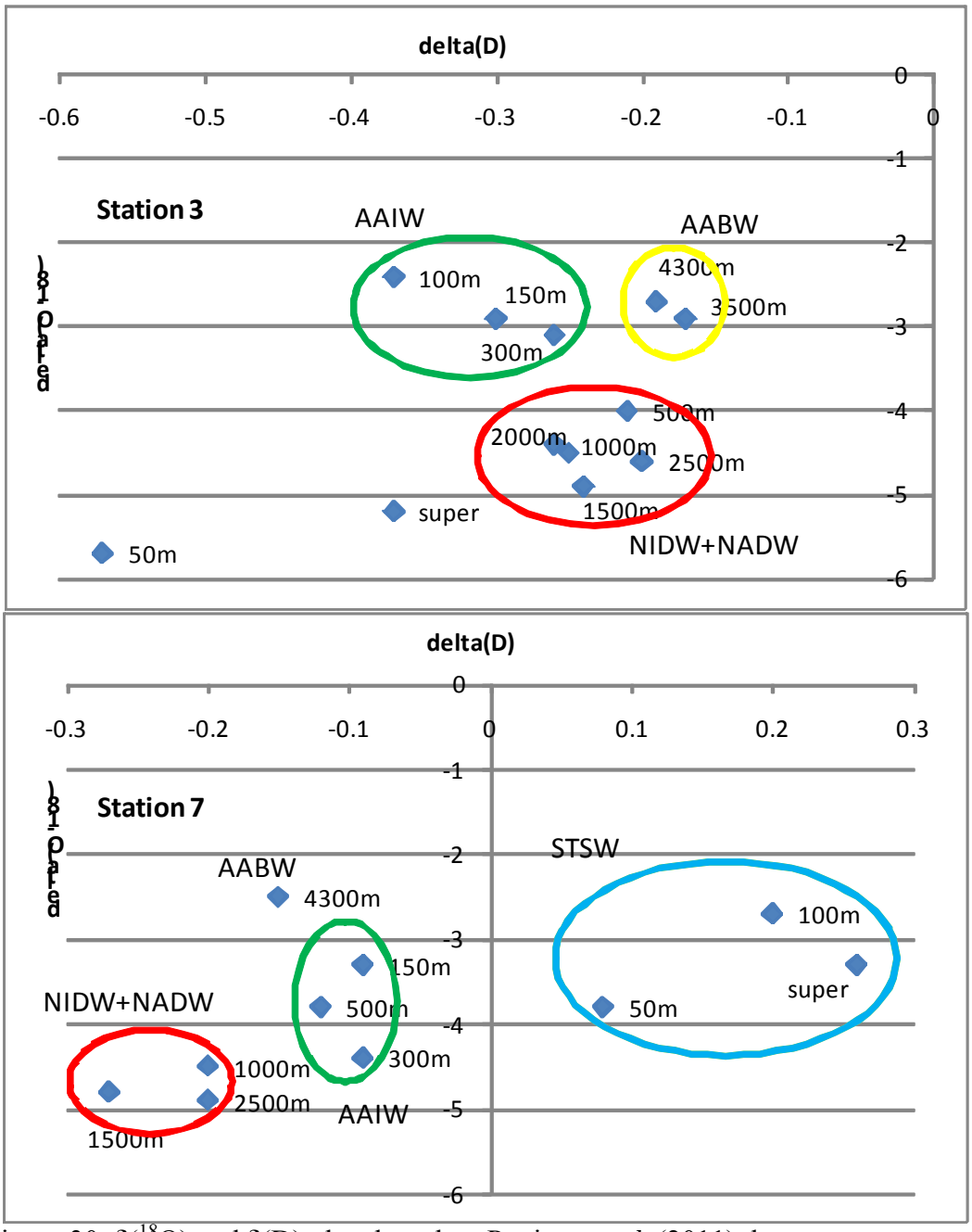

Figure 30: δ(^{18}O) and δ(D) plots based on Povinec *et al.* (2011) data

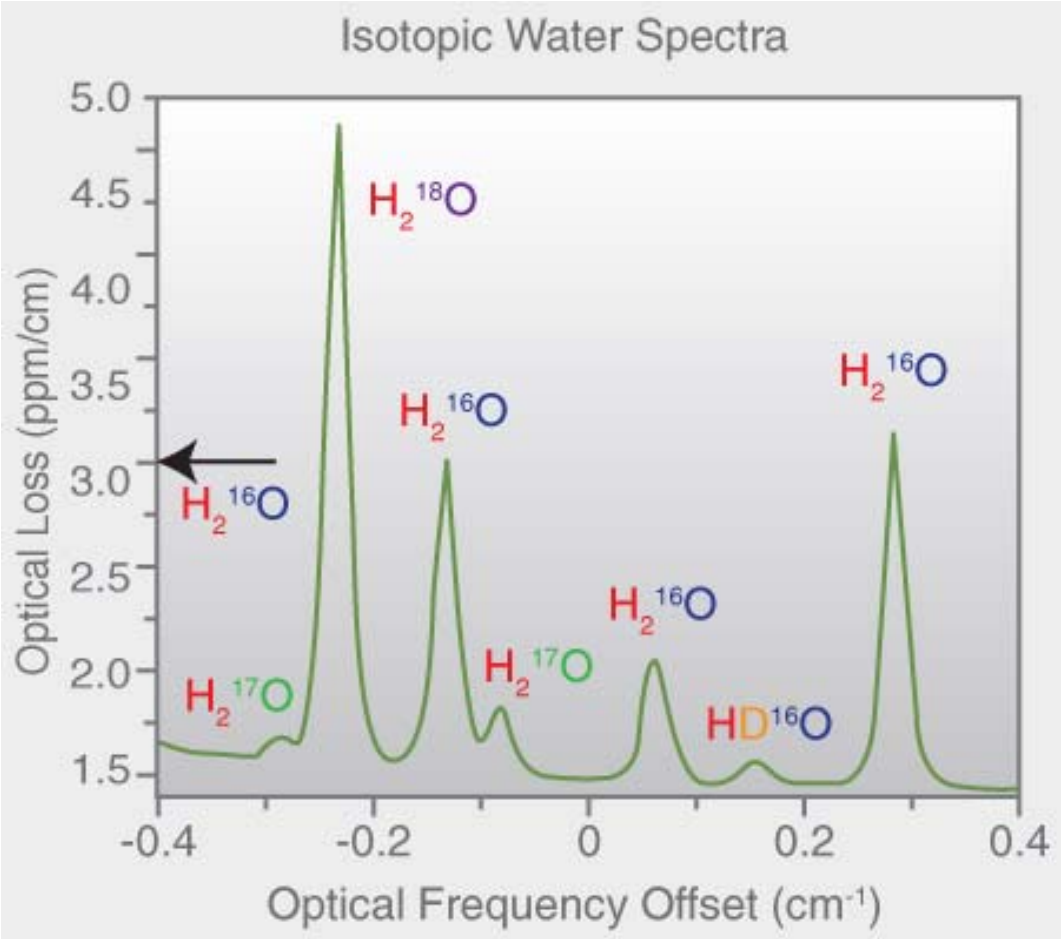

Figure 31: IR spectrum of water molecules obtained a Picarro spectrometer

References

Hoppema et al. (2010) Distribution of barium in the Weddell Gyre: Impact of circulation and biogeochemical processes, Marine Chemistry 112, 118-129

Povinec et al. (2011) Tracing of water masses using a multi isotope approach in the southern Indian Ocean, Earth and Planetary Sciences Letters 302, 14-26.

Souza et al. (2010) Use of multitracers for the study of water mixing in the Paraíba do Sul estuary, J. Environ. Radioactivity 101, 564-570

Turetta et al. (2010) The distribution of dissolved thallium in the different water masses of the western sector of the Ross Sea (Antarctica) during the austral summer, Microchem. Journal 96, 194-202

3.2.B. CO_2 and other transient anthropogenic tracers

3.2.B.1. Dissolved Inorganic Carbon, Total Alkalinity

Elizabeth Jones and Lesley Salt

NIOZ

Methodology

Sampling and analysis for carbonate system parameters broadly followed the standard operating procedures outlined by Dickson et al., 2007.

Water samples of 0.6 L were collected from the Large Volume CTD at one cast of every station, at all 24 depths, into borosilicate sample bottles with plastic caps, using silicone tubing. In each profile, three duplicate samples were collected at shallow, intermediate and deep parts of the profile. Samples analysis commenced immediately after collection. Analysis of profiles was in all cases completed within 12 hours after sampling. All analyses were performed on a VINDTA 3C (Versatile INstrument for the Determination of Total Alkalinity, designed and built by Dr. L. Mintrop, Marine Analytics and Data, Kiel, Germany). Samples were measured simultaneously on two instruments, referred to as A and B (VINDTA #14 and #17, respectively). These instruments were slightly modified: the peristaltic sample pump was replaced with an overpressure system (~0.5 bar overpressure) and a 1 m long (though coiled) 1/8" stainless steel counter-flow heat exchanger that was placed between the sampling line and the circulation circuit. This setup allows for the rapid, convenient and bubble-free loading of the pipettes with sample of 25 ºC (± 0.1 ºC), irrespective of the samples' initial temperature.

Duplicate samples were analyzed first followed by the depth profile beginning with surface samples. This assured that any 'startup drift' in the coulometric cells does not affect the deep samples. The use of two machines increases our confidence in final results, and allows demonstration and quantification of measurement errors of the machines that would otherwise go unnoticed. No formal analysis and correction of the result have been performed yet. Such a report on the treatment of the carbon data will, in due time, be available as a separate report.

On station 6, in addition to the regular sampling scheme, 6 depths were also sampled in triplicate. The samples were stored in 250 mL borosilicate bottles and poisoned with 0.175 mL of 50% saturated $HgCl_2$ for external and further internal analysis in due course. This will hopefully validate our data further.

Dissolved inorganic carbon (DIC)

Dissolved inorganic carbon (DIC) was determined by coulometric titration. An automated extraction line takes a 20 mL subsample which is subsequently purged of CO_2 in a stripping chamber containing ~1 mL of ~8.5% phosphoric acid (H_3PO_4). A stream of nitrogen carries the CO_2 gas into a coulometric titration cell via a condenser and acid trap, to strip the gas flow of any water. The CO_2 reacts with the cathode solution in the cell to form hydroxyethylcarbamic acid, which is then titrated with hydroxide ions (OH^-) generated by the coulometer. The current of the coulometer is then integrated over the duration of the titration to obtain the total amount of carbon titrated. The raw DIC data from all samples measured on VINDTA A is shown in Figure 32.

Total Alkalinity (TA)

Determinations of total alkalinity (TA) were performed by acid titration that combines aspects from both the commonly used 'closed cell' method and the 'open cell' method, following the VINDTAs standard settings. A single 20 L batch of acid of ~0.05M and salinity 35 was prepared to be used by both VINDTAs. Potential drift in acid strength due to HCl-gas loss to acid vessel headspace is not accounted for. The raw TA data from all samples measured on VINDTA A is shown in Figure 33.

Certified reference material (CRM, Batch #105) obtained from Dr. Andrew Dickson at Scripps Institute of Oceanography (San Diego, California) was used for calibration purposes and quality control for both DIC and TA.

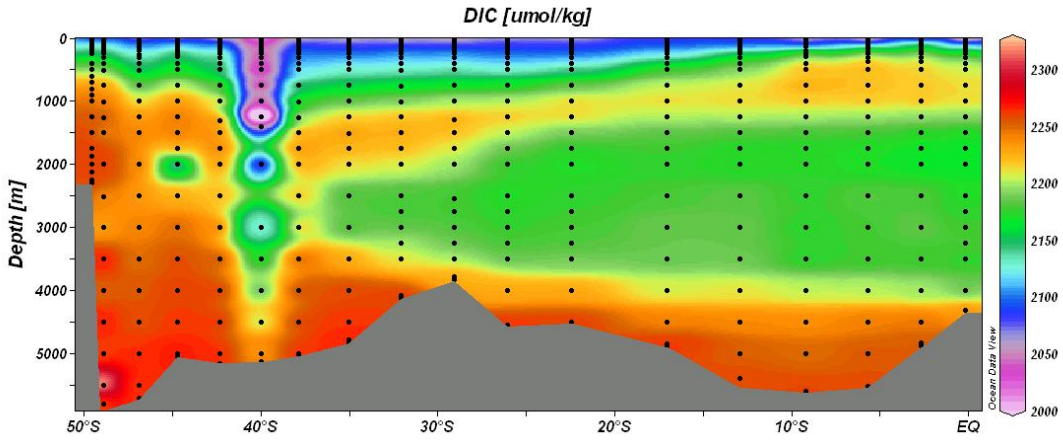

Figure 32. Raw DIC data from all depths along the transect.

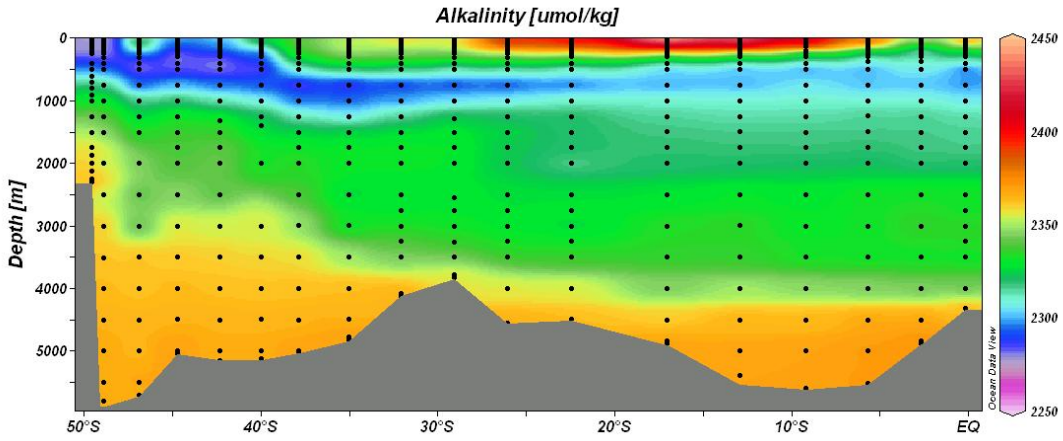

Figure 33. Raw TA data from all depths along the transect.

References

Dickson, A.G., Sabine, C.L. and Christian, J.R. (Eds.) 2007. Guide to best practices for ocean CO2 measurements. PICES Special Publication 3, 191 pp.

3.2.B.2. Isotopes of Dissolved Inorganic Carbon (DIC): δC13 and ΔC14

PI: Steven van Heuven[1]
Work on board: Patrick Schmidt[2]*, Lesley Salt*[3]*, Maaike Claus*[4]

[1] Centre for Isotope Research, RuG
[2] IUP
[3] NIOZ
[4] RuG

Background

In nature, three isotopes of carbon (C) exist: the common, stable ^{12}C (circa 99%), the rare, stable ^{13}C (circa 1%) and the exceptionally rare, unstable 'radiocarbon' ^{14}C (circa $1{\cdot}10^{-10}$ %, $T_{1/2} \approx 5730$ years). The ratios of the concentrations of the isotopes $^{13/12}C$ and $^{14/12}C$ are not exactly constant in place and time, and the deviations from 'normal' (referred to as δC13 and ΔC14, respectively) are of strong interest to environmental sciences. Determination of these deviations is challenging. For $^{13/12}C$, deviations from 'normal' are caused by isotopic fractionation in physical, chemical and biological processes (and are a measure of the strength of these processes, which is exactly what makes them interesting). Deviations of $^{14/12}C$ are not only the result of the aforementioned fractionation processes, but also of the steady decay of (atmospherically produced) ^{14}C, which becomes noticeable once seawater loses contact with the atmosphere (and thus stops exchanging $^{14}CO_2$). Additionally, anthropogenic changes in the atmospheric composition with respect to ^{13}C and ^{14}C (emissions of low-δC13 CO_2 by combustion of fossil fuels, and the large 'pulse' of ^{14}C produced by atomic bob tests in the 1950s and 1960s, respectively) also imprint on the oceanic values of δC13 and ΔC14. In the ocean, the cumulative effect of the aforementioned processes on δC13 is very small: the range of oceanic δC13 is approximately -1 ‰ to +2 ‰. Determination of δC13 is only possible by highly precise mass spectrometric analysis. The oceanic range of ΔC14 is much larger (circa -250 ‰ to +150 ‰) but the analysis (by Accelerator Mass Spectrometry; AMS) is nonetheless much more challenging due to the extremely low concentrations of ^{14}C in seawater.

Significant risk of contamination of the samples with non-natural ^{14}C was present during this cruise. Another research team on board conducted ^{14}C-spiking experiments for determination of microbial production. The initial spiking of microbial cultures was followed after 72 hours by acidification and filtration of acidified samples. During both activities, but especially the latter, large amounts of $^{14}CO_2$ are evolved, and were evacuated from the isotope container and vented over the back of the ship. Significant care was taken to avoid any work on the natural-^{14}C samples in the circa 20 hours after spiking activities. Additionally, a protocol intended to minimize the risk of physical contact between material from both activities was rigorously adhered to.

Samples collected

During this cruise, 468 samples were collected on 18 profiles for shore-based determination of carbon isotope ratios at the Centre for Isotope Research (CIO) at the University of Groningen. At each station, samples were collected from all bottles of the Ultra Clean CTD, directly into custom made, pre-baked, 250 ml glass ampoules. Several duplicates were collected at each station at the deep and shallow end of the profile.

To be able to rule out atmospheric ^{14}C-contamination during sampling (and thereby to increase our confidence in obtained ΔC14 dataset), air samples were collected in the UC-CTD

container during sample collection, by means of bubbling air through a strong solution of NaOH.

Methods

Empty ampoules were stored per 125 in new, nearly airtight Zarges aluminum boxes that were kept closed at all other times. Shortly before the UC-CTD came on deck, the required (circa 27) ampoules were removed from crates and labeled, using gloves. In the UC-CTD container, ampoules were gently filled from the bottom upwards using carefully prepared glass tubes connected with PVC tubing to a PTFE insert that connected the UC-CTD. Ampoules were flushed with circa 1-2 times their volume and preliminary capped without a headspace with a PTFE cap. Upon returning to the sample sealing lab each ampoule was treated as follows: the PTFE cap was removed, the neck of the ampoule was cleared of sample by blowing high-purity N_2 through a glass tube that was lowered into the neck. $HgCl_2$ (125 µl, 50% saturated) was added to the bottom of the neck (i.e., slightly above the sample) by means of a 1/8" Teflon tube attached to a dispensing pipette, while N_2 still flowed out of the glass tube, thereby preventing entry of lab air into the neck of the ampoule. The ampoule was subsequently flame sealed using a propane/butane (i.e., camping gas) torch, again with the N_2-tube still in place (albeit higher in the neck at this point). After cooling down, ampoules were cleaned, dried and stored in the Zarges boxes. All material used for sampling and poisoning was stored after each station in dilute HCl and soaked for a few hours in deep seawater before sampling.

3.2.B.3. Chlorofluorocarbons (CFC's)

Patrick Schmidt

IUP

Introduction

Chlorofluorocarbons (CFCs) are anthropogenic trace gases that enter the ocean by gas exchange with the atmosphere. The evolution of these transient tracers in the ocean interior is determined by their temporal increase in the atmosphere since the middle of the last century and the formation, advection and mixing processes of intermediate, deep and bottom water. Hence, these transient tracers enable to determine transit times, i.e. the time elapsed since the water has left the surface mixed layer.

Work at sea, water sampling, and analyzes in the IUP Bremen laboratories

In total 417 samples for chlorofluorocarbons (CFC-11 and CFC-12) distributed on 18 deep profiles were taken. Water samples from the CTD/rosette system were collected into 100 ml glass ampoules and sealed off after a CFC free headspace of pure nitrogen had been applied. The CFC samples are shipped home for analysis in the CFC-laboratory at the IUP Bremen. The determination of CFC concentration will be accomplished by purge and trap sample pre-treatment followed by gas chromatographic (GC) separation on a capillary column and electron capture detection (ECD). The amount of CFC degassing into the headspace will be accounted for during the measurement procedure in the lab. The system will be calibrated by analyzing several different volumes of a known standard gas. Additionally the blank of the system will be analyzed regularly. Due to limited measurement capacity and high number of samples analyzed in the laboraty, measurement will be probably finished in 2012.

3.2.C. Microbial oceanography: biodiversity and turnover rates of prokaryotes, eukaryotes and viruses

3.2.C.1. Microbial community composition and function through analysis of the Meta-Genome and Proteome

Kristin Bergauer

University of Vienna

Introduction

The deep sea, a vast, dark realm featuring distinctive organisms and serving as a massive reservoir of carbon, is the largest and least explored ecosystem on Earth. Ecological and biogeochemical processes in the dark ocean remain cryptic (the dim mesopelagic or 'twilight zone' plus the aphotic bathypelagic zone below) compared to processes in the euphotic zone being in the focus of several prior major interdisciplinary studies. The biological pump connects surface processes to the deepest ocean layers (Volk and Hoffert, 1985; Ducklow et al., 2001), where biological processes occur at low rates, and the biota may adapt unique metabolisms. These deep layers are characterized by significant decomposition, recycling, and repackaging of particulate and dissolved organic matter. Thus, we aim to analyze the structure and function of microbial assemblages sampled throughout the water column of the subtropical North Atlantic using molecular tools.

Objectives

1. To assess the community composition of prokaryotes in the major deep water masses
2. To assess the function of deep water versus subsurface microbial communities based on a meta-genomics and -proteomics approach
3. Temperature versus liability of DOM Experiment

Methods

1. Microbial community composition

Water samples were taken at every occupied station (total of 18) and at 8 depth layers. Water was collected from distinct water masses, identified based on their temperature and salinity characteristics and inorganic nutrient concentrations. Specifically, water was collected from the euphotic layer at 50m depth, the oxygen minimum zone, the Antarctic Intermediate Water (AAIW), the upper (uNADW), middle (mNADW) and lower North Atlantic Deep Water (lNADW) and the Antarctic Bottom Water (AABW). Additionally the oxygen minimum zone at the base of the euphotic realm, ranging between 250 and 1200m, was sampled. Samples were collected from 25 L Niskin bottles into acid rinsed polycarbonate carboys (10L). For each depth a total of ten liters of seawater was filtered through a 0.22 µm GTTP filter unit (Millipore) and the filters were stored at -80°C. Filtration of samples was accomplished within three hours after recovery the CTD rosette sampler. Overall, 144 filters were stored at – 80˚C for subsequent DNA extraction and analysis in the molecular laboratory of the University Vienna.

Terminal Restriction Fragment Length Polymorphism analysis

PCR reactions for T-RFLP will be performed with fluorescently labeled primers (bacterial primers 27F-FAM/1492R; archaeal primers 21F-FAM/958R) and digested with a tetrameric restriction enzyme (*Hha*I). Only the fragments carrying the fluorescent label are detected with the capillary sequencer using laser-induced fluorescence detection. The size of the FAM-labeled fragments (representing operational taxonomic units, OTUs) will be determined by comparison with the internal size standard using Fingerprinting II software of Bio-Rad.

The T-RFLP patterns will be analyzed by recording the numbers of peaks (presence versus absence). The similarities of the T-RFLP patterns between the different samples were assessed with the Bray-Curtis similarity index, which is similar to Sorenson's similarity index when applied to presence/absence data.

2. Meta-genomics and -proteomics

Water samples were taken at stations 2, 7, 11 and 16 (total of 4 stations). Water was collected from distinct water masses, identified based on their temperature and salinity characteristics and inorganic nutrient concentrations. Specifically, water was collected from the lower euphotic layer at 100m depth, the oxygen minimum layer, the Antarctic Intermediate Water (AAIW) and North Atlantic Deep Water (NADW). Samples were collected from 25L Niskin bottles into acid rinsed polycarbonate carboys (200L). Water samples were collected onto a 0.22µm ATTP filter (Millipore). Filtration of samples was accomplished within 3-4 hours after recovery the CTD rosette sampler. Overall, 2x 0.8µm and 8x 0.2µm filters (Table 4) were obtained and frozen in liquid nitrogen and finally stored at –80˚C for subsequent DNA extraction and analysis in the molecular laboratory of the University Vienna.

Table 4: Overview about stations sampled for Meta-omics approach

Station	Cast	Niskin #	Depth (m)	WM	Volume (L)
2	5	3-14	500	O_2 min	300
	5	15-19	100	sub-surface	100
7	3	3-14	1750	O_2 min	300
	2	15-19	100	sub-surface	100
11	3	3-14	600	O_2 min	300
	3	15-19	100	sub-surface	100
16	3	3-14	400	O_2 min	300
	3	15-19	100	sub-surface	100

3. Temperature versus liability of DOM Experiment

Water samples were taken at hyperstations 2, 7, 11 and 16 at 50m in the euphotic and at 3500m in the bathypelagic realm. Acid rinsed Nalgene bottles holding 20L of seawater were incubated at 2-4˚C and at the distinct surface water temperature, ranging between 15-25˚C.

Figure 34: Experimental setup

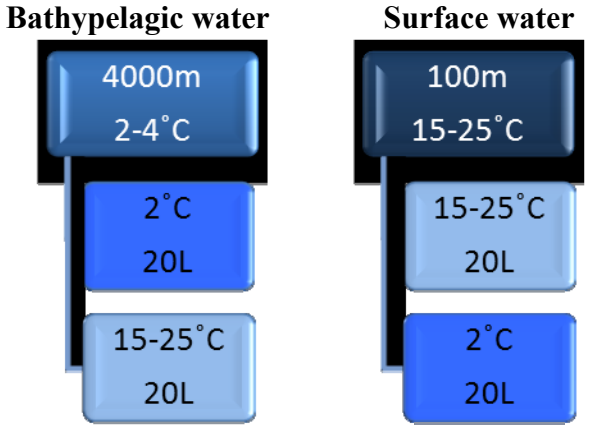

As soon as incubations were adjusted to the required temperatures, sub-sampling of water was accomplished over 5 days to measure following parameters: PA (Prokaryotic abundance), PHP (Prokaryotic heterotrophic production), FISH (Fluorescence in situ hybridization), MICRO-CARD-FISH (Microautoradiography-Catalyzed reporter deposition-FISH), DNA, Nutrients, DOC (dissolved organic carbon) and fDOM (fluorescent dissolved organic matter).

PA

1.5 ml of samples were fixed with glutaraldehyde (final concentration 0.5%), frozen in liquid nitrogen and stored at -80°C. The abundance of prokaryotes and viruses will be measured by flow cytometry (Beckton Dickinson) after nucleic acid staining with SyBR-Green I. The abundance will be estimated using an internal standard of fluorescent beads, and will be corrected by calculating the flow rate.

PHP

Microbial heterotrophic production was measured by incubating 5-40 ml of seawater (depending on the depth) in triplicate with 5 nM [3H]-leucine (final concentration, specific activity 120 Ci mmol-1, American Radiolabeled Chemicals) in the dark at in situ temperature (±1°C) for 1 to 24 h. Duplicate formaldehyde-killed blanks were treated in the same way as the samples. Incubations were terminated adding formaldehyde (2% final concentration) to the samples. Samples and blanks were filtered through 0.2-µm polycarbonate filters (Whatman Nuclepore, 25 mm filter diameter) supported by cellulose acetate filters (Millipore, HA, 0.45-µm pore size). Subsequently, the filters were rinsed twice with 5% ice-cold trichloroacetic acid, twice with Milli-Q and with 80% Ethanol. Subsequently filters were dried, 8 ml of scintillation cocktail (FilterCount, Canberra-Packard) added, and after about 18 h counted on board in a liquid scintillation counter (Perkin Elmer Tricarb). The instrument was calibrated with internal and external standards. The blank-corrected leucine incorporation rates were converted into microbial carbon production using the theoretical conversion of 1.55 kg mol-1 leucine incorporated (Kirchman, 1993; Simon and Azam, 1989).

MICRO-CARD-FISH

The relative abundance and activity of the major prokaryotic groups will be determined by MICRO-CARD-FISH analysis. Fifty milliliters were incubated with 3H- Leucine of high specific activity (10nM final concentration). After the incubations, the life samples were fixed by adding paraformaldehyde (2% final concentration) and, subsequently, stored at 4oC in the dark for 18 h. Thereafter the samples were filtered onto 0.2-µm polycarbonate filters and stored at -80oC.

The analysis of MICRO-CARD-FISH samples in the lab will be done as described elsewhere (Teira et al. 2004; see also http://www.microbial-oceanography.eu/methods.htm). To evaluate the relative abundance and activity of Bacteria we will use a probe mix of EUB338-II-III (EUB338: 5'-GCT GCC TCC CGT AGG AGT-3', EUB338-II: 5'-GCA GCC ACC CGT AGG TGT-3', EUB338-III: 5'-GCT GCC ACC CGT AGG TGT-3', see Daims et al., 1999). To target Crenarchaea we will use a probe mix of CREN537 and GI554 (CREN537: 5'-TGA CCA CTT GAG GTG CTG-3', Teira et al., 2004; GI554: 5'-TTA GGC CCA ATA ATC MTC CT-3', Massana et al., 1997). To cover Euryarchaea we will use the probe EURY806 (5'-CAC AGC GTT TAC ACC TAG-3'; Teira et al., 2004). To evaluate unspecific hybridization of probes and background fluorescence we will use antisense probes.
Microautoradiography will be performed on previously hybridized filter sections and processed as described in Teira et al. (2004). The slides will be examined under an epifluorescence microscope equipped with a 100-W mercury lamp and appropriate filter sets for DAPI and Alexa488. The presence of silver grains surrounding cells will be recorded by using the transmission mode of the microscope. The data will be expressed as percent of DAPI-stained cells.

Nutrients

Of each incubation experiment, 4 mL of seawater were 0.2µm pre-filtered in duplicate and collected in 5 ml polyethylene vials. Nutrient samples were subsequently analyzed on a Quatro auto-analyzer by Evaline van Weerle.

DOC and fDOM

In order to measure DOC, sub-surface incubations were pre-filtered (0.2µm) and collected in 10mL ampules. 8mL of seawater from the bathypelagic realm could be collected and amended with 6 drops of concentrated HCL without pre-filtration. Same procedure was applied to fDOM samples. Ampules were sealed and stored at – 20˚C.
Analysis of samples will take place at the University of Vienna.

References

Baltar, F., J. Arístegui, J. M. Gasol, E. Sintes, and G. J. Herndl. 2009. Evidence of prokaryotic metabolism on suspended particulate organic matter in the dark waters of the subtropical Atlantic. Limnol. Oceanogr. 54**:** 182-193.

Barber, R. T. 1986. Dissolved organic carbon from deep waters resists microbial oxidation. Nature 220**:** 274-275.

Daims, H., A. Bruhl, R. Amann, K. H. Schleifer, and M. Wagner. 1999. The domain-specific probe EUB338 is insufficient for the detection of all Bacteria: Development and evaluation of a more comprehensive probe set. Systematic and Applied Microbiology 22**:** 434-444.

Delong, E. F. 1992. Archaea in coastal marine environments. Proc. Natl. Acad. Sci. USA 89**:** 5685-5689.

Herndl, G. J., T. Reinthaler, E. Teira, H. Van Aken, C. Veth, A. Pernthaler, and J. Pernthaler. 2005. Contribution of Archaea to total prokaryotic production in the deep Atlantic Ocean. Appl. Environ. Microb. 71**:** 2303-2309.

Jannasch, H. W., and C. O. Wirsen. 1973. Deep-Sea Microorganisms: in-Situ Response to Nutrient Enrichment. Science 180**:** 641-643.

Kirchman, D. 2001. Production and growth rates from Leucine incroporation in natural aquatic environments, p. 227-237. Methods in microbiology. Academic Press.

Kirchman, D. 1993. Leucine incorporation as a measure of biomass production by heterotrophic bacteria, p. 509-512. *In* P. F. Kemp, B. F. Sherr, E. B. Sherr and J. J. Cole [eds.], Handbook of Methods in Aquatic Microbial Ecology. Lewis publishers.

Kirchman, D. L., H. Elifantz, A. I. Dittel, R. R. Malmstrom, and M. T. Cottrell. 2007. Standing stocks and activity of Archaea and Bacteria in the western Arctic Ocean. Limnol. Oceanogr. 52**:** 495-507.

Lane, D. J. 1991. 16S/23S rRNA sequencing, p. 115-176. *In* E. Stackebrandt and M. Goodfellow [eds.], Nucleic acid techniques in bacterial systematics. John Wiley & Sons.

Massana, R., A. E. Murray, C. M. Preston, and E. F. Delong. 1997. Vertical distribution and phylogenetic characterization of marine planktonic Archaea in the Santa Barbara Channel. Appl. Environ. Microb. 63**:** 50-56.

Moeseneder, M. M., C. Winter, J. M. Arrieta, and G. J. Herndl. 2001. Terminal-restriction fragment length polymorphism (T-RFLP) screening of a marine archaeal clone library to determine the different phylotypes. J. Microbiol. Meth. 44**:** 159-172.

Reinthaler, T., H. Van Aken, C. Veth, J. Aristegui, C. Robinson, P. J. L. Williams, P. Lebaron, and G. J. Herndl. 2006. Prokaryotic respiration and production in the meso- and bathypelagic realm of the eastern and western North Atlantic basin. Limnol. Oceanogr. 51**:** 1262-1273.

Simon, M., and F. Azam. 1989. Protein content and protein synthesis rates of planktonic marine bacteria. Mar. Ecol. Prog. Ser. 51**:** 201-213.

Teira, E., T. Reinthaler, A. Pernthaler, J. Pernthaler, and G. J. Herndl. 2004. Combining catalyzed reporter deposition-fluorescence in situ hybridization and microautoradiography to detect substrate utilization by bacteria and archaea in the deep ocean. Appl. Environ. Microb. 70**:** 4411-4414.

Varela, M. M., H. M. Van Aken, and G. J. Herndl. 2008. Abundance and activity of Chloroflexi-type SAR202 bacterioplankton in the meso- and bathypelagic waters of the (sub)tropical Atlantic. Environ. Microbiol. 10**:** 1903-1911.

3.2.C.2. Prokaryotic abundance and ectoenzymatic activity

Adam Klimiuk

University of Vienna, Austria

Prokaryotic abundance

To evaluate the dynamics of the microbial food web samples for prokaryotic and viral abundance were collected in every station and depth from the surface to the bottom layers. 1.5 ml of samples were fixed with glutaraldehyde (final concentration 0.5%), frozen in liquid nitrogen and stored at -80°C. The abundance of prokaryotes and viruses will be measured by

flow cytometry (Beckton Dickinson) after nucleic acid staining with SyBR-Green I. The abundance will be estimated using an internal standard of fluorescent beads, and will be corrected by calculating the flow rate.

Ectoenzymatic activity of prokaryotic communities and end product inhibition experiment

The ectoenzymatic activity (EEA) of prokaryotic organisms was determined adding a specific substrate attached to a fluorochrome to water samples of 5 different depths. EEA was measured in unfiltered samples (total EEA) as well as samples filtered through 0.2μm Acrodisc syringe filter (EEA of free dissolved ectoenzymes). The samples were incubated in the dark at *in situ* temperature during 24-120 h, depending on the expected enzymatic activity. The substrates used were 4-methylumberlliferyl (MUF)-alpha-glucoside, MUF-phosphate and 4-methylcoumarinyl-7-amide (MCA)-leucineaminopeptide, to assess the ectoenzymatic activity of alpha-glucosidase, phosphatase and leucine-aminopeptidase, respectively. Fluorescence is observed after enzymatic splitting of the substrate and the fluorochrome. The activity of the different enzymes is linearly related to the fluorescence and was detected on the spectrofluorometer using an excitation wavelength 365 nm and an emission of 445 nm. Fluorescence will be transformed to substrate concentrations by using a standard curve in which the fluorochromes (MUF and MCA) were added to 0.2 μm filtered sample water (Acrodisc syringe filter) at concentrations ranging from 2.5 to 100 nM. The cleavage activity will be calculated from the change of each substrate concentration over time.

To investigate EEA regulation of specific enzymes by mechanism of end product inhibition, glucose or sodium phosphate were added at different concentrations to water samples containing substrates for alpha-glucosidase or phosphatase, respectively. Samples were incubated in the dark at *in situ* temperature during 24-120 h. After incubation fluorescence was measured and cleavage activity will be calculated as described above. Inhibition rate will be calculated from difference of final product concentration in samples containing inhibitor at various concentrations, as compared to samples without inhibitor.

3.2.C.3. Prokaryotic Activity in the major water masses of the South Atlantic

Itziar Lekunberri

University of Vienna

Introduction

The microbial loop hypothesis postulates a major role for bacteria in the oceanic carbon cycle (Pomeroy 1974, Williams 1981, Azam et al. 1983), actively growing through the consumption of DOC. Bacterioplankton can consume 30-60% of the primary production via dissolved organic matter (Williams 1981, Azam et al. 1983, Cole et al. 1988), reaching close to 100% in very oligotrophic sites (Gasol et al. submitted). Bacterial biomass often comprises a major fraction of particulate organic carbon, in oligotrophic systems at times even surpassing phytoplankton biomass (Cho & Azam 1988, Fuhrman et al. 1989, Simon et al. 1992, Gasol et al. 1997).

It is generally accepted that bacterial communities seem to be rather similar at relatively large spatial scales (Acinas et al. 1997, Baldwin et al. 2005) on the horizontal axis, except

where different water masses meet (Suzuki et al. 2001, Pinhassi et al. 2003). Since the biggest distinction in microbial communities occurs at the boundary of the euphotic and aphotic zones, light and the vertical distribution of autotrophs seem to be an important factor determining bacterial distributions, through their effects on the DOC pool.
Geotraces provides a good opportunity to relate the different water masses well characterized by the different trace metal with the prokaryotic activity.

Objective

To study the heterotrophic activity and chemoautotrophic activity of prokaryotes in the major water masses of the South Atlantic.

Methods

Samples were taken at every station (total of 18) and at 8 depth layers. The depth layers were chosen to cover the bottom waters, Antartic Bottom Water (AABW), Antartic Intermediate Water (AAIW), North Atlantic Deep Water (NADW). Additionally the oxygen minimum zone, the base of the euphotic zone (~250m) and the subsurface at 50m were sampled. Samples were transferred from the CTD 25L bottles into acid rinsed polycarbonate bottles. Filtration and/or fixing of samples was done within 15 min after sampling the CTD 25L.

Prokaryotic heterotrophic production using the filter method

Immediately after the recovery of the CTD 25L, samples for microbial heterotrophic production and DIC fixation measurements were collected from the Niskin bottles. Samples were taken at 50 m, 250 m, 400 or 500 m, 1250 m, 2000 m, 3000 m, 4000 m depth. Processing of the samples, from collecting water from the Niskin bottles to incubating the samples with the radiolabeled tracers in temperature-controlled incubators, took less than 15 min.

Microbial heterotrophic production was measured by incubating 5-40 ml of seawater (depending on the depth) in triplicate with 5 nM [3H]-leucine (final concentration, specific activity 120 Ci mmol-1, American Radiolabeled Chemicals) in the dark at in situ temperature (±1°C) for 1 to 24 h. Duplicate formaldehyde-killed blanks were treated in the same way as the samples. Incubations were terminated by adding formaldehyde (2% final concentration) to the samples. Samples and blanks were filtered through 0.2-µm polycarbonate filters (Whatman Nuclepore, 25 mm filter diameter) supported by cellulose acetate filters (Millipore, HA, 0.45-µm pore size). Subsequently, the filters were rinsed twice with 5% ice-cold trichloroacetic acid, twice with Milli-Q and with 80% Ethanol. Subsequently filters were dried, 8 ml of scintillation cocktail (FilterCount, Canberra-Packard) added, and after about 18 h counted on board in a liquid scintillation counter (Perkin Elmer Tricarb). The instrument was calibrated with internal and external standards. The blank-corrected leucine incorporation rates were converted into microbial carbon production using the theoretical conversion of 1.55 kg mol-1 leucine incorporated (Kirchman, 1993; Simon and Azam, 1989).

DIC fixation was measured via the incorporation of [14C]-bicarbonate (3.7 x 106 Bq, Amersham) in 50 ml seawater samples. Triplicate samples and formaldehyde-fixed blanks were incubated in the dark at in situ temperature for 72 h. Incubations were terminated by adding glutaraldehyde (2% final concentration) to the samples, filtered onto 0.2-µm polycarbonate filters and rinsed with 10 ml 0.2 µm filtered seawater. Subsequently, the filters were fumed with concentrated HCl for 12 h. The filters were then processed as described above and counted in the scintillation counter for 10 min. The resulting mean disintegrations

per minute (DPM) of the samples were corrected for the mean DPM of the blanks and converted into organic carbon fixed over time and corrected for the natural DIC.

Prokaryotic heterotrophic production using the microcentrifuge method

3H-leucine incorporation rate was determined as a proxy for prokaryotic production (Kirchman 2001, Methods in microbiology, vol. 30), Figure 35. Triplicate subsamples (1.5 mL) dispensed into screw-capped centrifuge tubes amended with 10 nmol L-1 (final concentration) of [3H]-leucine (Cat#: ART0840, American Radiolabeled Chemicals, Inc.) and incubated at in situ temperature (± 2oC) in the dark. One trichloroacetic acid (TCA) killed blank was prepared for each sample. Incubation periods were 2 hour and 24 hours for the upper (0 – 250 m) and deeper (300 – bottom) water layers, respectively. After the incubation, proteins were TCA (final conc. 5%) extracted twice by centrifugation (12000 rpm, 10 min), followed by the extraction with ice-cold 80% ethanol. The samples were radioassayed with a liquid scintillation counter (Tri-Carb 3100TR, PerkinElmer) using Ultima-GOLD (Packard) as scintillation cocktail. Quenching was corrected by External standard channel ratio. The disintegrations per minute (DPM) of the TCA-killed blank was subtracted from the average DPM of the samples, and the resulting DPM was converted into leucine incorporation rates.

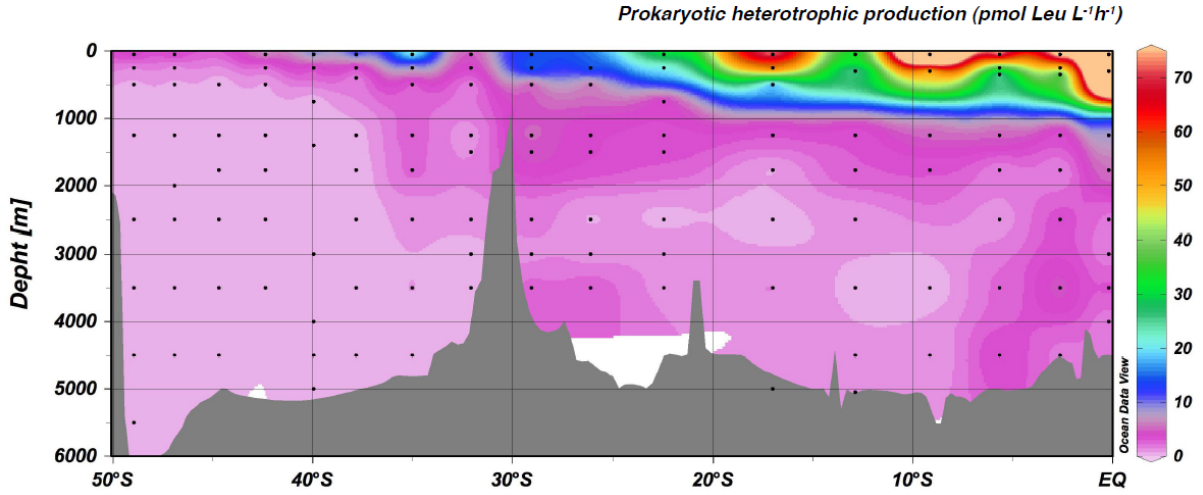

Figure 35. The prokaryotic heterotrophic production (pmol Leu L-1h-1) in the Southwest Atlantic Ocean as determined using the microcentrifuge methodology.

MICRO-CARD-FISH

The relative abundance and activity of the major prokaryotic groups will be determined by MICRO-CARD-FISH analysis. Fifty milliliters were incubated with 3H- Leucine of high specific activity (10nM final concentration). After the incubations, the life samples were fixed by adding paraformaldehyde (2% final concentration) and, subsequently, stored at 4ºC in the dark for 18 h. Thereafter the samples were filtered onto 0.2-µm polycarbonate filters and stored at -80^{o}C.

The analysis of MICRO-CARD-FISH samples in the lab will be done as described elsewhere (Teira et al. 2004; see also http://www.microbial-oceanography.eu/methods.htm). To evaluate the relative abundance and activity of Bacteria we will use a probe mix of EUB338-II-III (EUB338: 5'-GCT GCC TCC CGT AGG AGT-3', EUB338-II: 5'-GCA GCC ACC CGT AGG TGT-3', EUB338-III: 5'-GCT GCC ACC CGT AGG TGT-3', see Daims et

al., 1999). To target Crenarchaea we will use a probe mix of CREN537 and GI554 (CREN537: 5'-TGA CCA CTT GAG GTG CTG-3', Teira et al., 2004; GI554: 5'-TTA GGC CCA ATA ATC MTC CT-3', Massana et al., 1997). To cover Euryarchaea we will use the probe EURY806 (5'-CAC AGC GTT TAC ACC TAG-3'; Teira et al., 2004). To evaluate unspecific hybridization of probes and background fluorescence we will use antisense probes. Microautoradiography will be performed on previously hybridized filter sections and processed as described in Teira et al. (2004). The slides will be examined under an epifluorescence microscope equipped with a 100-W mercury lamp and appropriate filter sets for DAPI and Alexa488. The presence of silver grains surrounding cells will be recorded by using the transmission mode of the microscope. The data will be expressed as percent of DAPI-stained cells.

Estimation of marine microbial planktonic community respiration by in vivo electron transport system activity.

The respiration can be studied using enzyme analysis. In the enzymatic chain of Electron Transport Sys- tem (ETS), dehydrogenase enzymes and cythocrome electron carrier proteins are involved in electron transfer, and oxygen is used by aerobic organisms in the ter- minal steps of adenosine triphosphate (ATP) production in the respiratory process. The use of ETS activity as an estimate of respiration rates is based on the reduction of the tetrazolium salt 2-para (iodo- phenyl)-3(nitrophenyl)-5(phenyl) tetrazolium chloride (INT), a water- soluble, membrane-permeable salt, which passively penetrates into the cell (Dufour and Colon 1992), by dehy- drogenase enzymes present in the ETS, forming insoluble for- mazan crystals (INT-F). These dense stable colored, intracel- lular formazan granules can be detected spectrophoto- metrically or observed with bright-field. It has been demonstrated that ETS activity followed the same pattern as oxygen con- sumption, A quantitative approximation of the in vivo ETS assay is also possible through spectrophotometric or fluorometric analysis. It was found that in vivo INT reduction rates were highly correlated with microbial oxygen consumption**.** This procedure allows the determination of microplankton respiration rates at sea by using the in vivo INT-reduction method.

Sample volume 200 mL, incubation devices were made of polypropylene. Measurements were done on 4 replicates. One replicate was immediately fixed by adding paraformaldehyde (2% w/v final concentration) and used as killed controls. Fifteen minutes later all replicates were inoculated with a sterile solution of 7.9 mM INT to a final concentration of 0.2 mM. The solution was freshly prepared for each experiment using autoclaved Milli-Q water. After incubation, samples were fixed by adding paraformaldehyde in the same way as for the killed controls. After at least 15 minutes, samples were filtered through 25 mm diameter 0.2 μm pore size polycarbonate filters, air-dried for 1 min approximately, and stored frozen in 1.5 mL cryovials at –20°C until further processing.

References

Acinas et al. 1997, Acinas SG, Rodríguez-Valera F, Pedrós-Alió C (1997) Spatial and temporal variation in marine bacterioplankton diver- sity as shown by RFLP fingerprinting of PCR amplified 16S rDNA. FEMS Microbiol Ecol 24:27–40

Azam F, Fenchel T, Fleld JG, Gray JS, Meyer-Reil LA, Thingstad F (1983) The ecological role of water-column microbes in the sea. Mar Ecol Prog Ser 10:257-263

Baldwin AJ, Moss JA, Pakulski JD, Catala P, Joux F, Jeffrey WH (2005) Microbial diversity in a Pacific Ocean transect from the Arctic to Antarctic circles. Aquat Microb Ecol 41:91-102

Cho & Azam 1988, Cho BC, Azam F (1988) Major role of bacteria in biogeochem- ical fluxes in the ocean's interior. Nature 332:441-44

Cole et al. 1988 Cole JJ, Findlay S, Pace ML (1988) Bacterial production in fresh and saltwater ecosystems: a cross-system overview. Mar Ecol Prog Ser 43:l-10

Daims H, Brühl A, Amann R, Schleifer KH, Wagner M. (1999) The domain-specific probe EUB338 is insufficient for the detection of all Bacteria: Development and evaluation of a more comprehensive probe set. Syst Appl Microbiol 22: 434–444

Dufour, P., and M. Colon. (1992) The tetrazolium reduction method for assessing the viability of individual bacterial cells in aquatic environments: improvements, performance and applications. Hydrobiología 232:211-218.

Fuhrman et al. 1989, Fuhrman JA, Azam F (1982) Thymidine incorporation as a measure of heterotrophic bacterioplankton production in marine surface waters: evaluation and field results. Mar Bio166:109-1

Gasol J.M., del Giorgio P.A., Duarte C.M. (1997) Biomass distribution in marine planktonic communities. Limnol. Oceanogr. 42(6) 1353-1363.

Kirchman D. (2001) Measuring Bacterial Biomass production and growth rates from Leucine incorporation in natural aquatic environments. Methods in microbiology, vol. 30, 227-237

Kirchman, D.L., R.G. Keil*, M. Simon, and N.A. Welschmeyer. (1993) Biomass and production of heterotrophic bacterioplankton in the oceanic subarctic Pacific. Deep-Sea Res. 40:967-988.

Massana, R., A. E. Murray, C. M. Preston, and E. F. DeLong. (1997) Vertical distribution and phylogenetic characterization of marine planktonic Archaea in the Santa Barbara Channel.

Martínez-García S., Fernández E., Aranguren-Gassis M., and Teira E. (2009). In vivo electron transmport system activity: a method to estimate respiration in natural marine microbial planktonic communities. Limnol. Oceanogra. Methods 7, 459-469.

Pinhassi J. and Berman T. (2003) Differential Growth Response of Colony-forming α- and γ-Proteobacteria in Dilution culture and nutrient addition experiments from Lake Kinneret 8Israel), the Eastern Mediterranean Sea, and the Gulf of Eilat. Applied and Environmental Microbiology. 199-211

Pomeroy LR (1974) The ocean's food web, a changing paradigm. BioSci 24:499-504

Simon M., Cho C., and Azam E. (1992) Significance of bac- terial biomass in lakes and the ocean: Comparison to phyto- plankton biomass and biogeochemical implications. Mar. Ecol.

Simon, M., and F. Azam. (1989) Protein content and protein synthesis rates of planktonic marine bacteria. Mar. Ecol. Prog. Ser. 51:201-213.

Suzuki MT, Preston CM, Chavez FP, DeLong EF (2001) Quantitative mapping of bacterioplankton populations in seawater: field tests across an upwelling plume in Monterey Bay. Aquat Microb Ecol 24:117-127

Teira E, Reinthaler T, Pernthaler A, Pernthaler J, Herndl GJ (2004) Combining catalyzed reporter deposition-fluores- cence in situ hybridization and microautoradiography to detect substrate utilization by Bacteria and Archaea in the deep ocean. Appl Environ Microbiol 70:4411–4414

Williams PJleB (1981) Incorporation of microheterotrophic processes into the classical paradigm of the planktonic food web. Kieler Meersforsch Sonderh 5:l-28

3.2.C.4. ^{14}C Archaeal Incorporation

Santiago Gonzalez

NIOZ

Methods

Water was collected from 6 to 7 depths between 4500 and 250 m at all CTD cast. 5 Greiner tubes were filled with 50 ml water, 3 live samples and 2 glutaraldehyde-killed controls, posterior 40, 100 or 200 µCi Sodium Bicarbonate (^{14}C) was added. Samples were incubated for 72 hours at 4 and 10 ^{o}C. The incubation terminated adding 5 ml glutaraldehyde. After a couple of hours samples were filtered through polycarbonate 0.2 µm filters with a supporting 0.45 µm filter underneath. Filters were place for 1 d in desiccators with the fuming HCl.

For determining the ^{14}C incorporation, filters were placed in a labeled scintillation vial adding 8 ml scintillation cocktail Filter Counter (PerkinElmer) and let it sit about 18 hours before counting with a TriCarb 2810 Scintillation Counter. DPMs obtained were converted into Carbon fixed using the common primary production formula.

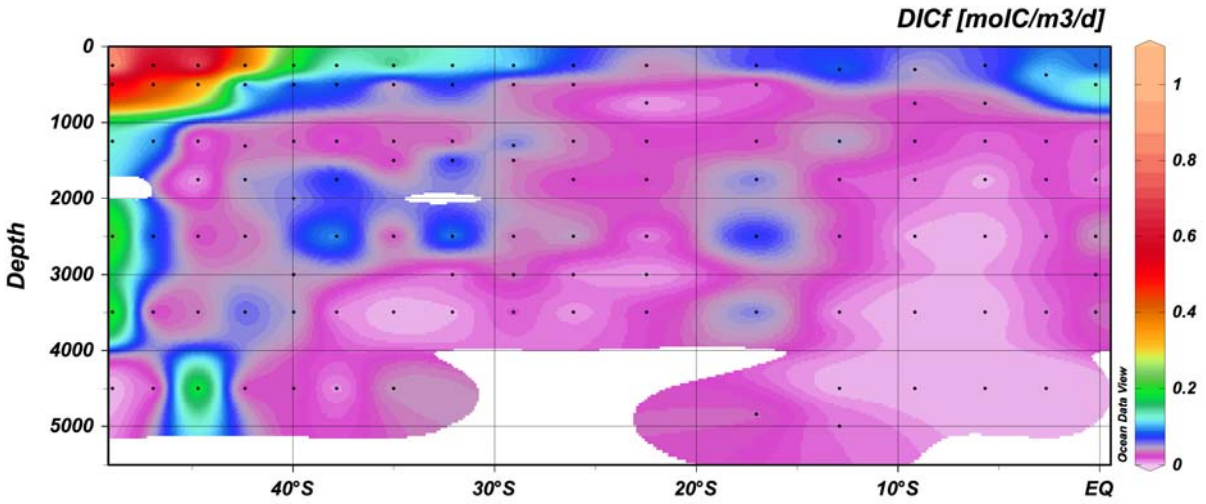

Figure 36. The Archaeal incorporation of ^{14}C via inorganic carbon in the Southwest Atlantic Ocean.

3.2.C.5. Dissolved Organic Carbon (DOC) and Fluorescent Organic Matter (FDOM) Sampling

Santiago Gonzalez

NIOZ

About 20 ml duplicates samples for DOC and FDOM were taken directly from the CTD in each station, DOC samples were acidified with 5-6 drops HCl 37 %. After sealing samples were stored a 4 ^{o}C and -20 ^{o}C for DOC and FDOM respectively. DOC and FDOM will be analysed in a land based laboratory.

Note: All samples from bottles 1-17 were unfiltered and the samples from 18-24 were 0.2 μm filtered.

Appendix 1.

Address list of scientist involved in data collection and analysis

Abouchami, Wafa: wafa.abouchami@mpic.de
Max-Planck-Institute for Chemistry
Biogeochemistry dept.
Postfach 3060
55020 Mainz
Germany
Tel: +49 6131 30 52 60
Fax: +49 6131 37 10 51

Achterberg, Eric: eric@noc.soton.ac.uk
Marine Biogeochemistry; School of Ocean & Earth Science
National Oceanography Centre Southampton; University of Southampton
Southampton SO14 3ZH
United Kingdom
Tel Direct: 02380-593199
Tel Secretary: 02380-592011
FAX: 02380-593059

Anderson, Per: per.andersson@nrm.se
Per Andersson
Laboratory for Isotope Geology, Swedish Museum of Natural History, Sweden
P.O. Box 50007, SE-104 05, Stockholm, Sweden
Phone: +46 8 5195 4038
Mobile +46 70 493 0782
Fax: +46 8 5195 4031

de Baar, Hein: NIOZ; Hein.de.Baar@nioz.nl
Royal Netherlands Institute for Sea Research
P.O. Box 59 1790 AB Den Burg The Netherlands
telephone 31 222 369465 telefax 31 222 319674
University of Groningen
Department Ocean Ecosystems
P.O. Box 14, 9750 AA Haren (Groningen)
secretariat phone: 31 50 363 2259

Baker, Alex: UEA; Alex.Baker@uea.ac.uk
School of Environmental Sciences
University of East Anglia
Norwich NR4 7TJ
United Kingdom
phone: + (0)1603 591529
fax: + (0)1603 591327

Bergauer, Kristin: bergauer.kristin@gmx.net
(Address details see Gerard Herndl)

Berube, Paul: pmberube@MIT.EDU
Postdoctoral Associate
Chisholm Laboratory
Massachusetts Institute of Technology
Department of Civil and Environmental Engineering, USA

Boye, Marie: Marie.Boye@univ-brest.fr
Laboratoire des Sciences de l'Environnement Marin (LEMAR), CNRS-UMR 6539 Institut Universitaire Europaen de la Mer (IUEM)
Technopole Brest-Iroise
Place Nicolas Copernic
29280 PlouzanÃ©- FRANCE
Phone: 33 2 98 49 86 51 - Fax : 33 2 98 49 86 45

Buesseler, Ken: kbuesseler@whoi.edu
Department of Marine Chemistry and Geochemistry
Woods Hole Oceanographic Institution
Clark-447, MS#25 WHOI
Woods Hole, MA 02543, USA
Phone: 001-508-289-2309
Fax: 001-508-457-2193

Claus, Maaike: maaike.e.claus@gmail.com
(Address details see Hein de Baar)

Cobelo, Antonio: acobelo@iim.csic.es
Marine Biogeochemistry Research Group
Instituto de Investigacións Mariñas (IIM-CSIC)
Rúa Eduardo Cabello 6
36208 Vigo (Spain)
Tel. +34 986 231 930 Ext 145
Fax +34 986 292 762

Deng, Feifei: Feifei.Deng@earth.ox.ac.uk
(Address details see Gideon Henderson)

Dérot, Jonathan: jonathan.derot@etumel.univmed.fr
(Address details see Marie Boye)

Galer, Stephen: sjg@mpch-mainz.mpg.de
Max-Planck-Institut fur Chemie
Department of Geochemie
PO box 3060
55020 Mainz, Germany
Phone: 0049-6131-305-220
Fax: 0049-6131-371-051

Gerringa, Loes J.A., NIOZ; Loes.Gerringa@nioz.nl
Royal Netherlands Institute for Sea Research
BIO-Chemical Oceanography
PO Box 59 1790 AB Den Burg
The Netherlands
tel 31(0)222369436
fax 31(0)222319674

Godoy, José Marcus: jmgodoy@puc-rio.br
Departamento de Quimica
Pontifical Catholic University of Rio de Janeiro (PUC-RIO)
Rua Marques de Sao Vicente 255
Gavec, Rio de Janeiro, Brazil
CEP 22453-900
Phone: 0055-21-3527-1322/1802/1854
Fax: 0055-21-3527-1854

Goldstein, Steve; steveg@ldeo.columbia.edu
Lamont-Doherty Earth Observatory of Columbia University
Department of Geochemistry
61 Route 9W
Palisades, NY 10964
213 Comer Building
Phone: 001-845-365-8787
Fax: 001 845-365-8155

Gonzalez, Santiago: NIOZ; Santiago.Gonzalez@nioz.nl

Groot, Lennart: lennart.groot@student.hu.nl
(Address details see Loes Gerringa)

Hartman, Alison; ahartman@ldeo.columbia.edu
(Address details see Steve Goldstein)

Henderson, Gideon: gideonh@earth.ox.ac.uk
Department of Earth Sciences
Oxford University
South Parks Road, Oxford
OX1 3AN, UK
Phone: 0044-1865 282123
Fax: 0044-1865 272072

van Heuven, Steven: svheuven@gmail.com
Centrum voor Isotopen Onderzoek (CIO)
Energy and Sustainability Research Institute Groningen (ESRIG) Rijksuniversiteit Groningen
Nijenborgh 4, 9747 AG Groningen, Netherlands
tel +31-50-3634760 fax +31-50-3634738

Herndl, Gerhard: gerhard.herndl@univie.ac.at
Professor, Chair of Marine Biology
University of Vienna
Althanstrasse 14
A-1090 Vienna
Austria
phone: +43-(0)1-4277-57100
cell phone: +43-699-1908-1166
fax: +43-(0)1-4277-9571

and
Dept. of Biological Oceanography
Royal Netherlands Institute for Sea Research (NIOZ)
P.O. Box 59
1790 AB Den Burg
The Netherlands

Jones, Elizabeth (Libby): NIOZ; Elizabeth.Jones@uea.ac.uk

de Jong, Jeroen: jdejong@ulb.ac.be
Université Libre de Bruxelles
Department of Earth and Environmental Sciences CP 160/02
Unit Isotopes, Petrology and Environment
Avenue F.D. Roosevelt 50
1050 Brussels
Belgium
PHONE:
+32-2-650-2236 (office)
+32-2-650-4169 (Nu Plasma mass spec room)
FAX: +32-2-650-3748

Klimiuk, Adam: adam.klimiuk@nioz.nl
(Address details see Gerard Herndl)

Laan, Patrick: NIOZ; email: Patrick.Laan@nioz.nl

Lamborg, Carl: WHOI; e-mail: clamborg@whoi.edu
Department of Marine Chemistry and Geochemistry
Woods Hole Oceanographic Institution
Clark-447, MS#51 WHOI
Woods Hole, MA 02543, USA
Phone: 001-508-289-2556

Lekunberri, Itziar: itzileku@gmail.com
(Address details see Gerard Herndl)

Lopez Sanchez, Daniel Eduardo: dels@iim.csic.es
(Address details see Antonio Cobelo)

Meijer, Harro: h.a.j.meijer@rug.nl
Centrum voor Isotopen Onderzoek (CIO)
Energy and Sustainability Research Institute Groningen (ESRIG) Rijksuniversiteit Groningen
Nijenborgh 4, 9747 AG Groningen, Netherlands
tel +31-50-3634760 fax +31-50-3634738

Middag, Rob: NIOZ; email: rob.middag@nioz.nl
Present address:
Department of Ocean Sciences & Institute of Marine Sciences
University of California Santa Cruz, CA 95064, USA

Ober, Sven: NIOZ; Sven.Ober@nioz.nl

Orellana, Mónica: morellan@systemsbiology.org
Institute for Systems Biology
1441 N 34th street
Seattle WA 98103, USA
Phone 001-206 732-1302
FAX 001-206 732-1299

Owens, Stephanie: sowens@whoi.edu
(Address details see Ken Buesseler)

Pena, Leopold (Leo); leopoldo@ldeo.columbia.edu
(Address details see Steve Goldstein)

Pichevin, Laetitia: laetitia.pichevin@ed.ac.uk
The University of Edinburgh
Address: Grant Institute, The King's Buildings, West Mains Road,
Edinburgh EH9 3JW
Phone: 0044 131 650 5980

Rafter, Patrick: prafter@princeton.edu
Dept. of Geosciences
Guyot Hall
Princeton University
Princeton, NJ 08544
phone: 001-858-405-0539

Rijkenberg, Micha: NIOZ, email: micha.rijkenberg@nioz.nl
Royal Netherlands Institute for Sea Research
P.O. Box 59 1790 AB Den Burg The Netherlands
Phone: 0031 222 369456
Fax: 0031 222 319674

Salt, Lesley: NIOZ; email:lesley.salt@nioz.nl

Schmidt, Patrick: Universitat Bremen; psbschmidt@googlemail.com
(Address details see Reiner Steinfeldt)

Schoemann, Veronique: NIOZ; email: Veronique.schoemann@nioz.nl

Steinfeldt, Reiner; rsteinf@physik.uni-bremen.de
Universitaet Bremen, FB 1
Abt. Ozeanographie
Postfach 330440
D-28334 Bremen
Germany
Tel: +49 (0)421 218-62154
Fax: +49 (0)421 218-7018

de Visser, Jan Dirk: NIOZ; JanDirk.de.Visser@nioz.nl

van Weerlee, Evaline: NIOZ; Evaline.van.Weerlee@nioz.nl

Weiss, Dominik: d.weiss@imperial.ac.uk
Department of Earth Science and Engineering
Royal School of Mines
Imperial College London
South Kensington Campus
Exhibition Road
London SW7 2AZ
Phone: 0044-20-7594-6383
Fax: 0044-20-7594-7444

Wuis, Leon: NIOZ; Leon.Wuis@nioz.nl

Appendix 2. Station list & devices deployment

CTD25L is the high volume 25L CTD
UCC is the ultra clean CTD
ISP are the *in situ* pumps

Station	Cast	Device	Action	date	time	Longitude	Latitude
1	1	UCC	start	5-Mar-11	18:00	-52.6877	-49.5468
1	1	UCC	end	5-Mar-11	20:16	-52.6877	-49.5468
1	2	CTD25L	start	5-Mar-11	20:56	-52.6885	-49.5475
1	2	CTD25L	end	5-Mar-11	23:51	-52.6885	-49.5475
2	1	UCC	start	6-Mar-11	15:08	-48.8790	-48.9675
2	1	UCC	end	6-Mar-11	19:21	-48.8790	-48.9675
2	2	CTD25L	start	6-Mar-11	19:40	-48.7933	-48.9358
2	2	CTD25L	end	6-Mar-11	23:53	-48.7933	-48.9358
2	3	ISP	start	7-Mar-11	0:08	-48.7177	-48.8987
2	3	ISP	end	7-Mar-11	2:28	-48.7177	-48.8987
2	4	UCC	start	7-Mar-11	2:52	-48.6615	-48.8642
2	4	UCC	end	7-Mar-11	6:55	-48.6615	-48.8642
2	5	CTD25L	start	7-Mar-11	7:22	-48.6070	-48.8087
2	5	CTD25L	end	7-Mar-11	9:28	-48.6070	-48.8087
3	1	UCC	start	7-Mar-11	23:15	-47.2202	-46.9330
3	1	UCC	end	8-Mar-11	2:57	-47.2202	-46.9330
3	2	CTD25L	start	8-Mar-11	3:21	-47.1790	-46.9070
3	2	CTD25L	end	8-Mar-11	7:20	-47.1790	-46.9070
4	1	UCC	start	8-Mar-11	23:42	-45.5457	-44.7020
4	1	UCC	end	9-Mar-11	3:02	-45.5457	-44.7020
4	2	CTD25L	start	9-Mar-11	3:22	-45.5265	-44.7117
4	2	CTD25L	end	9-Mar-11	6:03	-45.5265	-44.7117
5	1	UCC	start	9-Mar-11	23:14	-44.0198	-42.3785
5	1	UCC	end	10-Mar-11	2:24	-44.0198	-42.3785
5	2	CTD25L	start	10-Mar-11	2:43	-44.0318	-42.3640
5	2	CTD25L	end	10-Mar-11	6:16	-44.0318	-42.3640
6	1	UCC	start	10-Mar-11	22:47	-42.4877	-39.9685
6	1	UCC	end	11-Mar-11	1:57	-42.4877	-39.9685
6	2	CTD25L	start	11-Mar-11	2:17	-42.4232	-39.9648
6	2	CTD25L	end	11-Mar-11	5:47	-42.4232	-39.9648
6	3	ISP	start	11-Mar-11	6:19	-42.3609	-39.9590
6	3	ISP	end	11-Mar-11	7:53	-42.3609	-39.9590
6	4	UCC	start	11-Mar-11	8:16	-42.3460	-39.9568
6	4	UCC	end	11-Mar-11	11:36	-42.3460	-39.9568
7	1	CTD25L	start	12-Mar-11	1:56	-41.1248	-37.8305
7	1	CTD25L	end	12-Mar-11	5:30	-41.1248	-37.8305
7	2	UCC	start	12-Mar-11	5:49	-41.1305	-37.8382
7	2	UCC	end	12-Mar-11	8:55	-41.1305	-37.8382
7	3	CTD25L	start	12-Mar-11	9:19	-41.1382	-37.8522
7	3	CTD25L	end	12-Mar-11	11:34	-41.1382	-37.8522
8	1	UCC	start	13-Mar-11	9:07	-39.4425	-35.0083
8	1	UCC	end	13-Mar-11	13:24	-39.4425	-35.0083
8	2	CTD25L	start	13-Mar-11	13:43	-39.4310	-35.0093
8	2	CTD25L	end	13-Mar-11	17:10	-39.4310	-35.0093

9	1	UCC	start	14-Mar-11	15:38	-37.4633	-32.0860
9	1	UCC	end	14-Mar-11	18:27	-37.4633	-32.0860
9	2	CTD25L	start	14-Mar-11	18:45	-37.4563	-32.0920
9	2	CTD25L	end	14-Mar-11	21:33	-37.4563	-32.0920
9	3	ISP	start	14-Mar-11	21:45	-37.4480	-32.0991
9	3	ISP	end	14-Mar-11	23:48	-37.4480	-32.0991
10	1	UCC	start	15-Mar-11	20:38	-35.7842	-29.0620
10	1	UCC	end	15-Mar-11	23:23	-35.7842	-29.0620
10	2	CTD25L	start	15-Mar-11	23:40	-35.8078	-29.0538
10	2	CTD25L	end	16-Mar-11	2:18	-35.8078	-29.0538
11	1	CTD25L	start	17-Mar-11	0:34	-34.2585	-26.0867
11	1	CTD25L	end	17-Mar-11	4:03	-34.2585	-26.0867
11	2	UCC	start	17-Mar-11	4:24	-34.2812	-26.0902
11	2	UCC	end	17-Mar-11	7:49	-34.2812	-26.0902
11	3	CTD25L	start	17-Mar-11	8:10	-34.3003	-26.0905
11	3	CTD25L	end	17-Mar-11	10:30	-34.3003	-26.0905
12	1	UCC	start	18-Mar-11	10:40	-32.7322	-22.4715
12	1	UCC	end	18-Mar-11	13:57	-32.7322	-22.4715
12	2	CTD25L	start	18-Mar-11	14:16	-32.7487	-22.4732
12	2	CTD25L	end	18-Mar-11	17:15	-32.7487	-22.4732
12	3	ISP	start	18-Mar-11	17:44	-32.7554	-22.4744
12	3	ISP	end	18-Mar-11	19:26	-32.7554	-22.4744
12	4	UCC	start	18-Mar-11	19:35	-32.7510	-22.4693
12	4	UCC	end	18-Mar-11	22:27	-32.7510	-22.4693
13	1	UCC	start	20-Mar-11	11:20	-30.5932	-17.0162
13	1	UCC	end	20-Mar-11	14:37	-30.5932	-17.0162
13	2	CTD25L	start	20-Mar-11	14:54	-30.6052	-17.0173
13	2	CTD25L	end	20-Mar-11	18:05	-30.6052	-17.0173
14	1	UCC	start	21-Mar-11	21:58	-29.2197	-12.8913
14	1	UCC	end	22-Mar-11	0:39	-29.2197	-12.8913
14	2	CTD25L	start	22-Mar-11	1:00	-29.2335	-12.8957
14	2	CTD25L	end	22-Mar-11	4:25	-29.2335	-12.8957
14	3	ISP	start	22-Mar-11	4:30	-29.2382	-12.9023
14	3	ISP	end	22-Mar-11	6:39	-29.2382	-12.9023
15	1	UCC	start	23-Mar-11	7:20	-27.9988	-9.1475
15	1	UCC	end	23-Mar-11	10:50	-27.9988	-9.1475
15	2	CTD25L	start	23-Mar-11	11:11	-28.0012	-9.1608
15	2	CTD25L	end	23-Mar-11	15:06	-28.0012	-9.1608
16	1	CTD25L	start	24-Mar-11	12:54	-28.4572	-5.6667
16	1	CTD25L	end	24-Mar-11	16:13	-28.4572	-5.6667
16	2	UCC	start	24-Mar-11	16:32	-28.4595	-5.6768
16	2	UCC	end	24-Mar-11	19:56	-28.4595	-5.6768
16	3	CTD25L	start	24-Mar-11	20:13	-28.4640	-5.6890
16	3	CTD25L	end	24-Mar-11	21:58	-28.4640	-5.6890
17	1	UCC	start	25-Mar-11	17:41	-28.9120	-2.6385
17	1	UCC	end	25-Mar-11	20:49	-28.9120	-2.6385
17	2	CTD25L	start	25-Mar-11	21:08	-28.9172	-2.6505
17	2	CTD25L	end	26-Mar-11	0:18	-28.9172	-2.6505
17	3	ISP	start	26-Mar-11	0:25	-28.9207	-2.6611
17	3	ISP	end	26-Mar-11	2:26	-28.9208	-2.6626
17	4	UCC	start	26-Mar-11	2:37	-28.9210	-2.6632
17	4	UCC	end	26-Mar-11	5:51	-28.9210	-2.6632

18	1	UCC	start	27-Mar-11	9:45	-32.8817	-0.1828
18	1	UCC	end	27-Mar-11	12:54	-32.8817	-0.1828
18	2	CTD25L	start	27-Mar-11	13:11	-32.8745	-0.1915
18	2	CTD25L	end	27-Mar-11	16:12	-32.8745	-0.1915

Appendix 3. Samples taken from FISH

FISH SAMPLING LOG

DATE	Ship's time	UTC	Latitude	Longitude	Serial # - bottle #	Nuts	DFe	DAl	DMn	Library	Library	FeL	Pt	Pt	Pb isotopes	Pb isotopes	Cd/Ni/Cr isotopes	$\delta^{18}O$ & Ba	Co	Co	Fe/Cu/Zn	Fe/Cu/Zn
dd-mm-yy	h-mm	h-mm			DFe, DAl, DMn, nuts	F	F	F	F	UF	F	F	UF	F	UF	F	F	F	UF	F	UF	F
06-03-11	0:00	2:00	-49.489368	-52.264051	1-1	X	X	X	X	X	X			X	X		X					
06-03-11	3:00	5:00	-49.371747	-51.54557	1-2	X	X	X	X	X	X											
06-03-11	6:00	8:00	-49.275286	-50.775327	1-3	X	X	X	X	X	X	X										
06-03-11	9:00	11:00	-49.130456	-49.918573	1-4	X	X	X	X	X	X											
07-03-11	9:00	11:00	-48.614396	-48.458567	1-5	X	X	X	X	X	X	X	X	X	X							
07-03-11	12:00	14:00	-48.177756	-48.197759	1-6	X	X	X	X	X	X						X					
07-03-11	15:00	17:00	-47.770845	-47.895827	1-7	X	X	X	X	X	X											
07-03-11	18:00	20:00	-47.363736	-47.577972	1-8	X	X	X	X	X	X											
07-03-11	20:00	22:00	-47.073879	-47.326468	1-9	X	X	X	X	X	X				X	X	X					
08-03-11	9:00	11:00	-46.383755	-46.797558	1-10	X	X	X	X	X	X											
08-03-11	12:00	14:00	-45.968047	-46.476438	1-11	X	X	X	X	X	X											
08-03-11	15:00	17:00	-45.561662	-46.186027	1-12	X	X	X	X	X	X											
08-03-11	18:00	20:00	-45.171255	-45.880133	1-13	X	X	X	X	X	X											
09-03-11					Station 4												X					
09-03-11	6:00	8:00	-44.592503	-45.431619	1-15	X	X	X	X	X	X	X					X					
09-03-11	9:00	11:00	-44.154034	-45.166047	1-16	X	X	X	X	X	X											
09-03-11	12:00	14:00	-43.722693	-44.907801	1-17	X	X	X	X	X	X											
09-03-11	15:00	17:00	-43.289558	-44.602612	1-18	X	X	X	X	X	X											
09-03-11	18:00	20:00	-42.836704	-44.321178	1-19	X	X	X	X	X	X	X										
09-03-11	20:00	22:00	-42.530415	-44.122746	1-20	X		X	X	X	X				X		X					
10-03-11	6:00	8:00	-42.144326	-43.897536	1-21	X		X	X	X	X											
10-03-11	9:00	11:00	-41.709791	-43.597825	1-22	X	X	X	X	X	X											
10-03-11	12:00	14:00	-41.244701	-43.300869	1-23	X	X	X	X	X	X											
10-03-11	15:00	17:00	-40.79212	-43.010474	1-24	X	X	X	X	X	X											
10-03-11	18:00	20:00	-40.348641	-42.722286	2-1	X	X	X	X	X	X											
10-03-11	20:00	22:00	-40.045987	-42.539157	2-2	X	X	X	X	X	X	X	X	X	X		X					
11-03-11	12:45	14:45	-39.471428	-42.016054	2-3	X	X	X	X	X	X											
11-03-11	15:00	17:00	-39.117695	-41.845621	2-4	X	X	X	X	X	X											
11-03-11	18:00	20:00	-38.653642	-41.596707	2-5	X	X	X	X	X	X											
11-03-11	21:00	23:00	-38.196245	-41.353216	2-6	X	X	X	X	X	X											
11-03-11	22:30	24:30	-37.98728	-41.220772	2-7	X	X	X	X	X	X	X		X	X	X	X					
12-03-11	15:00	17:00	-37.159514	-40.71651	2-8	X	X	X	X	X	X											
12-03-11	18:00	20:00	-36.773907	-40.500771	2-9	X	X	X	X	X	X											
12-03-11	21:00	23:00	-36.400018	-40.271211	2-10	X	X	X	X	X	X											
13-03-11	0:00	2:00	-36.019724	-40.038003	2-11	X	X	X	X	X	X											
13-03-11	3:00	5:00	-35.635422	-39.810751	2-12	X	X	X	X	X	X											
13-03-11	6:00	8:00	-35.250765	-39.576076	2-13	X	X	X	X	X	X	X										
13-03-11	7:00	9:00	-35.123316	-39.501029	2-14	X	X	X	X	X	X				X		X					
13-03-11	18:00	20:00	-34.644698	-39.211859	2-15	X	X	X	X	X	X											
13-03-11	21:00	23:00	-34.269917	-38.947559	2-16	X	X	X	X	X	X	X										
14-03-11	0:00	2:00	-33.897699	-38.678009	2-17	X	X	X	X	X	X											
14-03-11	3:00	5:00	-33.506063	-38.414266	2-18	X	X	X	X	X	X											
14-03-11	6:00	8:00	-33.104241	-38.151569	2-19	X	X	X	X	X	X	X										
14-03-11	9:00	11:00	-32.678118	-37.874819	2-20	X	X	X	X	X	X											
14-03-11	12:00	14:00	-32.278472	-37.590107	2-21	X	X	X	X	X	X		X	X	X		X					
15-03-11	0:00	2:00	-31.831019	-37.288668	2-22	X	X	X	X	X	X											
15-03-11	3:00	5:00	-31.377972	-37.063347	2-23	X	X	X	X	X	X											
15-03-11	6:00	8:00	-30.91283	-36.822114	2-24	X	X	X	X	X	X	X										
15-03-11	9:00	11:00	-30.470881	-36.549864	3-1	X	X	X	X	X	X				X							
15-03-11	12:00	14:00	-30.012107	-36.303372	3-2	X	X	X	X	X	X											
15-03-11	15:30	17:30	-29.480092	-36.01722	3-3	X	X	X	X	X	X											
15-03-11	17:15	19:15	-29.224207	-35.868244	3-4	X	X	X	X	X	X				X		X					
16-03-11	3:00	5:00	-28.704085	-35.62233	3-5	X	X	X	X	X	X											
16-03-11	6:00	8:00	-28.267671	-35.38694	3-6	X	X	X	X	X	X	X										
16-03-11	9:00	11:00	-27.827235	-35.145405	3-7	X	X	X	X	X	X				X							
16-03-11	12:00	14:00	-27.393826	-34.920715	3-8	X	X	X	X	X	X											
16-03-11	15:00	17:00	-26.961647	-34.699905	3-9	X	X	X	X	X	X											

FISH SAMPLING LOG
(continued)

DATE	Ship's time	UTC	Latitude	Longitude	Serial # - bottle #	Nuts	DFe	DAl	DMn	Library	Library	FeL	Pt	Pt	Pb isotopes	Pb isotopes	Cd/Ni/Cr isotopes	$\delta^{18}O$ & Ba	Co	Co	Fe/Cu/Zn	Fe/Cu/Zn
dd-mm-yy	h-mm	h-mm			DFe, DAl, DMn, nuts	F	F	F	F	UF	F	F	UF	F	UF	F	F	F	UF	F	UF	F
16-03-11	18:00	20:00	-26.527944	-34.481395	3-10	X	X	X	X	X	X											
16-03-11	20:00	22:00	-26.241634	-34.338002	3-11	X	X	X	X	X	X			X	X		X					
17-03-11	12:00	14:00	-25.572971	-34.038066	3-12	X	X	X	X	X	X											
17-03-11	15:00	17:00	-25.093627	-33.836437	3-13	X	X	X	X	X	X											
17-03-11	18:00	20:00	-24.612432	-33.638259	3-14	X	X	X	X	X	X											
17-03-11	21:00	23:00	-24.146774	-33.449182	3-15	X	X	X	X	X	X	X										
18-03-11	0:00	2:00	-23.698126	-33.251992	3-16	X	X	X	X	X	X											
18-03-11	3:00	5:00	-23.255295	-33.063874	3-17	X	X	X	X	X	X											
18-03-11	6:30	8:30	-22.752921	-32.841472	3-18	X	X	X	X	X	X				X		X					
20-03-11	18:00	19:00	-16.893893	-30.568491	3-19	X	X	X	X	X	X	X	X	X			X	X				
20-03-11	21:00	22:00	-16.429622	-30.392406	3-20	X	X	X	X	X	X											
21-03-11	0:00	1:00	-15.958817	-30.239811	3-21	X	X	X	X	X	X											
21-03-11	3:00	4:00	-15.48333	-30.083022	3-22	X	X	X	X	X	X											
21-03-11	6:00	7:00	-15.010162	-29.917191	3-23	X	X	X	X	X	X	X										
21-03-11	9:00	10:00	-14.542487	-29.764261	3-24	X	X	X	X	X	X											
21-03-11	12:00	13:00	-14.080714	-29.620481	4-1	X	X	X	X	X	X											
21-03-11	15:00	16:00	-13.625117	-29.463569	4-2	X	X	X	X	X	X											
21-03-11	19:00	20:00	-13.010745	-29.258974	4-3	X	X	X	X	X	X				X		X	X				
22-03-11	7:00	8:00	-12.719348	-29.176821	4-4	X	X	X	X	X	X	X										
22-03-11	9:00	10:00	-12.419519	-29.075357	4-5 (nuts), 4-9 Metals	X	X	X	X	X	X											
22-03-11	12:00	13:00	-11.95823	-28.919629	4-6	X	X	X	X	X	X											
22-03-11	15:00	16:00	-11.514409	-28.765014	4-7	X	X	X	X	X	X											
22-03-11	18:00	19:00	-11.050635	-28.615672	4-8	X	X	X	X	X	X											
22-03-11	21:00	22:00	-10.583887	-28.474137	4-10	X	X	X	X	X	X	X										
23-03-11	0:00	1:00	-10.113426	-28.316222	4-11	X	X	X	X	X	X											
23-03-11	4:00	5:00	-9.487074	-28.106269	4-12	X	X	X	X	X	X		X	X	X		X	X				
23-03-11	15:00	16:00	-9.028019	-28.024561	4-13	X	X	X	X	X	X											
23-03-11	18:00	19:00	-8.540772	-28.083967	4-14	X	X	X	X	X	X											
23-03-11	21:00	22:00	-8.06088	-28.152073	4-15	X	X	X	X	X	X	X										
24-03-11	0:00	1:00	-7.584942	-28.209921	4-16	X	X	X	X	X	X											
24-03-11	3:00	4:00	-7.103186	-28.268478	4-17	X	X	X	X	X	X											
24-03-11	6:00	7:00	-6.60833	-28.329512	4-18	X	X	X	X	X	X	X										
24-03-11	9:00	10:00	-6.113484	-28.398977	4-19	X	X	X	X	X	X											
24-03-11	11:00	12:00	-5.788679	-28.446064	4-20	X	X	X	X	X	X			X			X	X				
25-03-11	0:00	1:00	-5.247047	-28.519854	4-21	X	X	X	X	X	X											
25-03-11	3:00	4:00	-4.789459	-28.587208	4-22	X	X	X	X	X	X											
25-03-11	6:00	7:00	-4.311981	-28.664641	4-23	X	X	X	X	X	X	X										
25-03-11	9:00	10:00	-3.834169	-28.737596	4-24	X	X	X	X	X	X											
25-03-11	12:00	13:00	-3.350008	-28.80627	5-1	X	X	X	X	X	X											
25-03-11	15:30	16:30	-2.802932	-28.884277	5-2	X	X	X	X	X	X		X	X	X		X	X				
27-03-11					Station 18								X	X								
29-03-11	9:00	10:00	5.512366	-29.589137	5-3	X	X	X	X	X	X									X		
29-03-11	12:00	13:00	5.910358	-29.353456	5-4	X	X	X	X	X	X						X	X	X	X	X	X
29-03-11	15:00	16:00	6.309782	-29.121819	5-5	X	X	X	X	X	X								X	X		
29-03-11	18:00	19:00	6.711122	-28.894493	5-6	X	X	X	X	X	X	X						X	X	X	X	X	X
29-03-11	21:00	22:00	7.107818	-28.66495	5-7	X	X	X	X	X	X								X	X		
30-03-11	0:00	1:00	7.516702	-28.440713	5-8	X	X	X	X	X	X						X	X	X	X	X	X
30-03-11	3:00	4:00	7.922042	-28.199197	5-9	X	X	X	X	X	X								X	X		
30-03-11	6:00	7:00			5-10	X	X	X	X	X	X	X						X	X	X	X	X	X
30-03-11	9:00	10:00	8.745727	-27.712489	5-11	X	X	X	X	X	X								X	X		
30-03-11	12:00	13:00	9.147204	-27.470508	5-12	X	X	X	X	X	X						X	X	X	X	X	X
30-03-11	15:00	16:00	9.546186	-27.241617	5-13	X	X	X	X	X	X								X	X		
30-03-11	18:00	19:00	9.940646	-27.004103	5-14	X	X	X	X	X	X	X					X	X	X	X	X	X
30-03-11	21:00	22:00	10.337994	-26.762798	5-15	X	X	X	X	X	X								X	X		
31-03-11	0:00	1:00	10.74078	-26.534807	5-16	X	X	X	X	X	X						X	X	X	X	X	X
31-03-11	3:00	4:00	11.140221	-26.302202	5-17	X	X	X	X	X	X	X					X	X	X	X	X	X